LIVRO DE RESUMOS

CBrAVIC 2022

08 a 12 de agosto de 2022

Sociedade Brasileira de Vácuo – SBV

XLIII CBrAVIC
CONGRESSO BRASILEIRO DE APLICAÇÕES DE VÁCUO NA INDÚSTRIA E NA CIÊNCIA
Sorocaba - SP
08-12 de Agosto de 2022

Livro de resumos - CBrAVIC 2022

Formato: Livro digital
Veiculação: Digital
ISBN: 978-65-00-78788-7

XLIII CONGRESSO BRASILEIRO DE APLICAÇÕES DE VÁCUO NA INDÚSTRIA E NA CIÊNCIA

É com grande satisfação que anunciamos a 43ª edição do Congresso Brasileiro de Vácuo na Indústria e na Ciência – CBrAVIC 2022, a ser realizada entre os dias 08 e 12 de agosto de 2022, no Parque Tecnológico de Sorocaba - PTS, em Sorocaba -SP, que conta excelente infraestrutura de auditórios e salas para a realização de palestras convidadas, palestras técnicas de empresas expositoras, sessões orais, apresentações de pôsteres e também para exposição de empresas parceiras.

A Comissão Organizadora envidará todos os esforços para propiciar um ambiente oportuno para ricas discussões e interações entre pesquisadores, professores e estudantes de graduação e pós-graduação, público alvo deste evento, e empresas parceiras, abordando temas relevantes nas áreas de pesquisa e desenvolvimento em Ciência e Tecnologia de Vácuo.

É nosso maior objetivo que o CBRAVIC 2022 ofereça a seus participantes a oportunidade de apresentar e discutir seus trabalhos e que seja instrumento para estimular novas e frutíferas colaborações. Palestrantes nacionais e internacionais apresentarão os últimos desenvolvimentos científicos e tendências futuras, englobando as áreas de Engenharia, Física, Química, Ciência dos Materiais e assuntos interdisciplinares.

Esperamos encontrá-los em breve em Sorocaba, cidade sede de muitas empresas de tecnologia e centros de pesquisa, rica em parques e atividades culturais e com povo muito hospitaleiro.

Luciana Sgarbi Rossino
Presidente do CBrAVIC 2022

Nazir Montero dos Santos
Presidente da SBV

TEMAS DO CONGRESSO

a) Ciência e Tecnologia de Vácuo (CTV);

b) Ciência e Tecnologia de Plasmas (CTP);

c) Ciência e Tecnologia dos Materiais (CTM);

d) Superfícies, Interfaces e Filmes Finos (SIFF);

e) Tratamento e Modificações de Materiais (TMM);

f) Energia: Fontes Renováveis e Tecnologia (EFRT);

g) Biomateriais, Biofilmes e Bioprocessos: Ciência e Tecnologia (BBBCT);

h) Vácuo na Indústria (VA);

i) Ciência e Tecnologia de Sensores e Dispositivos (CTSD);

j) Nanociência, Nanotecnologia e Nanomateriais (NNN).

TEMAS DOS MINICURSOS

a) Introdução à Ciência e Tecnologia do Vácuo

b) Tratamento de Superfície a Plasma – Teoria

c) Tratamento de Superfície a Plasma – Prática

d) Filmes Finos: Métodos de Deposição e Caracterização em Superfície

e) Vacuum Metrology

f) Dinâmica de Gases Rarefeitos: Teoria e Aplicações do Vácuo

g) Aprendizagem Ativa: Uma abordagem que faz pensar

h) Interação de Íons com a Matéria: Da Deposição à Modificação de Materiais

PROGRAMAÇÃO

Segunda-feira – 08/08/2022

	Unesp Sorocaba/SP		Fatec Sorocaba/SP	
08:30 - 09:30	Minicurso: "Introdução a Ciência e Tecnologia do Vácuo" – Prof. Dr. Francisco Tadeu Degasperi e Dr. Marcelo Juni Ferreira	Minicurso: "Filmes Finos: Métodos de Deposição e Caracterização de Superfície" – Profª. Drª. Nazir Monteiro dos Santos, Prof. Dr. Conrado Ramos Moreira Afonso, Prof. Dr. Pedro A. P. Nascente e Prof. Dr. Angelo L. Gobbi	Minicurso: "Tratamento de Superfície a Plasma - Teoria" – Prof. Dr. Rodrigo S. Pessoa	Minicurso: "Tratamento de Superfície a Plasma - Prática" – Prof. Msc. Marcos Dorigão Manfrinato e Profª. Drª. Luciana Sgarbi Rossino
09:30 - 10:00				
10:00 - 10:30	Coffee Break		Coffee Break	
10:30 - 12:30	Minicurso: "Introdução a Ciência e Tecnologia do Vácuo" - – Prof. Dr. Francisco Tadeu Degasperi e Dr. Marcelo Juni Ferreira	Minicurso: "Filmes Finos: Métodos de Deposição e Caracterização de Superfície" – Profª. Drª. Nazir Monteiro dos Santos, Prof. Dr. Conrado Ramos Moreira Afonso, Prof. Dr. Pedro A. P. Nascente e Prof. Dr. Angelo L. Gobbi	Minicurso: "Tratamento de Superfície a Plasma - Teoria" – Prof. Dr. Rodrigo S. Pessoa	Minicurso: "Tratamento de Superfície a Plasma - Prática" – Prof. Msc. Marcos Dorigão Manfrinato e Profª. Drª. Luciana Sgarbi Rossino
12:30 - 14:00	Almoço		Almoço	
14:00 - 18:00	Minicurso: "Vacuum Metrology" – Dr. Matthias Bernien	Minicurso: "Filmes Finos: Métodos de Deposição e Caracterização de Superfície" – Profª. Drª. Nazir Monteiro dos Santos, Prof. Dr. Conrado Ramos Moreira Afonso, Prof. Dr. Pedro A. P. Nascente e Prof. Dr. Angelo L. Gobbi	Minicurso: "Tratamento de Superfície a Plasma - Teoria" – Prof. Dr. Rodrigo S. Pessoa	Minicurso: "Tratamento de Superfície a Plasma - Prática" – Prof. Msc. Marcos Dorigão Manfrinato e Profª. Drª. Luciana Sgarbi Rossino
18:00 - 19:00	Livre		Jantar	
19:00 - 23:00				

Terça-feira – 09/08/2022

	Unesp Sorocaba/SP			Fatec Sorocaba/SP			UFSCar Sorocaba/SP
08:30 - 09:30	Minicurso: "Introdução a Ciência e Tecnologia do Vácuo" – Prof. Dr. Francisco Tadeu Degasperi e Dr. Marcelo Juni Ferreira	Minicurso: "Filmes Finos: Métodos de Deposição e Caracterização de Superfície" – Profª. Drª. Nazir Monteiro dos Santos, Prof. Dr. Conrado Ramos Moreira Afonso, Prof. Dr. Pedro A. P. Nascente e Prof. Dr. Angelo L. Gobbi	Minicurso: "Dinâmica de Gases Rarefeitos: Teoria e Aplicações do Vácuo" – Prof. Dr. Felix Sharipov	Minicurso: "Tratamento de Superfície a Plasma - Prática" - Prof. Msc. Marcos Dorigão Manfrinato e Profª. Drª. Luciana Sgarbi Rossino	Aprendizagem Ativa : "Uma Abordagem que faz Pensar" – Prof. Dr. Álvaro José Damião		Minicurso: "Interação de Íons com a Matéria: da Deposição à Modificação de Materiais" – Prof. Dr. Tiago Fiorini da Silva
09:30 - 10:00							
10:00 - 10:30	Coffee Break			Coffee Break			Coffee Break
10:30 - 12:30	Minicurso: "Introdução a Ciência e Tecnologia do Vácuo" – Prof. Dr. Francisco Tadeu Degasperi e Dr. Marcelo Juni Ferreira	Minicurso: "Filmes Finos: Métodos de Deposição e Caracterização de Superfície" – Profª. Drª. Nazir Monteiro dos Santos, Prof. Dr. Conrado Ramos Moreira Afonso, Prof. Dr. Pedro A. P. Nascente e Prof. Dr. Angelo L. Gobbi	Minicurso: "Dinâmica de Gases Rarefeitos: Teoria e Aplicações do Vácuo" – Prof. Dr. Felix Sharipov	Minicurso: "Tratamento de Superfície a Plasma - Prática" - Prof. Msc. Marcos Dorigão Manfrinato e Profª. Drª. Luciana Sgarbi Rossino	Visita ao Campus da Fatec Sorocaba	Oficina: "Mulheres na Ciência com integrantes do Projeto Mulheres em STEM2D" – Profª. Drª. Leila Ribeiro dos Santos, Ma. Lia Junqueira Pimont e Engª. Mariana Conti Tarifa	Minicurso: "Interação de Íons com a Matéria: da Deposição à Modificação de Materiais" – Prof. Dr. Tiago Fiorini da Silva
12:30 - 14:00	Almoço			Almoço			Almoço
	Parque Tecnológico de Sorocaba/SP						
14:00 - 16:00	Credenciamento e Recepção aos Participantes						
16:00 - 16:30	Abertura						
16:30 - 18:30	**Conferência: Ciência e Tecnologia do Vácuo: Um Olhar para o Futuro** Vacuum Metrology - Dr. Matthias Bernien Vacuum Calculations Methods - Dr. Roberto Kersevan Ciência e Tecnologia do Vácuo e as Atividades Desenvolvidas no Laboratório de Tecnologia do Vácuo – LTV – Dr. Francisco Tadeu Degasperi Vácuo na Indústria – Gustavo Pitaro (PIAB), João Carmo Vendramim (ISOFLAMA Processos Térmicos) e Ricieri do Amaral (Villares Metals)						
18:30 - 24:00	Coquetel de Abertura						

Quarta-feira - 10/09/2022

	Parque Tecnológico de Sorocaba/SP	
08:30 - 09:15	Palestra Magna: Plasma Applications in the Enviroment: What's New - Dr. Jacopo Profili	
09:15 - 10:00	Palestra Magna: Chemical Speciation and Structural Evolution of Rhodium and Silver Surfaces with High Oxygen Coverages - Dr. Dan Killelea	
10:00 - 10:30	Coffee Break	
10:30 - 12:35	Sessão de Apresentação de Trabalhos - Oral	
	Sessão Oral 1	Sessão Oral 2
	Chair: Elidiane Cipriano Rangel e Nazir Monteio dos Santos	**Chair: Marcos Dorigão Manfrinato e Ronaldo Camara Cozza**
10:30 - 10:50	ID: 489809	ID: 487900
10:50 - 11:05	ID: 489573	ID: 489638
11:05 - 11:20	ID: 499189	ID: 489681
11:20 - 11:35	ID: 490884	ID: 506334
11:35 - 11:50	ID: 493938	ID: 517309
11:50 - 12:05	ID: 492177	ID: 497067
12:05 - 12:20	ID: 496726	ID: 492136
12:20 - 12:35	ID: 492190	ID: 489649
12:35 - 14:00	Almoço	
13:00 - 14:00	Dinâmica destinada para mulheres com o Projeto Mulheres em STEM2D – Dra. Leila Ribeiro dos Santos, Ma. Lia Junqueira Pimont e Engª. Mariana Conti Tarifa	
14:00 - 14:45	Palestra: Mulheres na Ciência – Profª. Drª. Leila Ribeiro dos Santos, Ma. Lia Junqueira Pimont e Engª. Mariana Conti Tarifa	
14:45 - 15:30	Palestra Magna: Dinâmica dos Gases Rarefeitos: Aplicações na Tecnologia do Vácuo - Dr. Felix Sharipov	
15:30 - 16:00	Coffee Break	
16:00 – 16:45	Palestra Magna: On-Surface Synthesis of New Functional 2D Materials: From Doped Graphene to Porous Organic Frameworks - Dr. Abner de Siervo	
17:00 - 17:30	Sessão 1 de Apresentação de Trabalhos - Pôster (Link abaixo)	
17:30 - 18:00	Sessão 2 de Apresentação de Trabalhos - Pôster (Link abaixo)	
18:30 - 20:00	Livre	
20:00 - 24:00	Confraternização – Petra Bar Wanel Ville	

Quinta-feira – 11/08/2022

	Parque Tecnológico de Sorocaba/SP	
08:30 - 09:15	Palestra Magna: Trabalhando na interface entre física nuclear e de materiais - Dr. Tiago Fiorini Silva	
09:15 - 10:00	Palestra Magna: Diffusion layers integrity assessment through cyclical contact loading: contact fatigue case studies - Dr. Roberto Carlos Veja Moron	
10:00 - 10:30	Coffee Break	
10:30 - 12:30	Sessão de Apresentação de Trabalhos - Oral	
	Sessão Oral 3	Sessão Oral 4
	Chair: Silvia Pierre Irazusta e Eliana Aparecida de Rezende Duek	**Chair: Odila Florêncio e Felipe Caneiro da Silva**
10:30 - 10:50	ID: 497246	ID: 497063
10:50 - 11:05	ID: 489184	ID: 497164
11:05 - 11:20	ID: 497387	ID: 496449
11:20 - 11:35	ID: 489196	ID: 496260
11:35 - 11:50	ID: 497157	ID: 489827
11:50 - 12:05	ID: 489193	ID: 493690
12:05 - 12:20	ID: 494045	ID: 493936
12:20 - 12:35	ID: 489729	ID: 493937
12:35 - 14:00	Almoço	
14:00 - 14:45	Palestra Magna: Atuação do Inmetro na Área de Vácuo: das normas ao padrão primário – Dr. Luciano Nascimento Batista	
15:00 – 15:30	Sessão 3 de Apresentação de Trabalhos - Pôster (Link abaixo)	
15:30 – 16:00	Coffee Break	
16:00 - 18:05	Sessão de Apresentação de Trabalhos - Oral	
	Sessão Oral 5	Sessão Oral 6
	Chair: Adriana de Oliveira Delgado Silva e Diego Nespeque Corrêa	**Chair: Marcos Dorigão Manfrinato e Maíra de Lourdes Rezende**
16:00 - 16:20	ID: 490669	ID: 499231
16:20 - 16:35	ID: 517309	ID: 494139
16:35 - 16:50	ID: 489710	ID: 491778
16:50 - 17:05	ID: 497110	ID: 489500
17:05 - 17:20	ID: 496939	ID: 512160
17:20 - 17:35	ID: 487879	ID: 496943
17:35 - 17:50	ID: 489518	ID: 497230
17:50 - 18:05	ID: 489653	ID: 496800
18:10 - 19:10	Palestra Técnica – "Turbo Pump - Best Practices for Maximum Uptime." John Screech, Applications Engineer, Agilent Technologies (Vacuum Products). (Link abaixo)	

Sexta-feira – 12/08/2022

	Parque Tecnológico de Sorocaba/SP
08:30 - 09:00	Sessão 4 de Apresentação de Trabalhos - Pôster (Link abaixo)
09:00 - 09:30	Sessão 5 de Apresentação de Trabalhos - Pôster (Link abaixo)
09:30 - 10:00	Coffee Break
10:00 – 11:30	Mesa Redonda: "O Plasma sem Fronteiras: As Perspectivas para o Brasil" – Dr. Rodrigo Sávio Pessoa, Dr. Nilson Cristino da Cruz, Dr. Vladimir Jesus Trava-Airoldi, Dr. Munemasa Machida e Dr. Rogério Pinto Mota
11:30 – 12:00	Palestra Técnica - Edwards
12:00 - 13:00	Almoço
13:00 – 14:00	Assembléia
14:00 – 14:30	Encerramento

PALESTRAS CONVIDADAS

DATA	PALESTRANTE	TÍTULO
10/08 08:30 – 09:15	**Jacopo Profili**	Plasma Applications in the Environment: What's New
10/08 9:15 – 10:00	**Dan Killelea**	Chemical Speciation and Structural Evolution of Rhodium and Silver Surfaces with High Oxygen Coverages
10/08 14:00 – 14:45	**Leila Ribeiro dos Santos; Lia Junqueira Pimont e Mariana Conti Tarifa**	Mulheres na Ciência
10/08 14:45 – 15:30	**Felix Sharipov**	Dinâmica dos Gases Rarefeitos: Aplicações na Tecnologia do Vácuo
10/08 16:00 – 16:45	**Abner de Siervo**	On-Surface Synthesis of New Functional 2D Materials: From Doped Graphene to Porous Organic Framework
11/08 08:30 – 09:15	**Tiago Fiorini Silva**	Trabalhando na interface entre física nuclear e de materiais
11/08 09:15 – 10:00	**Roberto Carlos Vega Moron**	Diffusion layers integrity assessment through cyclical contact loading: contact fatigue case studies
11/08 14:00 – 14:45	**Luciano Nascimento Batista**	Atuação do Inmetro na Área de Vácuo: das normas ao padrão primário
11/08 18:10 – 19:10	**John Screech**	Turbo Pump – Best Practices for Maximum Uptime

Livro de resumos

APRESENTAÇÕES ORAIS

Quarta-feira – 10/08/2022

Apresentação - Quarta-Feira (10/08/2022)				
Sessão 1 - Oral				
Chair: Elidiane Cipriano Rangel e Nazir Monteio dos Santos				
Horário	**Área**	**Título do Trabalho**	**Apresentador**	**ID**
10:30 ás 10:50		PLASMA DEPOSITED SiOXCY-CeO2 PHOTOCATALYTIC NANOCOMPOSITE FILMS	Elidiane Cipriano Rangel	489809
10:50 ás 11:05		COMPARATIVE STUDY OF THE WEAR BEHAVIOR OF HARD COATING BY MICRO-ABRASIVE WEAR AND RUBBER WHEEL TEST	Maicon Roberto Teodoro	489573
11:05 ás 11:20		RHEOLOGICAL ANALYSIS OF FIBROIN-BASED BIOACTIVE GEL FROM SILK/PLDLA/SINVASTATIN FOR 3D PRINTING	Bianca Sabino Antunes	499189
11:20 ás 11:35		DESINFECTION OF N95 RESPIRATORS IN LOW PRESSURE PLASMA	Tania Aguiar Passeti	490884
11:35 ás 11:50		NICKEL OXIDE THIN FILMS GROWN BY HIMPS AT ROOM TEMPERATURE	Felippe Galindo	489311
11:50 ás 12:05		SYNTHESIS AND MECHANICAL CHARACTERIZATION OF GRADED TIN FILMS	Felipe Carneiro da Silva	492177
12:05 ás 12:20		EEFFECT OF MULTILAYER GRAPHENE OBTAINED BY PECVD ON ECOTOXICITY AND CELL VIABILITY	Larissa Solano de Almeida	496726
12:20 ás 12:35		PRESSURE FIELD AND ITS GRADIENT IN TUBE DEVICES IN HIGH VACUUM SYSTEMS	Regina Maria Ricotta	492190

Sessão 2 - Oral				
Chair: Marcos Dorigão Manfrinato e Ronaldo Camara Cozza				
Horário	**Área**	**Título do Trabalho**	**Apresentador**	**ID**
10:30 ás 10:50		CHARACTERIZATION OF STRONTIUM TITANATE (oo1) SURFACE BY X-RAY PHOTOELECTRON DIFFRACTION	Pedro Nascente	487900
10:50 ás 11:05		DEPOSITION OF TITANIUM THIN FILMS BY RF-MAGNETRON SPUTTERING	Antonio Carlos Santos de Arruda	489638
11:05 ás 11:20		EFFECT OF TEMPERING TEMPERATURE ON THE DEGREE OF SENSITIZATION OF AISI 420 STEEL	Guilherme Vacchi	489681
11:20 ás 11:35		EVALUATION OF DLC FILM DEPOSITION ON THE CUTTING TOOL SUBMITTED TO THE DRY DRILLING PROCESS IN THERMOSETTING POLYMER	Francisco Toti	506334
11:35 ás 11:50		CARBON NANOTUBES PRODUCED BY PECVD ARE LESS TOXIC THAN THOSE PRODUCED BY CVD METHOD	Kazys Serevincis	493938
11:50 ás 12:05		PLASMA EFFECT ON BEAN GRAIN ACTIVATION	Telma Vinhas Cardoso	497067
12:05 ás 12:20		REDUCING ZINC OXIDE DEGRADATION EFFECT ON POLY (ACID LACTIC) MATRIX BY PLASMA SURFACE TREATMENT	Teresa Tromm	492136
12:20 ás 12:35		NB2O5 FILMS PRODUCED BY PLASMA ELECTROLYTIC OXIDATION AND ANODIC DOPING USING RED MUD RESIDUE	Patrícia dos Santos Araújo	489649

Quinta-feira – 11/08/2022

Apresentação - Quinta-Feira (11/08/2022)				
Sessão 3 - Oral				
Chair: Silvia Pierre Irazusta e Eliana Aparecida de Rezende Duek				
Horário	**Área**	**Título do Trabalho**	**Apresentador**	**ID**
10:30 ás 10:50		BETA-METASTABLE TI ALLOYS WITH LOW ELASTIC MODULUS FOR BIOMEDICAL APPLICATIONS	Carlos Roberto Grandini	497246
10:50 ás 11:05		MICROSTRUCTURE AND SELECTED MECHANICAL PROPERTIES OF AGED HIGH ENTROPY ALLOYS FOR POTENTIAL USE AS AN IMPLANTABLE MATERIAL	Jhuliene Elen Torrento	489184
11:05 ás 11:20		EFFECT OF NIOBIUM ON STRUCTURE, MICROSTRUCTURE AND SELECTED MECHANICAL PROPERTIES OF Ti-25Ta-xNb SYSTEM ALLOYS FOR BIOMEDICAL APPLICATIONS	Fernanda de Freitas Quadros	497387
11:20 ás 11:35		NATURAL RUBBER MODIFIED WITH HYALURONIC ACID FOR SKIN LESION APPLICATIONS	Bruna Quevedo	489196
11:35 ás 11:50		EFFECT OF HEAT TREATMENTS ON MICROSTRUCTURE, YOUNG'S MODULUS, AND VICKERS MICROHARDNESS OF a+ß AND ß Ti-5Mo-Nb SYSTEM ALLOYS FOR BIOMEDICAL APPLICATIONS	Giovana C. Cardoso	497157
11:50 ás 12:05		POLY(L-CO-D,L LACTIC ACID-CO-TRIMETHYLENE CARBONATE) 3D PRINTED SCAFFOLD CULTIVATED WITH MESENCHYMAL STEM CELLS DIRECTED TO BONE RECONSTRUCTION	Jéssica Asami	489193
12:05 ás 12:20		ELETROCHEMICAL ANALYSIS OF ZIRCONIA COATINGS ON THE Ti-6Al-4V ALLOY PRODUCED BY PLASMA ELECTROLYTIC OXIDATION	Aline Nanuh da Silva	494045
12:20 ás 12:35		TEMPORAL EVOLUTION OF PHYSICOCHEMICAL PARAMETERS IN PLASMA ACTIVATED LIQUIDS (PAL) BY GLIDING ARC PLASMA	Benedito Donizeti Botan Neto	489729

Sessão 4 - Oral				
Chair: Odila Florêncio e Felipe Carneiro da Silva				
Horário	**Área**	**Título do Trabalho**	**Apresentador**	**ID**
10:30 ás 10:50		DEVELOPMENT OF ULTRA-HARD METAL ALLOYS	Thomaz Augusto G. Restivo	497063
10:50 ás 11:05		DEVELOPMENT OF A SOFTWARE TO DESIGN ULTRA-HARD METAL ALLOYS	Thomaz Augusto G. Restivo	497164
11:05 ás 11:20		EVALUATION OF THE SPATIAL RESOLUTION OF CAMERAS FOR REMOTE SENSING APPLICATIONS IN THE VISIBLE SPECTRUM AND NEAR INFRARED	Jean dos Santos	496449
11:20 ás 11:35		METODOLOGIA PARA A CARACTERIZAÇÃO DE SISTEMAS NVG	Charles Bruno Duarte	496260
11:35 ás 11:50		ELECTROSPUN FIBERS OF PVP AND ALOE VERA - SOLVENT INFLUENCE	Ana Neilde Rodrigues da Silva	489827
11:50 ás 12:05		IONIZATION AS A TOOL FOR ANALYTIC DETERMINATIOS IN BIOLOGICAL ORGANISMS USED AS BIOINDICATORS	Leonardo Mestre	493690
12:05 ás 12:20		INFLUENCE OF TixW INTERLAYER SINTERED BY SPUTER RF IN ADHESION OF THE DIAMON LIKE CARBON COATINGS ONTO TOOL STEEL	Williams Steve Campos	493936
12:20 ás 12:35		DECREASING COEFFICIENT OF FRICTION WITH NANOZIRCONIA PARTICLES IN DLC FILMS	Williams Steve Campos	493937

Sessão 5 - Oral				
Chair: Adriana de Oliveira Delgado Silva e Diego Nespeque Corrêa				
Horário	**Área**	**Título do Trabalho**	**Apresentador**	**ID**
16:00 ás 16:20		PROCESSING OF PEO-COATINGS DECORATED WITH TA OXIDES IN LOW CARBON STEEL SAE 1020 TARGETING BIOMEDICAL APPLICATIONS	Diego Nespeque Corrêa	490669
16:20 ás 16:35		MICRO-RAMAN SPECTROSCOPY AND SEM/EDS APPLIED TO CRATON MINERALS FROM SÃO FRANCISCO: EVIDENCE OF BIOGENETICALLY MEDIATED PYRITE FORMATION AND ITS CONNECTIONS TO THE ORIGIN OF LIFE	Daniele Carolina Fonseca da Cruz	517309
16:35 ás 16:50		TRIBOLOGICAL STUDY OF STAINLESS STEEL 420 PLASMA NITROCEMENTATE	Rogério Varavallo	489710
16:50 ás 17:05		IN VITRO EVALUATION OF EXPOSURE OF TUMORAL CELLS TO SOLUTIONS TREATED WITH COLD ATMOSPHERIC PLASMA	Diego Verduino das Neves	497110
17:05 ás 17:20		CARBON NANOTUBES FUNCIONALIZED BY PLASMA FOR USE IN CANCER PHOTOTHERMICAL THERAPY USING LIGTH-EMITTING DIODE 660NM	Kaique Gomes Hergesel	496939
17:20 ás 17:35		PROPOSED MECHANISM FOR THE FORMATION OF SiOxCyHz-TIOx NANOCOMPOSITE THIN FILMS BY PECVD USING DATA FROM IRRAS, PM-IRRAS, AND XPS	Rafael Parra Ribeiro	487879
17:35 ás 17:50		BIOASSAY USING ONION AND LETTUCE SEEDS TO EVALUETE BIOPOLYMERS RESIDUES	Giovanna Moura Silva	489518
17:50 ás 18:05		SYNTHESIS OF TANTALUM-DOPED IRON OXIDE COATINGS ON AISI 304 STEEL WITH PLASMA ELECTROLYTIC OXIDATION FOR USE WITH BIOMATERAL	João Proença	489653

Sessão 6 - Oral				
Chair: Marcos Dorigão Manfrinato e Maira de Lourdes Rezende				
Horário	**Área**	**Título do Trabalho**	**Apresentador**	**ID**
16:00 ás 16:20		VACUUM PRESSURE METROLOGY BY THE STATIC EXPANSION METHOD	Luciano Nascimento Batista	499231
16:20 ás 16:35		STUDY OF THE DOPED DLC FILM DEPOSITION WITH NITROGEN GRADIENT ON THE WEAR RESISTANCE OF THE 321H STAINLESS STEEL	Cesar Augusto Antônio Jr.	494139
16:35 ás 16:50		EFFECT OF THE NITROGEN AND SILICIUM ADDITION IN THE DLC FILM ON TRIBOLOGICAL BEHAVIOR OF TOOL STEEL AISI M2	Miguel Rubira Danelon	491778
16:50 ás 17:05		EFFECTS OF LOW-TEMPERATURE PLASMA TREATMENT ON SUGARCANE BAGASSE-BIOCHAR	Angie Paola Santacruz	489500
17:05 ás 17:20		WEAR PROPERTIES OF AISI 4340 STEEL TREATED BY NITRIDING, DLC FILM AND DUPLEX COATING	Edson Alberto Silva Filho	512160
17:20 ás 17:35		COMPARATIVE STUDY OF PLASMA AND SOLID BORIDING PROCESS OF THE TI6AL4V	Felipe Lopes Fonseca da Silva	496943
17:35 ás 17:50		STUDY OF CORROSION RESISTANCE OF AISI 4340 STEEL WITH DUPLEX TREATMENTS OF NITRIDING AND DLC FILM DEPOSITION	Lucas de Almeida Pires de Campos	497230
17:50 ás 18:05		BACTERIA ANTI-ADHERENT SURFACES PRODUCED BY DBD PLASMAS	Nilson Cruz	496800

Legenda
Superfícies, Interfaces e Filmes Finos - SIFF
Ciência e Tecnologia de Plasmas - CTP
Tratamento e Modificações de Materiais - TMM
Ciência e Tecnologia de Sensores e Dispositivos - CTSD
Ciência e Tecnologia dos Materiais - CTM
Ciência e Tecnologia de Vácuo - CTV
Biomateriais, Biofilmes e Bioprocessos: Ciência e Tecnologia - BBBCT
Nanociência, Nanotecnologia e Nanomateriais - NNN

APRESENTAÇÕES DE PÔSTERES

Quarta-feira – 10/08

Sessão 1 - Pôster - 17:00 ás 17:30				
TV	Área	Título do Trabalho	Apresentador	ID
1		INFLUENCE OF THE ABRASIVE WEAR MODES ON THE FRICTION COEFFICIENT OF THIN FILMS	Ronaldo Câmara Cozza	489592
2		DEPOSITION OF SIO2 THIN FILMS USING TRIS(DIMETHYLAMINO) SILANE BY PLASMA ENHANCED ATOMIC LAYER DEPOSITION	Daniele Spigarollo	488582
3		OXIDE FILMS DEPOSITED ON ALUMINUM ACETYLACETONATE PLASMA	Adriano Luiz da Silva Souza	488694
4		TI-NB-ZR ALLOY COATINGS SPUTTER-DEPOSITED ON AISI 316L STAINLESS STEEL	Sidney Cherman	496805
5		OPTICAL SENSORS: TERRESTRIAL DATA COLLECTION	Micaela Almeida Silva	494029
6		SYNTHESIS OF CU/NI-DOPED TITANIUM OXIDE CERAMIC COATINGS BY PEO PROCESS AND THEIR PHOTOCATALYTIC PERFORMANCE	Uanderson Garcia	494081
7		DEVELOPMENT OF TI-(10-X)AL-XV (X=0,2, AND 4% WT%) ALLOYS FOR USE SINGLE-AXIS KNEE PROSTHESES	Diego Rafael Nespeque Correa	484806
8		MECHANICAL PROPERTIES OF BULK METALLIC GLASSES BASED IN ZIRCONIUM ALLOYS	Cícero Lustosa	493961
9		DEVELOPMENT OF A HYBRID JOINT BETWEEN THE AA2024-T3 TREATED BY PLASMA ELECTROLYTIC OXIDATION (PEO) WITH PEI/GLASS FIBER LAMINATE	Rogério P. Mota	489766

Sessão 2 - Pôster - 17:30 ás 18:00				
TV	Área	Título do Trabalho	Apresentador	ID
1		EFEITO DE TRATAMENTOS TÉRMICOS EM LIGAS Ti-10Mo-xMn (x = 0, 2, 4, 6 e 8 %p) PARA APLICAÇÕES BIOMÉDICAS	Mariana Luna Louenço	497566
2		POLYMER FILM DEPOSITION ON METALLIC SURFACES THROUGH ELECTROPOLYMERIZATION ACTIVATED BY PULSED VOLTAGE BIAS	Amanda Valcanaia	494046
3		CO2 SENSORS AND MINIBIOREACTORS APPLIED ON RESEARCH AND TEACHING	Maria Lúcia P. Silva	490357
4		EFFECT OF PLASMA-ENHANCED CHEMICAL VAPOR DEPOSITION ON LYSOZYME AND ITS ANTIMICROBIAL PROPERTIES	Luis Fernando Bandeira Miranda	496332
5		CLASSIFICATION OF IMAGES REMOTE THERMAL SENSING	Micaela Almeida Silva	489751
6		AVALIAÇÃO DA TRIBOLOGIA DE FILMES DE TIN DOPADOS COM COBRE DEPOSITADOS PELA TÉCNICA MAGNETRON SPUTTERING	Felipe M. do Amaral Pereira	497175
7		UV-VIS SPECTROSCOPY AS A TOOL FOR DETECTION OF LONG-LIVED REACTIVE SPECIES IN PLASMA-ACTIVATED LIQUIDS	Luan Gonçalves de Lima	489331
8		VEGETABLE IVORY MICROPARTICLES COATED BY PLASMA JET ACTIVATION OF SILICONE OIL AND MULATEIRO EXTRACT	Yuri Ferreira da Silva	517268
9		STUDY OF THE EFFECT OF TEMPERING TEMPERATURE AND CARBON ADDITION EFFECT ON THE PROPERTIES OF THE SAE 8640 STEEL SUBMITTED TO PLASMA NITRIDING	Luciana Sgarbi Rossino	489507

Quinta-feira – 11/08

Sessão 3 - Pôster - 15:00 ás 15:30				
TV	Área	Título do Trabalho	Apresentador	ID
1		SURFACE TREATMENT OF POLYPROPYLENE USING A CONICAL APPJ-LIKE	Bruno Henrique da Silva Leal	488701
2		COMPARATIVE ANALYSIS BETWEEN PLASMA DEPOSITION TO FORM TIN FILMS IN NICR ALLOY FOR DENTAL APPLICATION	Larissa Solano de Almeida	489686
3		DEVELOPMENT OF PLASMA BORIDING USING SOLID PASTE ON 304 STAINLESS STEEL	Otávio Augusto	489185
4		CONTACT FATIGUE ASSESSMENT OF NITRIDED AISI 321 STEEL	Marcos Dorigão Manfrinato	489716
5		THE CORROSION BEHAVIOR OF A COMMON CARBON STEEL (SAE 1030) IN DIFFERENT CORROSIVE MEDIA	Paulo Bálsamo	497178
6		DETERMINATION OF ELECTRICAL PROPERTIES OF THIN FILMS BY UV-VIS SPECTROSCOPY	Diego Albuquerque	490995
7		ABRASIVE WEAR IN WHITE CAST IRON HIGH CHROMIUM	Odila Florêncio	493967
8		Ag-DOPED NANOCELULOSE FILMS FROM SPUTTERING OF AgNO3 POWDER IN ARGON PLASMAS	Adriana Delgado	490942
9		EFFECTS OF FREQUENCY AND POLARIZATION ON MAGNESIUM CORROSION TREATED BY PLASMA ELECTROLYCTIC OXIDATION	Thaís Matiello Gonçalves	489709

Sexta-feira – 12/08

Sessão 4 - Pôster - 8:30 ás 9:00				
TV	Área	Título do Trabalho	Apresentador	ID
1		INFLUENCE OF PH ON THE EFFICIENCY OF GRAPHENE DEPOSITION IN POLYESTER TEXTILES USING PULSED ELECTRICAL DISCHARGE IN AQUEOUS MEDIUM	Verônica Pazda	493943
2		ROLE OF MOLECULAR SPECIES IN COLD ATMOSPHERIC ARGON PLASMA: A GLOBAL MODEL STUDY	Júlia Karnopp	489696
3		GENERATION OF IRON OXIDES LAYERS IN ELECTRIC STEELS THROUGH PULSED BIPOLAR PLASMA	Paula Fin	489505
4		IMPROVED WETABILITY OF POLYDIMETHSILOXANE (PDMS) SAMPLE THROUGH PLASMA JET AT ATMOSPHERIC PRESSURE	Ananias Alves Barbosa	489704
5		THE TARGET DISTANCE INFLUENCE ON THE POWER OF A TRANSFERRED COLD ATMOSPHERIC PRESSURE PLASMA JET	Kleber Petroski	489748
6		UV-VIS SPECTROSCOPY AND MULTIPARAMETER METER TO STUDY THE PLASMA ACTIVATED DEIONIZED WATER CONSERVATION AT A LOW TEMPERATURE	Michaela Shiotani	489338
7		EFFECTS OF LOW TEMPERATURE ATMOSPHERIC PRESSURE PLASMA ON BONE LOSS OF INDUCED PERIODONTAL DISEASE IN RATS	Marina Tiburcio Bento	494035
8		OPTICAL CHARACTERIZATION OF APPJs PRODUCED INSIDE A TUBE FROM MASSIVEOES AUTOMATION USING DIFFERENT SETTINGS	Ana Carla de Paula Leite	492195
9		DEVELOPMENT OF SHAPE MEMORY ALLOY SOLUTIONS FOR SCRAMJET MOTORS IN HYPERSONIC VEHICLES: NUMERICAL AND EXPERIMENTAL VALIDATION	Alana Aíres	496107
10		CHARACTERIZATION OF RETAINED AUSTENITE BY X-RAY DIFFRACTION IN A Z-TUFF PM TOOL STEEL	Larissa Meincke Eickhoff	497219

Sessão 5 - Pôster - 09:00 ás 9:30				
TV	Área	Título do Trabalho	Apresentador	ID
1		EFFECT OF CARBON NANOTUBE DEPOSITION THROUGH PULSED ELECTRICAL CURRENT IN WATER/CNT SOLUTION ON ELECTRICAL CONDUCTIVITY OF THE JUTE FIBRES	Kelvin Masakazu	497241
2		ANALYSIS OF TRIBOLOGICAL PROPERTIES OF ANODIZED 6061 ALUMINIUM ALLOY	Andreia Larissa	489717
3		ARTIFACTS IN XPS ANALYSIS DUE TO INCORRECT SAMPLE HANDLING	Teresa Tromm Steffen	488538
4		STABILITY OF Gd/GdN MULTILAYERS DEPOSITED BY DC GRID-ASSISTED MAGNETRON SPUTTERING SYSTEM	Francisco Alfaro	493986
5		ZINC-NITRIDING TROUGH PLASMA: A SIMULTANEOUS ZN FILM DEPOSITION AND NITRIDING PROCESS	Amanda Valcanaia	493933
6		CARBON FIBERS FUNCTIONALIZATION THROUGH ACTIVE SCREEN PLASMA FOR POLYANILINE GRAFTING PURPOSE	André Felipe Deziderio	493883
7		EFFECT OF SAMPLE SHAPE ON PLASMA TREATMENT BY A CONICAL SHAPED APPJ	Thayna Fernandes	502342
8		APPLICATION OF FUNNEL-SHAPED COLD PLASMA JETS FOR PIGMENTATION ENHANCEMENT OF COMMERCIAL TEXTILES	Bruno Henrique da Silva Leal	489587
9		CONVOLUTIONAL NEURAL NETWORK ASSESSMENT FOR PERSON DETECTION ON WATER USING INFRARED IMAGERY	Rafael Marinho de Andrade	503091
10		AGEING EFFECTS ON PLASMA POLYMERS FROM ETHYLENEDIAMINE/C2H2 AND 2-METHYL-2-OXAZOLINE FOR BIOMEDICAL APPLICATIONS	Pedro William P. Moreira	489553

Legenda
Superfícies, Interfaces e Filmes Finos - SIFF
Ciência e Tecnologia de Plasmas - CTP
Tratamento e Modificações de Materiais - TMM
Ciência e Tecnologia de Sensores e Dispositivos - CTSD
Ciência e Tecnologia dos Materiais - CTM
Ciência e Tecnologia de Vácuo - CTV
Biomateriais, Biofilmes e Bioprocessos: Ciência e Tecnologia - BBBCT
Nanociência, Nanotecnologia e Nanomateriais - NNN

ORGANIZAÇÃO

Comitê Organizador

Luciana Sgarbi Rossino (Presidente)
Adriana de Oliveira Delgado Silva
Alessandro Augusto Jordão
Diego Aparecido Carvalho Albuquerque
Diego Rafael Nespeque Correa
Elaine Conceição de Oliveira
Eliana Aparecida de Rezende Duek
Elidiane Cipriano Rangel
Francisco Tadeu Degasperi
José Martins de Oliveira Junior
Marcos Dorigão Manfrinato
Nazir Monteiro dos Santos
Odila Florêncio
Silvia Pierre Irazusta

Comitê Científico

Adriana de Oliveira Delgado Silva | UFSCar Sorocaba
Álvaro Damião - IEAv
Antonio Renato Bigansolli | UFRRJ
Carlos Roberto Grandini | UNESP Bauru
Felipe Carneiro da Silva | Fatec-Cotia
Konstantin G. Kostov | UNESP Guaratinguetá
Luciana Sgarbi Rosisno | Fatec-Sorocaba
Marcos Dorigão Manfrinato | Fatec-Sorocaba
Pedro Nascente | UFSCar – São Carlos
Ronaldo Câmara Cozza | Fatec-Mauá
Silvia Pierre Irazusta | Fatec-Sorocaba
Steven Frederick Durrant | UNESP Sorocaba

Comitê Acadêmico

Cesar Augusto Antônio Junior | UFSCar - Sorocaba
Giovanna Gonçalves do Nascimento | Fatec - Sorocaba
Kaique Gomes Hergesel | Fatec - Sorocaba
Kazys Serenvivices | Fatec - Sorocaba
Larissa Solano de Almeida | UFSCar - Sorocaba
Miguel Rubira Danelon | UFSCar - Sorocaba
Felipe Lopes Fonseca da Silva | UFSCar - Sorocaba
Kauan Victor de Lima Ribeiro | UNIP - Sorocaba
Rafael Parra Ribeiro | UNESP - Sorocaba
Rian de Oliveira Rodrigues | UNIP - Sorocaba

Diretoria da Sociedade Brasileira de Vácuo

Presidente: Nazir Monteiro dos Santos
1º Vice Presidente: Luis Cesar Fontana
2º Vice Presidente: Antonio Renato Bigansolli
1º Diretor Secretário: Carlos Roberto Grandini
2º Diretor Secretário: Luciana Sgarbi Rossino
1º Diretor Tesoureiro: Rogério Pinto Mota
2º Diretor Tesoureiro: Maria Lucia Pereira da Silva
Diretor Científico: Júlio César Sagas
Diretor Cultural: Álvaro José Damião

PATROCINADORES

APOIO

REALIZAÇÃO

DETERMINATION OF ELECTRICAL PROPERTIES OF THIN FILMS BY UV-VIS SPECTROSCOPY

Albuquerque, D. A. C.[1]*, Chaves, M.[1]
[1]*University of Sorocaba*

1. Introduction

Thin films of titanium oxide were deposited using the reactive RF sputtering technique, with different oxygen flows. This study is given as numerous applications of titanium oxide films, as in photovoltaic cell applications [1] and as layers in the battery structure [2]. The optical characterization of the films was performed using the UV-Vis spectrophotometry technique. The use of the technique allows obtaining information on electrical properties of semiconductor materials, such as energy gap, which was obtained by different models.

2. Experimental

Samples with different deposition times and different oxygen flows were deposited. For all samples, the radio frequency used was 13.56 MHz and the Bias was -1000 V. The material used as target was metallic titanium and oxygen was introduced into the chamber, causing the reactive process and the formation of TiO_x. The pressure in the chamber before the inlet of the gases was maintained at 2.10^{-6} mbar. The total deposition pressure was 7.10^{-3} mbar. The optical UV-Visible measurements provided spectra of transmittance as a function of wavelength for samples in the wavelength range from 200 nm to 2500 nm. Different models were used to determine the gap band energy for the samples.

3. Results and Discussions

The characterization of films provided the transmission spectrum as a function of wavelength. Oxygen flow and deposition time were variable parameters during the deposition process. The energy gap was obtained using three different models. The Tauc model [3], E03 model and E04 model [4]. Regarding the transmission, it should be noted that the films presented average transmittance in the visible region above 70%. Fig. 1 presents the transmission spectrum of samples, while Fig. 2 presents an application of the E04 model to obtain the value of the gap energy. The results indicate the possibility of obtaining transparent thin films in the visible region and with semiconductor characteristics due to the gap energy obtained. Even with an oscillation in the stoichiometry obtained from the films and with a variation in the roughness, all the deposited films present average transparency above 70% and, regardless of the gap model used, all the films present an energy gap of 3.0 to 3.5 eV.

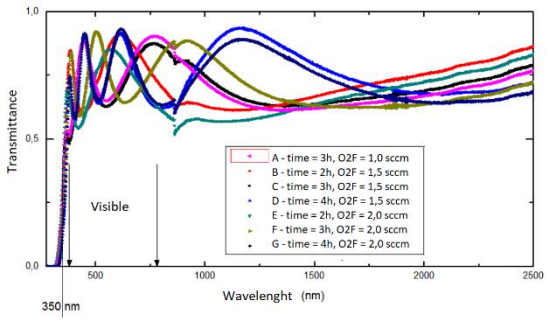

Fig. 1. *Transmittance spectrum for samples analyzed.*

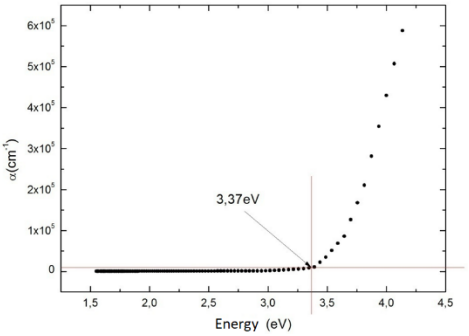

Fig. 2. *Energy gap determination using the E04 model.*

4. References

[1] A. A. Feitosa, et. al. Revista Interdisciplinar da Universidade Federal do Tocantins, **5**, 60-65 (2018).
[2] E. M. F. Vieira, et al. J. Electron. Mater. **45**, 910–916 (2016).
[3] J Tauc, R. Grigorovici, A Vancu. Physica Status Solidi B, **15**, 627-637, (1965).
[4] S. R. P, SILVA, Amorphous carbon thin films. In: NALWA, H. S. *Handbook of thin film materials*. Academic Press, San Diego v. 4, cap. 9, p. 403–505 (2002).

Acknowledgments
The authors thank LEFEO and the Surface Physics Laboratory at UNICAMP.

*Corresponding author: diego.albuquerque@prof.uniso.br

STABILITY OF Gd/GdN MULTILAYERS DEPOSITED BY DC GRID-ASSISTED MAGNETRON SPUTTERING SYSTEM

Alfaro, F.[1, 2]*, Sagás, J. C.[1], Fontana, L. C.[1].
[1]*Laboratório de Plasmas, Filmes e Superfícies, Universidade do Estado de Santa Catarina, Joinville, SC, Brazil*
[2]*Faculdade SENAI de Santa Catarina, Jaraguá do Sul, SC, Brazil*

1. Introduction

Gadolinium nitride (GdN) is one of the few promising intrinsic ferromagnetic semiconductors for spintronics applications [1-2], as well as the magnetic properties of Gd-based multilayered films and nanostructures [3], and possible applications include magnetic recording and nano-refrigeration. The current study describes the deposition of several multilayers of Gd/GdN using DC grid-assisted magnetron sputtering, as well as the structural and chemical stability of these samples.

2. Experimental

In addition to a pure Gd film, eight samples with different multilayer structures of Gd/GdN were deposited. They were grown on Si (100) with constant current (0.40 A), cathode power (~130 W), working gas pressure (~0.40 Pa), and without external heating. Ar and N_2 mass flow rates were set at 2.6 sccm and 1.3 sccm, respectively. The total film thickness is around 200 nm. The samples were analyzed by X-ray diffraction (XRD), X-ray photoelectron spectroscopy (XPS) using depth profile mode, and a scanning electron microscope (SEM).

3. Results and Discussions

The XPS analysis revealed a periodicity in the atomic concentration of nitrogen in agreement with the planned thicknesses. In Fig. 1, a maximum atomic concentration of 45% of nitrogen can be seen in films with a thickness of 20 nm of GdN, and 20% is perceived at a 10 nm GdN layer thickness in Fig. 2. The process used in the deposition of thin films on Si substrates in the grid-assisted magnetron sputtering configuration makes it possible to obtain multilayer films of Gd and GdN for conditions in which N_2 is allowed to enter the chamber for longer than 19 seconds. Two of the eight varied multilayer arrangements oxidized to the point of affecting the surface's look and topography. When GdN is exposed to oxygen, it becomes structurally and thermodynamically unstable. The 40 nm Gd cap protected the thinner inner layers of GdN in six of the eight multilayer samples from oxidation.

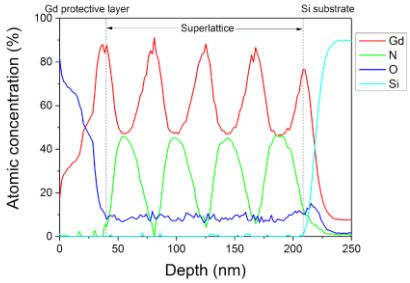

Fig. 1. *Atomic concentration of Gd, N, and O as a function of the depth of the sample layers with a thickness of 20 nm of GdN.*

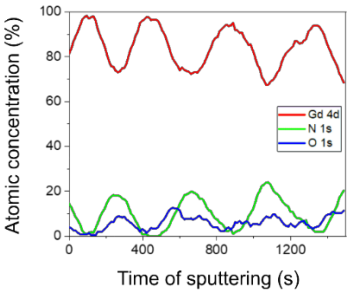

Fig. 2. *Atomic concentration of Gd, N, and O as a function of the sputtering time of the sample layers with a thickness of 10 nm of GdN.*

4. References

[1] A.V. Svalov, S.V. Andreev, A. Larrañaga, I. Orue, G.V. Kurlyandskaya. J. Magn. Magn. Mater., **490**, 165529, (2019).
[2] Maity, H. J. Trodahl, S. Granville, S. Vézian, F. Natali, and B. J. Ruck, J. Appl. Phys. **128**, 213901, (2020).
[3] I.S. Zhidkov, A.I. Kukharenko, N.O. Antropov, E.A. Kravtsov, M.V. Makarova, S.O. Cholakh, E.Z. Kurmaev, Thin Solid Films, **709**, 138251, (2020).

Acknowledgments

The authors thank PAP-FAPESC. This project was funded by the National Council for Scientific and Technological Development (UNIVERSAL/CNPq 455896/2014-3).

*Corresponding author: alfaro.professor@gmail.com

ANALYSIS OF TRIBOLOGICAL PROPERTIES OF ANODIZED 6061 ALUMINIUM ALLOY

Almeida, A. L. A de[1]*, Mello, C. B.[1], Savonov, G. da S.[1] Manfroi, L. A.[1], Miranda, E. L de[1]
[1] *Instituto Nacional de Pesquisas Espaciais*

1. Introduction

The AA6061 aluminum alloy is widely used in the aeronautical and aerospace sectors mainly due to its low density, but its low wear resistance limits its application in some components that require frictional contact [1]. One solution is to form a bed of aluminum oxide on the surface of the alloy, as this oxide has good wear resistance. This oxide can be formed from the anodizing process, in which aluminum is placed in an electrolytic bath and a potential difference is applied. The metal to be treated will be the anode. This reaction causes a controlled oxidation of the metal surface creating a protective oxide layer [2].

2. Experimental

To obtain the samples of AA6061, plates measuring approximately 220x2x19 mm were cut. Before anodizing, the plates underwent a physical and chemical cleaning process. To obtain the aluminum oxide coating, the alloy was anodized in an electrolytic solution of sulfuric acid at a concentration of 120 g/L, varying the time from 40 to 60 min and the current density from 1.2 to 2 A/dm^2. After that, the plate was cut into smaller samples for the analysis of roughness, friction wear resistance (tribometer) surface composition (EDS) and morphology (SEM).

3. Results and Discussions

The sample that was anodized for 60 min showed a greater number of cracks than the 50 min and 40 min samples. Anodizing performed with current density of 2 A/dm2 showed an oxide layer of approximately 20 µm, which is thicker compared to current density of 1.2 and 1.5 A/dm2. The figure 1 and figure 2 presents the SEM image of the sample anodized for 40 min and with a current density of 2 A/dm^2. Results about the roughness and friction wear resistance are under way and will be shown in the conference.

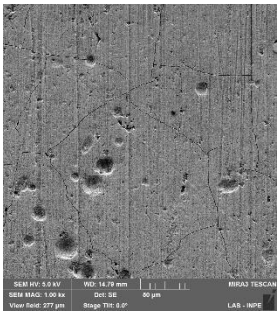

Fig. 1. *SEM top image of the sample anodized*

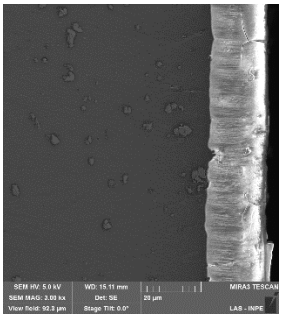

Fig. 2. *SEM cross-sectional image of the sample anodized*

4. References

[1] Mohitfar, S. H., et al. Journal of Alloys and Compounds, **842**, 155988, (2020).
[2] Grubbs, C. A. Anodizing of aluminum. Metal Finishing, **98**, 480– 496 (2000).

Acknowledgments
This research was support by CAPES, with the help of Laboratório de Tratamentos de Superfície (INPE) and Instituto de Pesquisa e Desenvolvimento (UNIVAP).

*Corresponding author: andreia.almeida@inpe.br

EFFECT OF MULTILAYER GRAPHENE OBTAINED BY PECVD ON ECOTOXICITY AND CELL VIABILITY

Almeida, L. S. de[1*], Serenvices, K.[2], Hergesel, K. G.[2], Nascimento, G. G.[2], Irazusta, S. P.[2], Oliveira, E. C. de[2], Manfrinato, M. D.[1,2], Rossino, L. S.[1,2]

[1] *Universidade Federal de São Carlos, PPGCM, UFSCar Campus Sorocaba, Sorocaba-SP*

[2] *Faculdade de Tecnologia do Estado de São Paulo (Fatec Sorocaba), CEETEPS, Sorocaba-SP*

1. Introduction

Graphene is a carbon nanostructure that has electrical, thermal, and mechanical properties, attractive for different applications. For this reason, the use of graphene has been growing in several areas of activity. On the other hand, graphene and carbon nanostructures discarded in the environment can interact with biological systems and generate toxicological effects. Thus, it is important to study the ecotoxicity and the toxicity cell of these carbon nanostructures [1]. The objective of this work is to study the ecotoxicity and cellular viability of multilayer graphene obtained by the Plasma Enhanced Chemical Vapor Deposition (PECVD) technique.

2. Experimental

For the plasma ablation process, nickel (Ni) was used as a substrate subjected to a mixture of argon (Ar - 80%) and hydrogen (H_2 - 20%) gases at a working pressure of 2.00 torr, with 350 V, and for 1 h. The precursor gases of methane (CH_4), H_2, and Ar in total gas pressure at 1.50 torr, with 700 V for 15 minutes, were used to synthesize graphene. The characterization of graphene was obtained by Raman spectrometry and contact angle. The aquatic toxicity test used algae of the species *Raphidocilis subcapitata*, at concentrations of 0.1 to 100 mg/L. The effect of cytotoxicity was evaluated by cell viability by MTT (L929 and B16F10).

3. Results and Discussions

The obtained material showed a Raman spectrum with D, G, and 2D bands, characteristic of defective multilayer graphene, as shown in Fig.1. In Fig. 2 (a), it is possible to observe the cell viability results. We can see that multilayer graphene does not affect the viability of non-tumor cells (murine fibroblast-L929). However, the opposite happens when we analyze the B16F10 tumor line, in which cell viability is affected when graphene is internalized. Figure 2 (b) shows the inhibition rate of algae at different concentrations of graphene, obtaining an EC_{50} of 9.316 mg/L, indicating that at concentrations below 10 mg/L, graphene has a negative effect on the death of the algae. The results show good prospects for the application of multilayer graphene obtained by plasma in biomedical and biological areas.

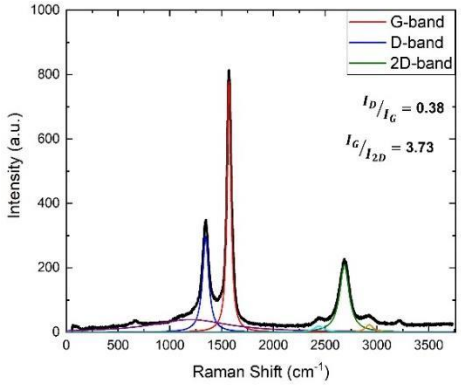

Fig. 1. *Defective multi-layer graphene Raman spectrum*

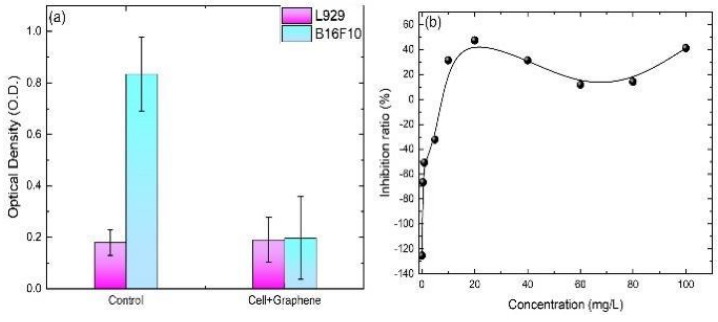

Fig. 2. *(a) Optical density for the control and cell + graphene with the L929 and B16F10 cells, (b) Inhibition ratio of algae at concentrations from 0.1 to 100mg/L.*

4. References

[1] J. Zhao, X. Cao, Z. Wang, Y. Dai, B. Xing. Water Res. **111**, 18-27, (2017).

Acknowledgments

The authors acknowledge FATEC-SO, UNICAMP, USP, and CAPES (001) for the financial support.

*Corresponding author: solano.larissa@gmail.com

OPTICAL CHARACTERIZATION OF APPJs PRODUCED INSIDE A TUBE FROM MASSIVEOES AUTOMATION USING DIFFERENT SETTINGS

Almeida, A. C. de P. L.[1]*, Barbosa, A. A.[1], Nascimento, F. do[1], Kostov, K. G.[1]
Faculty of Engieering – Campus of Guaratinguetá - FEG/Unesp

1. Introduction

Recent studies have shown that atmospheric pressure plasma jets (APPJs) are capable of generating cold plasma plumes in open space. They have a very reactive chemistry and ability to treat objects, making them suitable for many applications, including biomedicine. MassiveOES automation was used to obtain the rotational and vibrational temperatures of the excited species generated through the APPJs. In this work, we present Trot results obtained from N_2 molecules and the optical characterization of plasma jets applied inside a PDMS tube with different configurations.

2. Experimental

In this study, dimethylpolysiloxane (PDMS) was inserted into a polyvinyl chloride (PVC) tube, where an APPJ had the purpose of carrying out its treatment. The plasma jets were produced inside a silicone tube and at the end of a long and flexible plastic tube, with the last one connected to a dielectric barrier discharge (DBD) reactor. The DBD reactor is a cylindrical pin-electrode type, to which high voltage pulses were applied (Fig.1). We employed different configurations for the long tube by changing the number of holes from which the APPJ were extracted to be applied into the PDMS. Helium was used as the working gas, and a flow rate of 2.0 l/min was employed in all the experiments. Spectroscopic measurements were performed using a spectrometer from Avantes (model AvaSpec-ULS-RS-TEC), with spectral resolution of (0.784) nm. The temperatures resulting were estimated through the automation of the MassiveOES. For this purpose, it was used spectroscopic emissions from the N_2 molecular bands in the wavelength range from 360 to 382 nm.

3. Results and Discussions

Reactive oxygen and nitrogen species (RONS) generated from the interaction of APPJ with the external environment were verified and a high emission of molecular nitrogen (N_2) and hydroxyl molecules (OH) were observed (Fig.2). The results indicate that the use of He gas presents low rotational temperature and high vibrational temperature, favoring chemical reactions.

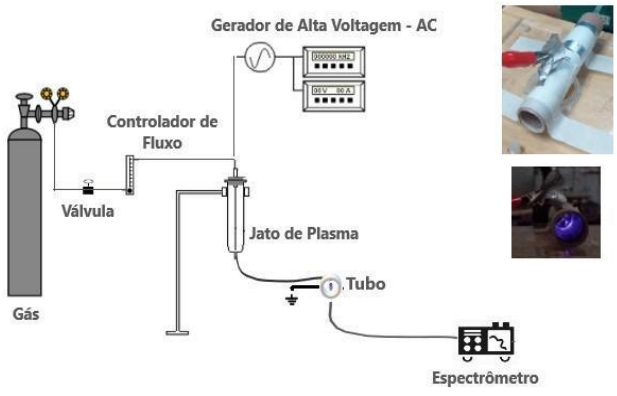

Fig. 1. *Schematic diagram of the experiment.*

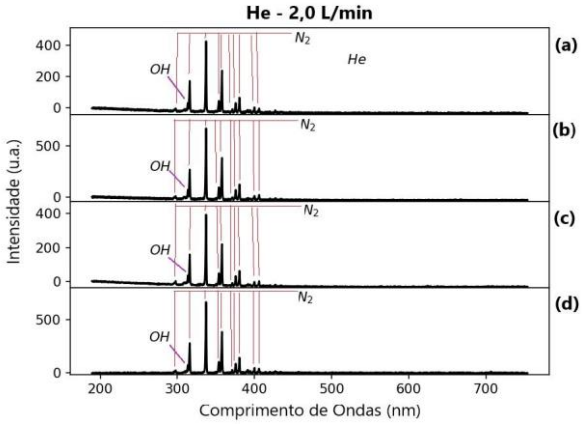

Fig. 2. *APPJ spectrum in end: (a) of the 2-hole tube. (b) the 3-hole tube, (c) the 4-hole tube and (d) the 6-hole tube.*

4. References

[1] X. Lu, G. V. Naidis, M. Laroussi et al, Phys. Rep., **630**, 1–84, (2016).

Acknowledgments:
This work was supported by CAPES - 88887.508483/2020-00 and FAPESP – 2019/05856-7.

*Corresponding author: ana.c.almeida@unesp.br

PLASMA DEPOSITED SiO_XC_Y-CeO_2 PHOTOCATALYTIC NANOCOMPOSITE FILMS

Antônio Junior, C. A.[1], Neves Filho, N. A.[2], Ribeiro, R. P.[2], Almeida, L. S. de[3], Cruz, N. C.[2], Rossino, L. S.[1], Rangel, E. C.[2]*

[1]*Sorocaba Technology College (FATEC), 2015 Engenheiro Carlos Reinaldo Mendes Av., Sorocaba, SP, Brazil*
[2]*Science and Technology Institute of Sorocaba (ICTS), São Paulo State University (UNESP), 511 Três de Março Av., Sorocaba, 18087-180, SP, Brazil*
[3]*Federal University of São Carlos (UFSCAR), Sorocaba Campus, Rod. João Leme dos Santos, km 110, 18052-780 Sorocaba, SP, Brazil*

1. Introduction

Photocatalytic nanocomposites represent a current alternative for the degradation of pollutants, inactivation of biofilms and for creation of photogenerated barriers against corrosion [1], but a simplified, economically viable and ecologically correct methodology for preparing it, is still a matter of future advances. In this context, it was evaluated the possibility of incorporating CeO_2 particles in Si-based films by means of a single step, low-pressure plasma deposition methodology.

2. Experimental

A plasma methodology that associates the deposition of films by PECVD, in atmospheres containing hexamethyldisiloxane (HMDSO) vapor, and the sputtering and/or sublimation of the cerium acetylacetonate compound, $Ce(acac)_3$, was employed. Substrates were placed on the lower electrode of a capacitively coupled plasma reactor, around 0.8 g of $Ce(acac)_3$. The plasma was established by applying pulsed direct voltage (400 W, 20 kHz) to the lower electrode in an atmosphere composed of 25 Pa of HMDSO, 41 Pa of Ar and 54 Pa of O_2, with a total working pressure of 138 Pa. The films' properties were evaluated as a function of the process time (t), that was changed between 2 to 23 min.

3. Results and Discussions

The increase in temperature with the process time produces sublimation of $Ce(acac)_3$ and pressure growth. The layer thickness tends to increase with t, producing a film that can be classified as a silicon oxycarbide with inclusions of Ce (Fig. 1 left). Samples' surface microstructure (Fig. 2) evidence a composite in which particulate material is dispersed in a uniform matrix. Particulates' dimensions and concentrations depend on t. All samples demonstrate photocatalytic effect (Fig. 1 right), the best result being obtained for the one prepared with 2 min, in which 30% of the dye was degraded after 15 min of irradiation and 100% after 60 min.

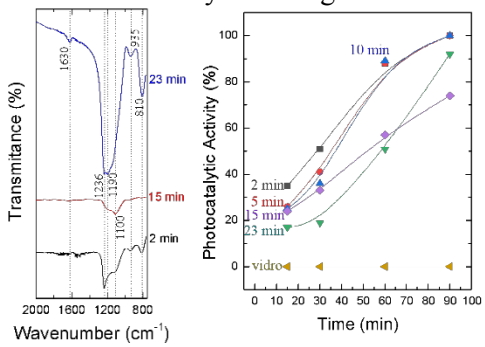

Fig. 1. *(left) PM-IRRAS spectra of the samples. (Right) Photocatalytic activity of the samples in the degradation of methylene blue as a function of UV irradiation time.*

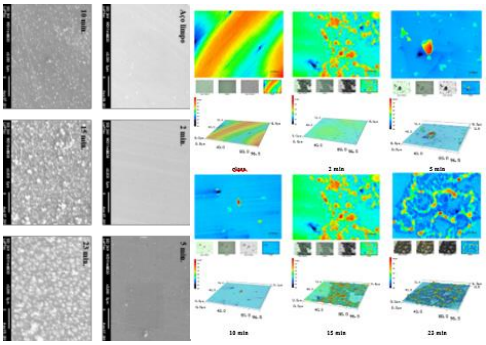

Fig. 2. *(Left) SEM and (right) Confocal images of the samples*

4. References

[1] M. Ramaprakash, G. Sreedhar, S. Mohan and S.K. Panda, Trans. IMF., **94**, 254–258, (2016).

Acknowledgments

Authors thank to MNF laboratory of LNNano/CNPEM, FAPESP (2017/21034-1), CNPq (48437/2018 and 47114/2018) and CAPES (1766917).

*Corresponding author: elidiane.rangel@unesp.br

STUDY OF THE DOPED DLC FILM DEPOSITION WITH NITROGEN GRADIENT ON THE WEAR RESISTANCE OF THE 321H STAINLESS STEEL

Antônio Junior, C. A.[1]*, Manfrinato, M. D.[2], Rossino, L. S.[1,2]
[1] *Universidade Federal de São Carlos, PPGCM, UFSCar Campus Sorocaba, Sorocaba-SP*
[2] *Faculdade de Tecnologia do Estado de São Paulo (Fatec Sorocaba), CEETEPS, Sorocaba-SP*

1. Introduction

The hydrogenated amorphous carbon (a-C:H) has excellent properties influenced by the balance of the sp^3 and sp^2 bonds that composes this film, but it presents low adhesion to metallic surfaces, due to high compressive stress, in contrast to the low density of chemical bonds at the interface of the films. The adhesion of a-C:H on the metal alloys is influenced by the affinity of the chemical interaction that exists at the interfaces [1,2]. The objective of this work is to study the effects of gradient deposition of the nitrogen-doped DLC film, obtain adherent films, and maintain the wear resistance in the material.

2. Experimental

The polished and clean 321H stainless steel was placed in the sealed reactor, and the plasma treatments were carried out by PECVD with a DC-Pulsed source. Plasma ablation cleaning was performed using 80% Ar and 20%H at 60 minutes and 285 V, followed by the interlayer deposition using 70%HMDSO and 30% Ar at 15 minutes and 500 V. After, the DLC film was deposited using 90%CH_4 and 10% Ar, while the nitrogen doped DLC film (DLC(N)) was carried out using 70%CH_4 and 30%N_2. The DLC film (DLC Grad) deposited by nitrogen gradient was carried out by decreasing the percentage of nitrogen in the DLC(N) film until a DLC film is formed. Raman spectroscopy, adhesion test, and micro-abrasive wear test by fixed ball were performed to characterize the formed films.

3. Results and Discussions

The Raman spectra (Figure 1) demonstrate the formation of the DLC film by the presence of the G and D bands. The increase in the intensity of the D band for the DLC(N) film is due to the presence of a nitrogen bond, increasing the reason for a relationship I(D)/I(G) due to aromatic rings. The atomic percentage of hydrogen is about 35-36%, characteristic of the hard a-C:H film [2]. It is observed, in Figure 2, that the films improved the surface resistance of the substrate. The DLC Grad showed lower wear volume compared to the DLC and DLC(N) film, along with better adhesion of this film to the substrate, indicating that the nitrogen gradient deposition of the DLC film improved the adhesion of the DLC film to the substrate influencing positively its wear resistance.

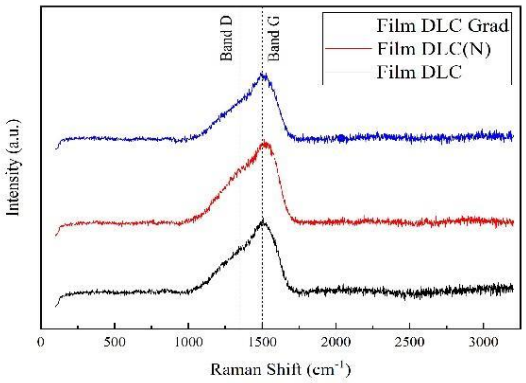

Fig. 1. *Raman spectra analysis of coatings.*

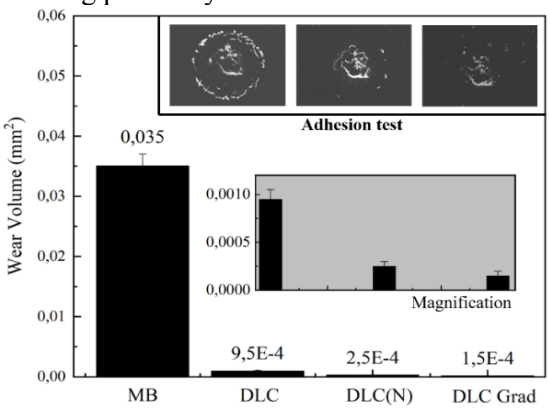

Fig. 2. *Wear Volume of coating and adhesion test.*

4. References

[1] D. Batory**.** Thin Solid Films*,* ***590****,* 299-305, (2015).
[2] J. Robertson. Materials Science and Engineering, **R 37**, 129-281, (2002).

Acknowledgments
The author thanks CAPES (nº 797983) and FATEC-SO for provide the laboratory.

*Corresponding author: cesar.augustoantoniojr@hotmail.com

RHEOLOGICAL ANALYSIS OF FIBROIN-BASED BIOACTIVE GEL FROM SILK/PLDLA/SINVASTATIN FOR 3D PRINTING

Antunes, B. S. L.[1], Komatsu, D.[2], Duek, E. A. R.[3]
[1] *Master's student in Materials Science, UFSCAR/ Sorocaba*
[2] *PhD in Sciences/Physical-Chemistry, UFSCAR*
[3] *PhD in Chemistry, UNICAMP*

1. Introduction

3D bioprinting has emerged to revolutionize the field of Bone Tissue Engineering (BTE), along with the release of osteogenic molecules such as simvastatin (SIN) [1]. However, their integration into a scaffold is a challenge. Silk fibroin (SF) is a biomaterial with adequate mechanical properties, biodegradable and has cell adhesion/proliferation [2]. The addition of other polymers has been studied in the SF solution, ensuring reproduction and quality of the printed structure. The objective of this work is to study the rheological properties of the gel based on FS and PLDLA [poly (L-co-D, L lactic acid)], with SIN, aiming at the printing of the 3D scaffold that will be used in the regeneration of bone tissue.

2. Experimental

SF/PLDLA solutions were analyzed in a DHR-2 Rheometer, TA Instruments at concentrations: SF 3%; 5% and PLDLA 3%; 5%; 7%; 10%, following a factorial experiment. Viscosity curves as a function of shear rate (0.01 to 1000 s^{-1}) in steady state were obtained. In oscillatory regime, the frequency tests were performed to obtain the loss modules (G") and storage (G') from the Linear Viscoelastic Region (LVR), which is previously obtained in the amplitude sweep test.

3. Results and Discussions

The PLDLA 7%/SF 5% solution (figure 1) had the highest viscosity value, caused by the interaction of the PLDLA entangled chains and the SF anti-parallel beta sheets. The pseudoplastic region of the curve is evidenced by the decrease in viscosity at high shear rates, a behavior that facilitates the extrusion of the material through the syringe nozzle. In the frequency test (figure 2), the PLDLA 7%/SF 5% solution also showed G'>G", suggesting a gel behavior, which is important for filament formation during the printing process. For the post-printing behavior, the thixotropy test will be performed to evaluate the viscosity recovery, avoiding the collapse of the printed structure.

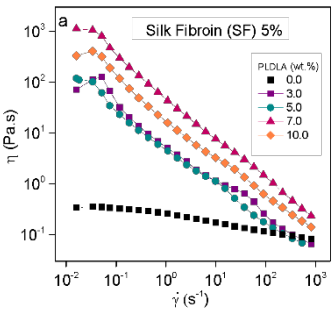

Fig. 1. *Viscosity x shear rate curves (5% SF varying concentrations of PLDLA)*

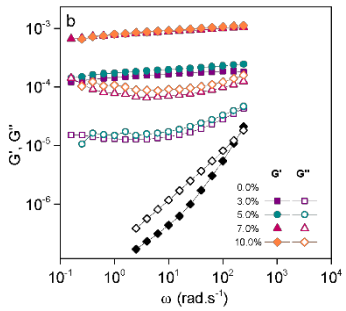

Fig. 2. *Curves of storage and loss modules (G', G") x angular frequency*

4. References

[1] Qiusheng, W, et al. Materials, **12**, 1-19, (2019).
[2] Ali, M, et al. Clinical and Experimental Pharmacology and Physiology, **43**, 659–684, (2016).
[3] Colby, Ralph H. Rheologica Acta, **49**, 425–442, 29, (2010).

Acknowledgments
FAPESP (2020/09917-8), CAPES, PPGCM-UFSCAR, Biomaterials Laboratory (LABIOMAT-PUC).

*Corresponding author: biasblanche@outlook.com

NB_2O_5 FILMS PRODUCED BY PLASMA ELECTROLYTIC OXIDATION AND ANODIC DOPING USING RED MUD RESIDUE

Araujo, P. S.[1], Batista, J. R. D. [1], Mendonça, V. R.[2], Trivinho-Strixino, F.[1]*
[1]*Federal University of São Carlos - UFSCar - Sorocaba*
[2]*Federal Institute – IFSP - Itapetininga*

1. Introduction

Plasma electrolytic oxidation (PEO) is a metal materials processing technique in which a high voltage potential is applied between two electrodes. During this process,a phenomenon called dielectric breakdown occurs by increasing the thickness of the oxide layer and causing micro discharges to occur throughout the substrate surface. The oxide layer produced under these conditions can have interesting characteristics, such as high mechanical strength or photoactivity [1]. Furthermore, processing conditions, such as composition, the concentration of reagents, or the temperature of the electrolyte used during film formation, affect the composition and morphology of the films produced, consequently also affecting their properties [2]. This work is about investigating the base electrolyte and later the insertion of Red Mud, a highly alkaline residue from the aluminum industry, in the PEO process for the production of Nb_2O_5 films.

2. Experimental

Niobium substrates were anodized in a low pH medium ($C_2H_2O_4$ and H_3PO_4) and high pH medium (KOH) using a system consisting of a direct current source in galvanostatic regime and electrolyte temperature control. Then, different percentages (mass/volume) of Red Mud were addedtothe $C_2H_2O_4$ solution, and new films were produced under the same synthesis parameters as in the previous work. The samples were characterized by techniques such as scanning electron microscopy (SEM), energy dispersive spectrometry (EDS), X-ray diffraction (XRD), and diffuse reflectance spectroscopy (DRS). The photocatalytic properties were investigated through photodegradation tests of an aqueous solution of Methylene Blue (MB).

3. Results and Discussions

Different Voltage (V) x Charge (C) curves were observed during the synthesis process according to the different electrolytes used. The micrographs indicated the formation of a porous film (fig.1-A), with higher pore density in the film produced in oxalic acid solution. Through the diffractograms, the formation of $Nb_2O_5$was observed. The bandgap calculation of the films for the samples produced in solutions of $C_2H_2O_4$, H_3PO_4, and KOH, showed values of 3.08, 3.35, and 3.19 eV, respectively. The sample anodized in the electrolyte solution containing 0.1 mol.L^{-1} of $C_2H_2O_4$ showed photocatalytic activity with significant degradation of the methylene blue dye (fig.1-B). After adding Red Mud to the electrolyte, there was a change in the electrochemical response during the synthesis, and elements such as Al and Fe were found in the films produced.

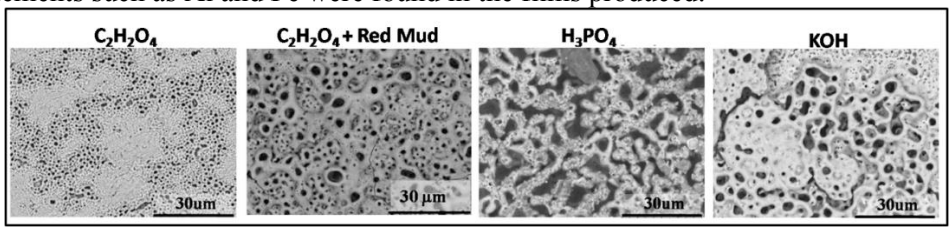

Fig. 1. *Micrographs of samples produced in different electrolytic solutions.*

4. References

[1] Yerokhin, A. L.; Nie, X.; Leyland, A.; Matthews, A.; Dowey, S. J. Surf. & Coat. Tech., **122**, 73–93, (1999).
[2] Santos, J. S.; Trivinho-Strixino, F.; Pereira, E. C. Corrosion science, **73**, 99–105, (2013).

Acknowledgments
This work received support from the following agencies: FAPESP (# 2010 / 10813-0), CNPq (# 443125 / 2014-7 and # 408250 / 2016-0) and CAPES (# 1838556).

*Correspondent author: fstrixino@ufscar.br

DEPOSITION OF TITANIUM THIN FILMS BY RF-MAGNETRON SPUTTERING

Arruda, A. C. S. de[1]*, Durrant, S. F.[2], Mansano, R. D.[3]
[1]*Instituto de Ciência e Tecnologia de Sorocaba – Universidade Estadual Paulista - UNESP*
[2]*Instituto de Ciência e Tecnologia de Sorocaba – Universidade Estadual Paulista - UNESP*
[3]*Laboratório de Sistemas Integráveis da Escola Politécnica da Universidade de São Paulo – USP*

1. Introduction

Over the last few decades, a wide variety of thin films has been extensively investigated for different applications. Titanium films are commonly used for dental applications because of their excellent biocompatibility and corrosion resistance [1, 2]. Several techniques can be used for the deposition and formation of thin films, such as sol-gel, chemical vapor deposition, electron beam evaporation and sputtering. Among the different deposition techniques, radiofrequency (RF) magnetron sputtering stands out for its capacity to deposit uniform, high quality films which exhibit good adhesion [3].

2. Experimental

The equipment used for the deposition of the films was a RF (13.56 MHz) magnetron sputtering reactor from the Laboratory of Integrated Systems (LSI) at EPEUSP. In all processes the base pressure of the equipment was 2.5x10-5 Torr, which was produced by a turbomolecular pump connected in series with a mechanical pump. A six inch diameter titanium target of 99.99% purity was used. The distance between the substrate and target was fixed (at about 18 cm). Argon gas (99.999% purity) was injected into the chamber through a mass flow controller. The titanium films were deposited for 60 minutes onto monocrystalline silicon wafers, which were p-type, of (100) orientation, three inches in diameter, 380 ⌠m thick, with a resistivity of 1 to 10 Ω.cm. To measure the thickness and roughness of the deposited films, a Veeco perfilometer (model Dektak 6M) was used. A process pressure of 8.0 mTorr was used and the applied RF power was varied between 150 and 400 W.

3. Results and Discussions

Table 1 shows the deposition conditions with the resulting film thickness and root mean square (RMS) roughness. The results revealed a deposition rate that depends linearly on the RF applied power over the range studied. Good uniformity of the titanium films was obtained on the silicon substrates. More detailed studies of the dependence of the roughness on the applied RF power are currently underway. Additional analyses using AFM, SEM and X-Ray Diffraction are planned to understand more clearly the surface morphology and crystallographic orientations of the films.

Sample	Power (W)	Thickness (nm)	RMS (nm)
A1	150	301	3.3
A2	200	329	2.7
A3	250	551	5.2
A4	300	504	2.0
A5	350	726	2.1
A6	400	795	25.4

Table 1. *Average thickness and RMS roughness at different RF applied powers.*

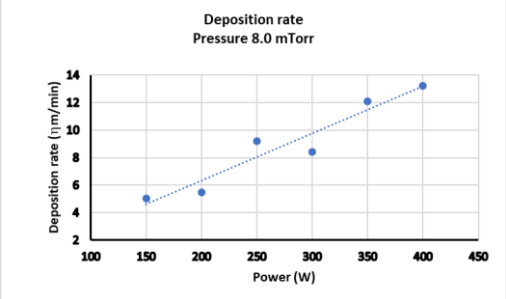

Fig. 1. *Deposition rate of Ti as a function of RF applied power.*

4. References

[1] H. Chouirfa et al, *Acta Biomaterialia.*, **83**, 37-54 (2019).
[2] X. Wang et al, *The Journal of Prosthetic Dentistry*., **116**, issue 3, 450-456 (2016).
[3] S. Calderon Velasco et al, *Progress in Materials Science.,* **84**, 158-191 (2016).

Acknowledgments
This work was supported in part by Capes (Code 001), EPEUSP – Laboratório de Sistemas Integraveis, UNESP and Faculdade de Tecnologia–Fatec Osasco.

*Corresponding author: antonio.arruda@unesp.br

POLY(L-CO-D,L LACTIC ACID-CO-TRIMETHYLENE CARBONATE) 3D PRINTED SCAFFOLD CULTIVATED WITH MESENCHYMAL STEM CELLS DIRECTED TO BONE RECONSTRUCTION

Asami J.[1], Moema A. H.[1], Komatsu D.[1], Ferreira L. M.[1], Silva, G. B. G. Silva[1], Silva L C. S. C. Silva[1], Baldo D. A. [3], Oliveira Jr J. M. [3], Motta A. C. [1] and Duek E. A. R. [1,2].
[1]*Pontifical Catholic University of São Paulo (PUC-SP), Sorocaba, SP, Brazil*
[2]*State University of Campinas (UNICAMP), Campinas, SP, Brazil*
[3]*University of Sorocaba (UNISO), Sorocaba, SP, Brazil*

1. Introduction

Biomaterials can be used on bone tissue engineering, such as natural or synthetic polymer-based materials, and even metal or ceramics approaches [1]. In this way, the terpolymer based on Poly (L-co-D,L lactic acid-co-Trimethylene Carbonate) (PLDLA-TMC) 3D printed scaffold came out recently. It was developed by our research group as a promising material, due capacity of PLDLA-TMC to its biological reabsorption abilities and biocompatibility. In addition, the Mesenchymal Stem Cells (MSCs) have immunoregulatory ability and modulation of the inflammatory process that occurs in bone injuries.

2. Experimental

3D scaffold based on Poly(L-co-D,L lactic acid-co-Trimethylene Carbonate) (PLDLA-TMC), which was designed in Solidworks™ software, projected in 3D Slicer™, 3D printed in filament extrusion. The culture with mesenchymal stem cells (MSCs) was tested *in vitro*. For *in vitro* study, the MSCs were seeded in a PLDLA-TMC 3D scaffold with 600 µm pore size and submitted to proliferation and osteogenic differentiation. The samples were stained with osteopontin and analyzed by Laser Confocal Scan Microscopy (LCSM).

3. Results and Discussions

Both PLDLA-TMC+MSCs submitted or not to osteogenesis presented increased signal of bone markers (Fig. 1 b-c). Therefore, the osteogenesis in this case was not only attributed to the specific inductive medium but also to the material itself. As previously reported in several other studies some materials properties such as porous structures, unique chemical compositions and the 3D configuration engenders an important role in the materials function, which assists and induces the osteoblastic differentiation without external stimuli as a supplemented medium of calcium, phosphate, and osteogenic factors, becoming an osteoinductive material. Moreover, some scaffolds based on synthetic polymers have the ability to activate the Runx2 transcription factor, responsible for the cell signaling cascade of bone formation [2].

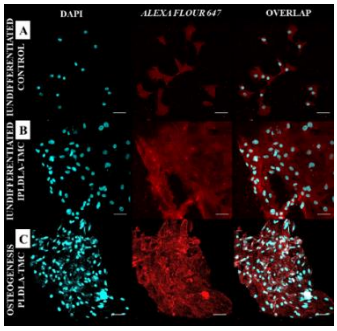

Fig. 1. LCSM images of Osteopontin staining.

4. References

[1] Howard D, et al. J Anat; **213**, 66–72 (2008).
[2] Rao SH, et al. Int j Biol Macromolecules; **110**, 88-96 (2018).

Acknowledgments
The authors gratefully acknowledge for the financial support from the Coordination for the Improvement of Higher Education Personnel (CAPES). (FINEP, n 01.14.0119.03), São Paulo Research Foundation (FAPESP).

*Corresponding author: jessicaasami@gmail.com

COMPARATIVE ANALYSIS BETWEEN PLASMA DEPOSITION TO FORM TIN FILMS IN NICR ALLOY FOR DENTAL APPLICATION

Balica, N. M. P.[1]*, Almeida, L. S. de[2], Rossino, L. S.[3], Sousa, R. R. M. de[1], Santos, R. L. P.[1], Nunes, L. C. C.[1]
[1]*Postgraduate Program in Materials Science and Engineering (PPGCM), Federal University of Piauí-UFPI, Teresina-PI, Brazil.*
[2]*University of São Paulo at Ribeirão Preto School of Dentistry, USP, Ribeirão Preto - SP, Brazil.*
[3]*Federal University of São Carlos, UFSCar/FATEC, Sorocaba - SP, Brazil.*

1. Introduction

Metal alloys have become widely used as biomaterials, so their applications in dentistry have been greatly developed, due to their excellent mechanical and biological properties [1]. NiCr-based dental prostheses may undergo changes in their structure when remaining in an unfavorable environment such as the oral cavity, where they may undergo rapid changes such as the surface corrosion process, depending on the variation of pH and temperature, typically related to changes in the diet of the patient [2,3].

2. Experimental

The present work aims to make a comparison between the cathodic cage and hollow cathode methods, in which a treatment of deposition of thin films of plasma titanium nitride (TiN) was carried out on circular samples of NiCr, to later be evaluated their properties. wear properties for each method. In both methods, the experiment was divided into two parts: pre-sputtering, lasting 1h at 350°C in the presence of argon and hydrogen gases, and sputtering, lasting 4h at 400°C in the presence of argon gases, nitrogen and hydrogen. X-Ray Diffraction analyzes were used to determine the phases present in the deposited layers and also in the base material. The fluorescence spectra and the semi-quantitative analysis of the elements present in the obtained systems were determined through energy dispersive X-ray fluorescence spectroscopy (FRX).

3. Results and Discussions

The presence of the titanium nitride phase comes from the titanium cathode cage after reacting with nitrogen gas in a plasma environment and being deposited on the sample surface. It is also possible to identify the phases of the Ni and Cr elements in isolation. For the untreated samples, it was possible to identify the NiCr phases, as well as in isolation for these elements. Through XRF analysis, it was possible to observe that with the cathodic cage method, the percentage of titanium on the sample surface decreased with increasing pH. The opposite occurred for the samples treated via hollow cathode, where there was an increase in the percentage.

Fig. 1. *Process for film deposition on NiCr samples.*

4. References

[1] Zhang, E., Zhao, X., Hu, J., Wang, R., Fu, S., Qin, G., **6**, 2569-2612, (2021).
[2] Turdean, G. L., Craciun, A., Popa, D., Constantiniuc, M. Materials Chemistry and Physics, **233**, 390-398, (2019).
[3] Liang, R., Xu, Y., Zhao, M., Han, G., Li, J., Wu, W., Dong, M., Yang, J., Liu, Y. Materials Science and Engineering: C, **106**, 110156, (2020).

Acknowledgments
CAPES, UFPI (Federal University of Piauí).

*Corresponding author: naassonbalica@gmail.com

CARBON FIBERS FUNCTIONALIZATION THROUGH ACTIVE SCREEN PLASMA FOR POLYANILINE GRAFTING PURPOSE

Borges, A. F. D.[1]*, Dalmolin C., Fontana, L. C.[1]
[1]*Universidade do Estado de Santa Catarina – Centro de Ciências Tecnológicas*

1. Introduction

Lately, supercapacitors have shown great promise in energy storage systems with their high capacitance and low internal resistance[1]. A route to produce electrodes suitable for supercapacitors is through the deposition of conductive polymers, such as polyaniline, on conductive substrates, like carbon fiber cloth. Although simple in concept, this method requires that the polymer is chemically bonded to the substrate to reduce the resistance to charge transfer[2], but usually, it is expensive and environmentally harmful to do so due to the chemicals and conditions involved. Treatment of the substrate in a low pressure active screen plasma may be an alternative treatment that is both cheaper, faster aAnd environmentally friendlier while producing promising results[3].

2. Experimental

Samples of carbon fiber cloth were coated with aniline through vapor deposition. Then, the samples were treated during 10 minutes inside an active screen plasma system. The plasma was generated in a 20% Ar / 80% N_2 atmosphere. The other plasma parameters were the following: pressure of 0,5 Torr; pulsed voltage of -400V at peak; pulsing frequency of 20, 100 and 200 KHz. The treated samples were then treated through electrochemical process to graft polyaniline on the surface. The samples were characterized through cyclic voltammetry (CV) and electrochemical impedance spectroscopy (EIS).

3. Results and Discussions

The results of CV and EIS for samples with and without plasma treatment are shown in figures 1 and 2, respectively. CV results show that the sample activated in N_2/Ar plasma at100 KHz and, subsequently, grafted with polyaniline shows higher peak current and higher charging capacity than the untreated sample. Figure 2 shows that the treated sample also displayed a smaller overall impedance than the untreated one at a potential of 0,5V vs. SCE. Those results show that the plasma activation is effective in improving the electrochemical characteristics of the final electrode. Further analyses are being performed to determine what exact changes in the surface chemistry on the fibers were responsible for activation.

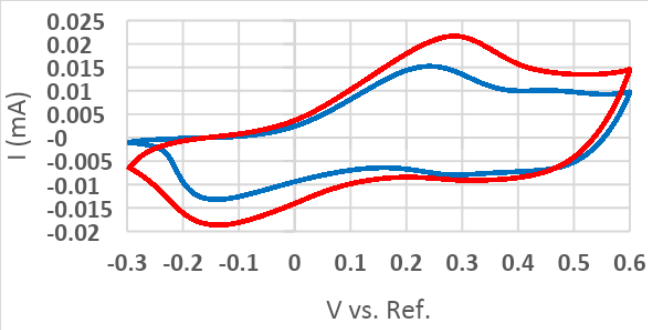

Fig. 1. *Cyclic Voltametry of Polyaniline deposited onto Carbon Fiber samples. The blue curve show the sample with no plasma activation; the red curve show the sample with plasma activation.*

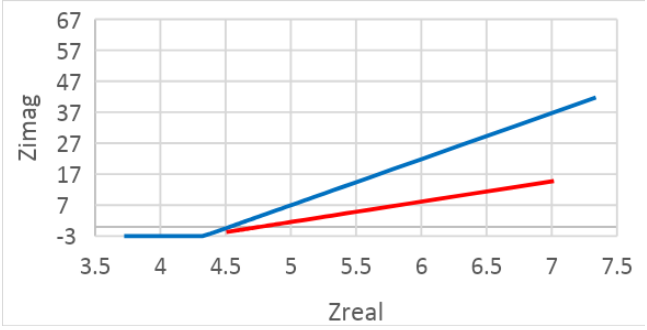

Fig. 2. *Nyquist plot of the electrochemical impedances. The red points correspond to the sample with no plasma activation and the red points refer to samples activated by plasma. .*

4. References

[1] T. Brousse et al. Nature Materials, **7**, 845-854, (2008).
[2] W.-M. Chang et al. Electrochimica Acta, **212**, 130-140, (2016).
[3] J. Xie et al. Surf. & Coat. Tech., **206**, 191-201 (2011).

Acknowledgments
The authors are thankful for the Multi-User Facility infrastructure from Santa Catarina State University's Technological Sciences Center. We would also like to thank the excellent analysts from the Multi-User Facility for their help and the CAPES, FAPESC and PROMOP-UDESC for the research funding.

*Corresponding author: andreso.felipe@gmail.com

DEVELOPMENT OF SHAPE MEMORY ALLOY SOLUTIONS FOR SCRAMJET MOTORS IN HYPERSONIC VEHICLES: NUMERICAL AND EXPERIMENTAL VALIDATION

Brito, A. A. R.[1]*, Costa, F. J.[2], Lima, M. S. F. [3], Paula A. S.[4]
[1]*Instituto Tecnológico de Aeronáutica – PG-CTE, São José dos Campos - SP*
[2]*BRENG Engenharia e Tecnologia Ltda, São José dos Campos - SP*
[3]*Instituto de Estudos Avançados- Divisão de Aerotermodinâmica e Hipersônica, São José dos Campos – SP*
[4]*Instituto Militar de Engenharia – Seção de Engenharia de Materiais, Rio de Janeiro – RJ*

1. Introduction

Advances in propulsion systems, aerothermodynamics, and flight control design have allowed aerospace vehicles to operate at hypersonic speed, however, many problems still exist owing to aerodynamic heating and shock wave interactions, resulting in high temperatures in the airframe causing thermal stresses and rapid ablation. Shape Memory Alloys (SMAs) have become a leading class of smart materials in aeronautics because of their excellent mechanical properties that allow them to withstand high speeds and temperatures [1]. To avoid any kind of ablation when exposed to high temperatures, some solutions are necessary, such as thermal barrier coatings, usually called TBC (Thermal Barrier Coatings) or Selective Laser Melting (SLM) in order to obtain an optimization of the metallic alloy will be studied [2]. Numerical model validation (*Auricchio*) using ANSYS software was used to analyze the alloy behavior.

2. Experimental

In additive manufacturing, also known as 3D printing, parts are manufactured by depositing materials. It is a relatively fast process; therefore, the metal parts are structured layer-by-layer. To succeed in the process, the deposition source to sinter the material was laser melted, which featured powder layer fusion and directed energy deposition. This production mode is fundamental for obtaining parts with good mechanical properties and low porosities. Another solution is the application of the TBC system, which is a chemical and thermal protection coating composed of three layers, two chemical protection layers: Bond Coated (BC) formed by an MCrAIY alloy (M= Ni/Co/Fe) and a Thermally Grown Oxide (TGO) layer and a thermal protection layer consisting of a ceramic coating [3]. For the development of the numerical model, a more detailed analysis of the pseudoelastic behavior of the alloy phase transaction is used in the ANSYS software, obtaining results very close to the experimental results, which are based on the model proposed by *Auricchio* [4].

3. Results and Discussions

It could be concluded that throughout the experimental tests that will be carried out on shape memory alloys using the following analytics studied in this project, in order to gather post and/or counter arguments within the framework of the manufactured alloy microstructure, identifying possible defects, critiquing the influence of process parameters, and evaluating the mechanical and metallographic properties of the post-processed material.

4. References

[1] Brito A. A. R.; Costa F. J.; Passaro A.; Lima M. S. F., Rev. Bras. de Apl. De Vácuo, **40**, 1 – 7, (2021).
[2] Sallet, E. H.; Oliveira, R. V.; Rodrigues, P. F.; Sousa, T. G.; Teixeira, R. S.; Sénéchal, N. V. L.; Gonçalves, D. A. C.; Paula, A. S.; Netto, P. I.; Silva, J. V. L. In: 74º Congresso Anual da ABM, São Paulo, 3095-3106, (2019).
[3] Teleginski, V. *"Deposição de revestimentos com laser de CO_2 para proteção térmica de palhetas de turbinas aeronáuticas e industriais"*, 85p, (2016).
[4] Silva, P. C. S.; Grassi, E. N. D.; Savi, M. A.; Araújo, C. J.; Santos, N. C. *"Simulação numérica do comportamento superelástico de mini molas de NiTi usando ansys."* (2014).

Acknowledgments
The authors thank the Breng Engenharia, company and partial financial support from CAPES (Edital Pró-Defesa IV- Processo 88887.285953/2018-00). Thanks, are also due to Military Institute of Engineering (IME) and the Institute of Advanced Studies (IEAv) for the support and availability of the material and the laboratories.

*Corresponding author: alanarb21@gmail.com

STUDY OF CORROSION RESISTANCE OF AISI 4340 STEEL WITH DUPLEX TREATMENTS OF NITRIDING AND DLC FILM DEPOSITION.

Campos, L. A. P. de[1]*, Almeida, L. S. de[1], Danelon, M. R.[1], Silva, B. P. da[2], Aoki, I. V.[2], Manfrinato, M. D.[1.3], Rossino, L. S.[1.3]
[1]*Universidade Federal de São Carlos – Campus Sorocaba*
[2]*Universidade de São Paulo*
[3]*Faculdade de Tecnologia de Sorocaba*

1. Introduction

The evolution of studies in surface treatments propose new alternatives to treat superficially the materials, as an example we have the duplex treatments (multilayer) that achieves better resistance corrosion properties that materials treated with only one surface treatment process [1]. The objective of this work is to evaluate the corrosion resistance of AISI 4340 steel coated DLC film and with duplex treatment of nitriding + DLC film deposition.

2. Experimental

The material studied were the AISI 4340 steel. The treatments were performed in two conditions, the first condition were the DLC film deposition on substrate, and the second condition were DLC film deposition on nitriding layer. DLC film deposition was performed using 90% CH_4 + 10% Ar at 200ºC for 2 hours. Duplex treatment was performed using 80% N_2 + 20% H_2 at 450ºC for 5 hours to nitriding followed DLC film deposition. The evaluation of corrosion resistance were carried out by SVET (Scanning Vibration Electrode Technique) in both conditions. The tests were carried out in a 0.05 $molL^{-1}$ NaCl solution, and SVET scans were performed every hour totalizing 9 hours of test.

3. Results and Discussions

The Fig. 1 show the SVET analysis performed on AISI 4340 steel with DLC film deposition, and it's possible observe points with a red color, indicating regions susceptible to corrosion, these points is referent to the defects in DLC film, thus the corrosive solution is in direct contact with the ferrous substrate. The Fig. 2 show the SVET analysis of AISI 4340 steel with DLC film deposited on nitrided layers, and it's possible observe that the nitriding layer (FeN and Fe_2N) has a greater corrosion resistance, protecting the surface of substrate, avoiding contact between the corrosive solution and the ferrous substrate.

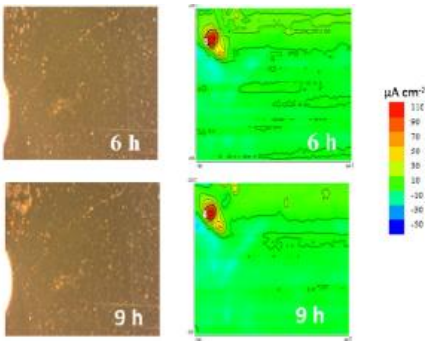

Fig. 1. *Scanning Vibration Electrode Technique (SVET) maps of DLC deposition film on substrate AISI 4340 steel.*

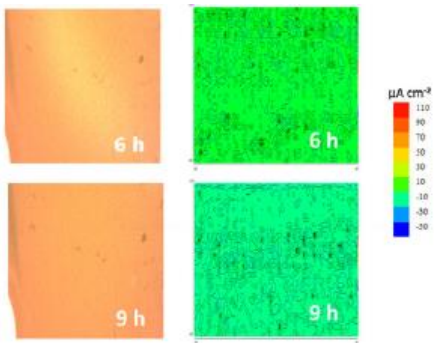

Fig. 2. *Scanning Vibration Electrode Technique (SVET) maps of DLC film deposition on nitriding layer of AISI 4340 steel.*

4. References

[1] L. Almeida, et al. JMEPEG. **29**, 8107-8121 (2020).

Acknowledgments
The authors are grateful to CAPES and CNPq scholarship - Brazil for the financial support.

*Corresponding author: lucasalmeidamk@gmail.com

LIKE CARBON COATINGS ONTO TOOL STEEL

Campos, W. S. H.[1]*, Bernal, J. M. G.[1,2], Trava-Airoldi, V. J.[3], Capote, G.[4]
[1] *Fundación Universitaria Los Libertadores. Facultad de Ingeniería y ciencias básicas. GIDAD Research group. Colombia.*
[2]*Universidad Nacional de Colombia. Escuela de Diseño Industrial. Colombia.*
[3]*Laboratorio associado de Sensores e Materiais. Instituo Nacional de Pesquisas Espaciais, INPE. Brasil.*
[4]*Universidad Nacional de Colombia. Facultad de Ciencias, Departamento de Física. Colombia.*

1. Introduction

Diamon Like Carbon or DLC coating has a disadvantage and that is low adhesion on different metallic substrates such as steels. This problem is mainly due two reason, the first is the difference in the coefficient of thermal expansion between the substrate and the DLC coating [1], [2] and the other is the high diffusion between of carbon and the substrate [3], [4]. With the aim of improving the adhesion of DLC coatings to AISI H13 tool steel, an interlayer will deposit of TixW. Titanium multilayer systems have been used as an interface in some investigations, showing good results in increasing the adhesion of DLC protective coatings and diamond coatings on metal surfaces, because Ti can form chemical bonds with Fe [5].

2. Experimental

A heat-treated AIS H13 tool steel with a hardness of 52 Rc was chosen as a sample to emulate the working conditions of the material, then the TixW film was grown using the magnetron sputtering technique R.F, DLC was deposited with PCVD assist for plasma. The growth conditions are better shown in the research [6] , the only thing that changes are the growth times since they were adjusted for the TixW objective and to have the required thicknesses. This was done by growing the films on Si(100) samples, also in the investigation [6] the characterization techniques used are mentioned.

3. Results and Discussions

The XRD showed the presence of two independent phases Ti and W and no new phase. The DLC was deposited however after the deposition was evident the detachment of the DLC. New film DLC were made with less pressure in Brazil, however the phenomenon of detachment persistent. In doing a mapping of the samples, it was observed that was peeled off with the TiW interlayer.

4. References

[1]V. J. Trava-Airoldi, L.F. Bonetti, et. al, Thin Solid Films, **516**, 272–276, (2007).
[2]X. Xiao, B. W. Sheldon, E Konca, L. C. Lev, M. J. Lukitsch, Diam. Relat. Mater. **18**, 1114–1117, (2009).
[3]Fan Hua Qi, Fernandes, Grácio J, Diam. Relat. Mater., **7**, 603–606, (1998).
[4]J. Spinnewyn, M. Nesládek, and C. Asinari, Diam. Relat. Mater., **2**, 361–364, (1993).
[5]M. Madej, *Wear*, **317**, 179–187, (2014).
[6]W. S. Hincapie C, J. M. Gutiérrez B, et al, *Diam. Relat. Mater.* **109**, (2020).

*Corresponding author: wshincapiec@libertadores.edu.co

EFFECT OF HEAT TREATMENTS ON MICROSTRUCTURE, YOUNG'S MODULUS, AND VICKERS MICROHARDNESS OF α+β AND β Ti-5Mo-Nb SYSTEM ALLOYS FOR BIOMEDICAL APPLICATIONS

Cardoso, G. C.[1]*, Grandini, C. R.[1,]
[1]*UNESP - Univ Estadual Paulista, Laboratório de Anelasticidade e Biomateriais, 17.033-360, Bauru, SP, Brazil*

1. Introduction

From the past few years, β-Ti alloys have been widely studied in the medical field. They have an excellent combination of attractive properties for a biomaterial, such as excellent chemical and mechanical properties and biocompatibility with human tissue [1]. Besides the composition of the alloying elements, thermomechanical treatments also modify the microstructure and mechanical properties of the alloys due to strain-induced stresses [2]. Thus, this work studied the microstructure and selected mechanical properties of four alloys of the Ti-5Mo-Nb system after several thermomechanical processing.

2. Experimental

The ingots of four alloys of the Ti-5Mo-xNb system (x = 0, 10, 20, and 30 %wt) were produced by arc melting. After melting, a homogenization heat treatment was performed, the ingots were hot-rolled, and finally, an annealing heat treatment was performed [3]. The structure and microstructure of the samples were analyzed by XRD and optical and scanning electron microscopy images. After each processing condition, the Vickers microhardness of the samples was measured, and Young's modulus was analyzed after hot rolling and annealing due to the shape of the samples.

3. Results and Discussions

As expected, because of the thermomechanical treatments, the microstructure of the samples has changed. Figure 1 shows, after refinement by the Rietveld method, that the alloy with 30% Nb suffered fewer variations in its microstructure due to higher stabilization of the β-phase. Due to the change in the microstructure of the samples, the measured mechanical properties have also changed. Figure 2 shows the samples' microhardness variation after each processing condition. Among all the samples produced, the Ti-5Mo-30Nb alloy samples showed the most promising results for the properties analyzed for use as a biomaterial.

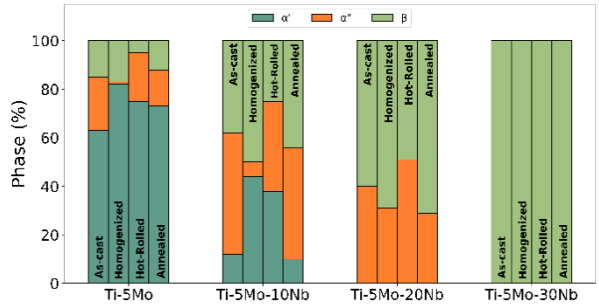

Fig. 1. *Phase composition of Ti-5Mo-xNb alloys, after each processing condition.*

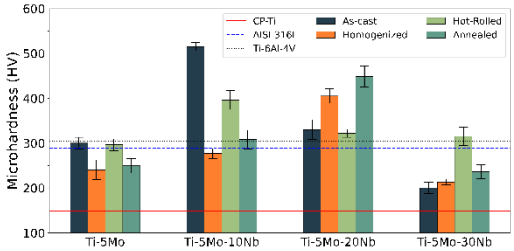

Fig. 2. *Microhardness of Ti-5Mo-xNb alloys, after each processing condition.*

4. References

[1] S.S. Sidhu, H. Singh and M.A.-H. Gepreel, Materials Science and Engineering: C, **121**, 111661 (2021).
[2] S. Semiatin, Metallurgical and Materials Transactions A **51(6)**, 2593-2625 (2020).
[3] G. Cardoso et al. Metals **12(5)**, 788 (2022).

Acknowledgments
The authors thank CAPES, CNPq, and FAPESP for financial support, PosMat, and the laboratory's colleagues collaborating with the research.

*Corresponding author: giovana.collombaro@unesp.br

PLASMA EFFECT ON BEAN GRAIN ACTIVATION

Cardoso, T. V.[1*], Almeida, L. S. de[2], Rossino, L. S.[1,2]
1 - Faculdade de Tecnologia José Crespo Gonzales – Fatec Sorocaba, Sorocaba – SP
2 - Universidade Federal de São Carlos – UFSCAR Campus Sorocaba, Sorocaba - SP

1. Introduction

Presently, some climatic factors negatively affect the production, germination, growth, and yield of crops all over the world. A few studies report the use of technological plasmas to increase the germination rate and reduce seed dormancy. Plasma provides surface modification without damaging the seed, in addition to being an ecologically correct technique [1]. Therefore, the objective of this work is to evaluate the effect of plasma on bean activation.

2. Experimental

Bean grains were selected for similarity in size from a commercial package of edible beans. Fifteen lots were selected, each with 14 seeds to form the test groups, being groups 1, 2, 3, 4, and control (no treatment). The groups were exposed to plasma of 100% oxygen (O_2), 100% Argon (Ar), and 50% Ar+ 50% O_2, with a power of 100 W for 2 minutes at a temperature of approximately 27° C. After the treatments, the groups of bean samples were placed in special papers, soaked in distilled water, rolled up and kept closed in labeled plastic envelopes to be opened and analyzed after 3, 5 and 7 days of treatment, following appropriate methodology of the Brazilian Ministry of Agriculture [2].

3. Results and Discussions

Following germination criteria [2], it was found that germination efficiency was higher for group 3 of the sample, which was exposed to oxygen plasma, as can be seen in Fig.1. In Fig.2. sprout lengths were observed for 3, 5, and 7 days, and it was found that similarity in sprout length in the control and 1 group (only vacuum), which suggests that the vacuum environment did not have a significant impact on the sprout length. On the other hand, group 3_100% O_2 and group 4_50% Ar+ 50% O_2 presented a sprout length about 10% and 20% greater than the control grain lengths (control group), respectively. Therefore, it is possible to observe the positive effect of plasma on the production, germination, growth, and yield of bean grains.

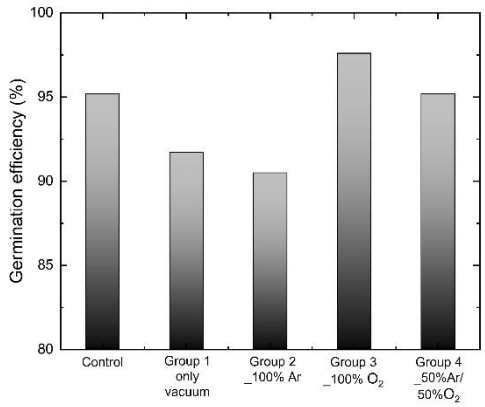

Fig. 1. *Germination efficiency for each sample group.*

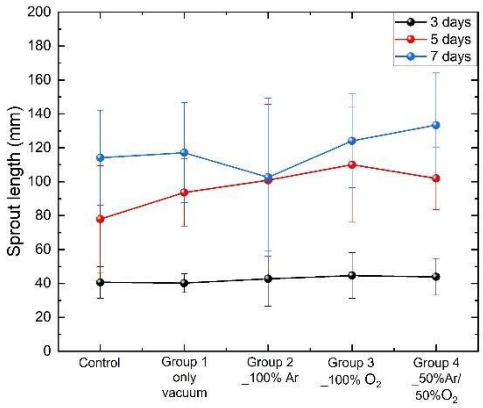

Fig. 2. *Sprout length with 3, 5 and 7 days for each sample group.*

4. References

[1] Sadhu, S., Thirumdas, R., Deshmukh, R. R., & Annapure. Food Science and Technology, **78**, 97–104 (2017).
[2] Brazil. Ministry of Agriculture, Livestock and Supply. Rules for seed analysis / Ministry of Agriculture, Livestock and Supply. Secretary of Agricultural Defense. Brasília: Mapa/ACS, 2009.

Acknowledgments
Cardoso and Rossino thank Centro Paula Souza and Fatec/Sorocaba for their financial support

*Corresponding author: telma.cardoso@fatec.sp.gov.br

LIOPHILIZATION AS A TOOL FOR ANALYTIC DETERMINATIOS IN BIOLOGICAL ORGANISMS USED AS BIOINDICATORS

Costa, L. A. M. da[1]*, Irazusta, S. P.[1,2], Almeida, L. S. de[4], Degasperi, F. T.[3]
[1] *Faculdade de Tecnologia de Sorocaba – José Crespo Gonzales, CEETEPS-SP, Brasil*
[2]*Programa de Mestrado Profissional em Gestão e Tecnologia dos Sistemas Produtivos-CEETEPS, SP, Brasil*
[3] *Faculdade de Tecnologia de São Paulo- CEETEPS, SP, Brasil*
[4]*Programa de Pós Graduação em Ciências dos Materiais – UFSCar- Sorocaba, SP, Brasil*

1. Introduction

Bioindicators are organisms sensitive to variations in the environment in which they live and, therefore, are excellent as representatives of the ecosystems [1]. In the terrestrial environment, the oligochaete *Eisenia andrei* is an important bioindicator, with proven and standardized tests to assess potential harmful impacts to the terrestrial environment [2, 3]. The limitation of the tests is precisely from the difficulty of preserving the sample for later characterizations. The objective of this work was to propose a method to preeserve these organisms after exposure, through the process of lyophilization, as a useful tool.

2. Experimental

In a plastic container, 150g of soil contaminated by metals (cadmium, copper and cobalt at a concentration of 10mg/kg) was prepared. Five earthworms *Eisenia andrei* were exposed to this soil for 14 days. After this period, the earthworms were removed from the container, washed in distilled water and sacrificed by cooling to 4°C. Then, the earthworms were placed in a stainless steel container and kept at -20°C until the moment of lyophilization. Lyophilization was carried out in a vacuum chamber, at a pressure of 0.4mbar, for 8 hours, for the processing. Finally, the samples were analysed by scanning electron microscopy (SEM)with energy dispersive spectroscopy (SED) to detect the absorption of metals.

3. Results and Discussions

SEM analysis (Figure 1A) and metal determinations by using SED showed that the organisms remained viable for analysis, it was possible demonstrate that there was incorporation of metals into earthworm tissues (Figure 1B). Then it was shown a interesting tool for analytical determinations in this bioindicator.

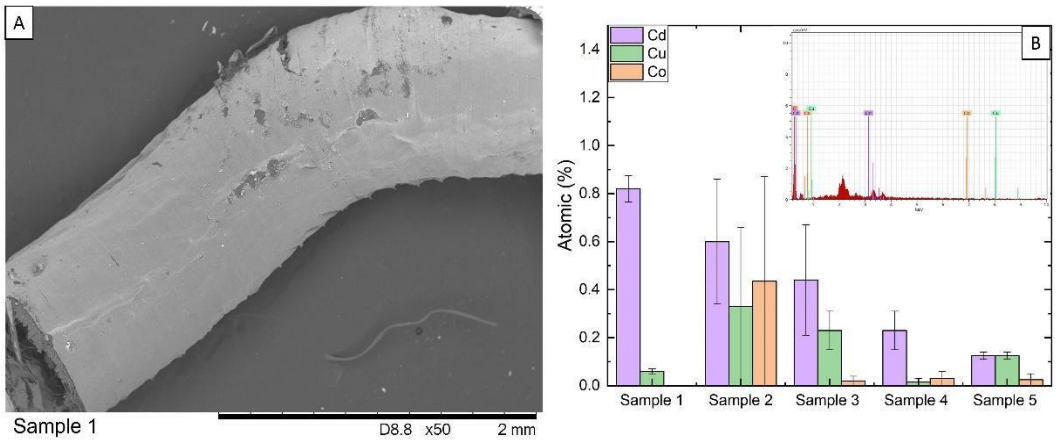

Fig. 1. *SEM image of the earthworm body (A) and EDS analysis of metals (B). It´s observed Co, Cd and Cu in the organism body.*

4. References

[1] S. Stankovic; P. Kalaba and A.R. Stankovic, Environ. Chem. Lett., **12**, 63-84 (2014).
[2] G. Muthukaruppan, Invertebrate Survival Journal, **12**, 237-245 (2015).
[3] J.B. Richardson *et* al., Soil Biology & Biochemestry, **85**, 190-198 (2015).

*Corresponding author: leonardo.aumestre@outlook.com

TI-NB-ZR ALLOY COATINGS SPUTTER-DEPOSITED ON AISI 316L STAINLESS STEEL

Costa, S. C. Z.[1], Lemos, L. L. A.[1], Gobbi, A. L.[2], Nascente, P. A. P.[1,3]
[1]*Federal University of São Carlos, Graduation Program in Materials Science and Engineering, 13565-905, São Carlos, SP, Brazil.*
[2]*Brazilian Center for Research in Energy and Materials, Brazilian Nanotechnology National Laboratory, 13083-970, Campinas, SP, Brazil.*
[3]*Federal University of São Carlos, Department Materials Engineering, 13565-905, São Carlos, SP, Brazil.*

1. Introduction

Although AISI 316L stainless steel (SS) is widely used as implant material, the release of corrosion products in the human body can be harmful. Thus, an interesting option to overcome this limitation is to coat a SS implant with Ti-Nb-Zr thin film that has a higher corrosion resistance and a better biocompatibility [1-3]. Ti, Nb, and Zr are non-toxic and non-allergenic elements that exhibit excellent biocompatibility and low cytotoxicity.

2. Experimental

Ti, Nb, and Zr disks with 2 in. diameter, 3 mm thickness, and 99.99% purity were used as targets. The substrates were made of 1 mm thick AISI 316L SS sheet, and 15 mm diameter disks were cut from this sheet to produce the substrates. An AJA Orion 8 Phase II J magnetron sputtering system was used to deposit coatings with the following nominal compositions: $Ti_{50}Nb_{30}Zr_{20}$, $Ti_{50}Nb_{25}Zr_{25}$, and $Ti_{45}Nb_{25}Zr_{30}$. X-ray diffraction (XRD) data were acquired by a Shimadzu diffractometer, model XRD-6100, using a Co K〈 source (L = 0.17889 nm), power given by 40 kV and 30 mA, in grazing incidence mode, and scan ranging from 0° to 90°.

3. Results and Discussions

Figure 1 presents the XRD diffractograms for the $Ti_{50}Nb_{30}Zr_{20}$, $Ti_{50}Nb_{25}Zr_{25}$, and $Ti_{45}Nb_{25}Zr_{30}$ coatings. Only the presence of the β (BCC) phase is observed; this phase is identified by the (110), (200), and (211) diffraction peaks (ICDD card No. 00-044-1288). Among the phases occurring in Ti-based alloys, the β phase exhibit the most adequate characteristics for biomedical application, such as low elastic modulus that is important because of the charge transfer between the implant and the neighbor tissue [3].

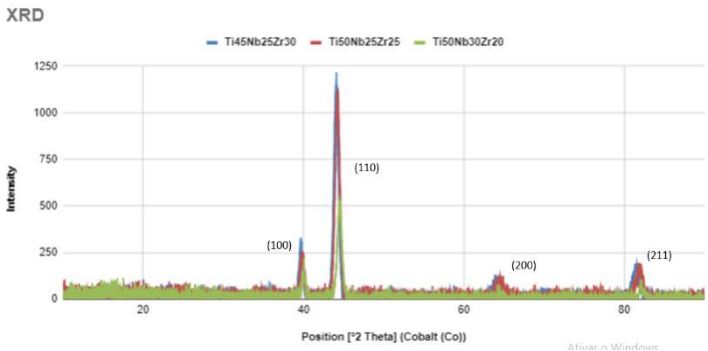

Fig. 1. *XRD diffractogram for the Ti-Nb-Zr coatings.*

4. References

[1] D.A. Tallarico *et al.*, Mater. Sci. Eng., **C 43**, 45-49, (2014).
[2] E.D. Gonzalez *et al.*, Surf. Coat. Technol., **326**, 424-428, (2017).
[3] E.D. Gonzalez *et al.*, Thin Solid Films, **721**, 138565, (2021).

Acknowledgments
This work was supported by FAPESP (process 2017/25983-8), CNPq (process 302450/2017-3), CAPES (Finance Code 001), and CNPEM/LNLS.

*Corresponding author: sidneycherman@gmail.com

EFFECT OF THE NITROGEN AND SILICIUM ADDITION IN THE DLC FILM ON TRIBOLOGICAL BEHAVIOR OF TOOL STEEL AISI M2

Danelon, M. R.[1]*, Almeida, L. S. de[1], Manfrinato, M. D.[1,2], Rossino, L. S.[1,2]
[1]*Universidade Federal de São Carlos, PPGCM, UFSCar Campus Sorocaba, Sorocaba-SP*
[2]*Faculdade de Tecnologia do Estado de São Paulo (Fatec Sorocaba), CEETEPS, Sorocaba-SP*

1. Introduction

DLC (Diamond-Like Carbon) film is an amorphous carbon thin film that contains carbon hybridizations sp^2 and sp^3 related to graphite and diamond, respectively. This combination provides high hardness and low friction coefficient improving the wear resistance of the material [1]. The doping of the DLC films with elements like N and Si can be an excellent alternative to change their properties and obtain different results, improving the adhesion or stability of these films at high temperatures. AISI M2 tool steel is high-speed steel, utilized in machining and cutting tools, due to its high hardness. The objective of this work is to compare the tribological behavior of the M2 steel with and without DLC, N-DLC, and Si-DLC film.

2. Experimental

DLC films were deposited by PECVD using a pulsed-DC power supply. Before treatments, an ablation treatment was performed with a gas mixture of 80%Ar/20%H_2 for 1h. Posteriorly, it was deposited an organosilicon film, to improve the DLC film adhesion, with a gas mixture of 70%HMDSO/30%Ar for 15min. Finally, DLC, N-DLC, and Si-DLC were deposited using a gas mixture of 90%CH_4/10% with 30sccm of gas flow, and 70%CH_4/30%N_2 with 40sccm of gas flow, and 90%CH/8%Ar/2%HMDSO with 30sccm of gas flow, respectively. Treatments were performed with a temperature of 200ºC for 2h. Micro-abrasive wear tests by fixed ball were performed for 600s with an 8N load and samples were characterized by Raman spectroscopy.

3. Results and Discussions

It's possible to observe in Figure 1 that all DLC film deposition improved the wear resistance of the samples when compared to untreated material. Si-DLC presented the best wear resistance and this can be explained by the low graphitization rate of the silicon doped DLC. On the other hand, the N-DLC presented the worst wear behavior when compared to other films and this is explained by the presence of N, which reduces the amount of sp^3 hybridizations decreasing the hardness of the film. These results are also explained by the coefficient of friction, where DLC and Si-DLC presented significantly lower coefficients when compared to the base material and N-DLC. Figure 2 presents the Raman spectroscopies, where is possible to observe the presence of D and G bands, around 1350 cm^{-1} and 1580 cm^{-1} respectively, these bands and the hydrogen percentage of 32,54% confirm the deposition of a-C:H DLC film. Thus, we can observe that doping DLC films with different elements can provide different tribological behaviors to the film.

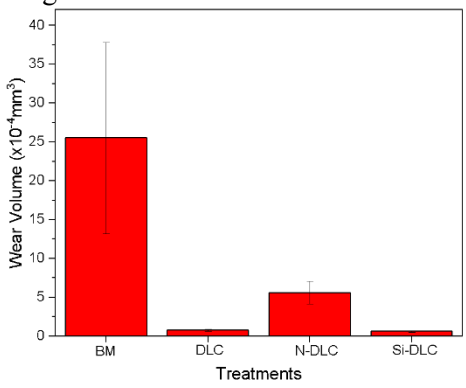

Fig. 1. *Wear Volume as a function of DLC films*

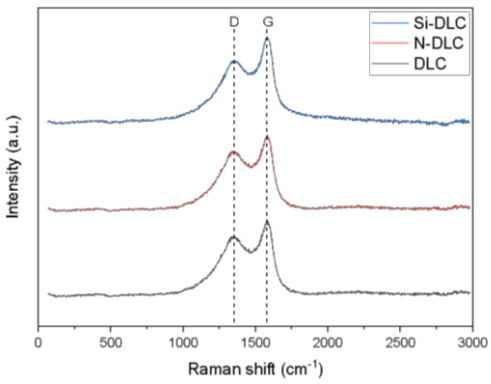

Fig. 2. *Raman Spectroscopy of DLC films*

4. References

[1] Franceschini, *et al.* Appl. Phys. Lett. **68**, 2645, (1996).

Acknowledgments
The authors acknowledge CAPES (001) for the financial support and FATEC-Sorocaba for the laboratory.

*Corresponding author: miguelrubida@gmail.com

Ag-DOPED NANOCELULOSE FILMS FROM SPUTTERING OF $AgNO_3$ POWDER IN ARGON PLASMAS

Delgado-Silva, A. O.[1]*, Matsuda, L. M. M.[2]
[1]*Universidade Federal de São Carlos, Centro de Ciências e Tecnologias para Sustentabilidade CCTS*
[2]*Universidade Federal de São Carlos, Centro de Ciências e Tecnologias para Sustentabilidade CCTS*

1. Introduction

Cellulose is a biodegradable material, flexible, with good mechanical resistance, from renewable source and widely available in nature. Beyond its several applications in the textile, paper and packaging industries [1], it has been attracting great interest in the production of biosensors and healing materials [2]. Cellulose membranes functionalized with silver nanoparticles has been reported as antimicrobial for wound-healing treatment [3]. In this context, the present work aimed to create and characterize nanocellulose (NC) films doped with silver (Ag-doped) from sputtering process of silver nitrate powder (AgNO3).

2. Experimental

The silver salt was placed in the lower electrode of a stainless steel plasma reactor while the NC films and a glass control sample were in the superior electrode (grounded), based on the approach described in [4]. The effectiveness of plasmas from argon and a mixture of argon and oxygen (90% and 10%, respectively) in silver incorporation was investigated. Radio frequency (RF) of 13.56 MHz was applied to the lower electrode, with power varying from 150 to 250 W, treatment time from 30 to 90 min, and working pressure from 8.8 to 14.9 Pa. After sputtering process, the Ag-doped NC films were characterized with X-ray diffraction (XRD), profilometry, absorption in the ultraviolet and visible region (UV-Vis), scanning electron microscopy (SEM), X-ray dispersive energy spectroscopy (EDS), water contact angle and microbiological analysis by Japanese Industrial Standard (JIS) Z 2801 test with *Staphylococcus aureus* e *Escherichia coli*.

3. Results and Discussions

The results obtained for the XRD showed diffraction angles at 14, 16 and 22°, characteristic of NC structure. Profilometry of the glass sample revealed the formation of a thin film on the surfaces, with thickness from 19 to 96 nm. SEM characterization exposed morphological changes in the surface topography dependent on the parameters of the plasma process, with Ag content on the membranes surface ranging from 3.6 to 31%, measured by EDS. Microbiological analysis, from JIS test revealed no growth of bacterial colonies for the films treated with 100% Ar plasmas under power of 150-200 W during 60 min and the lowest based pressure (1,7 Pa), related to the maximum of Ag incorporation and the thinnest deposited film. Therefore, the bactericidal activity of NC films could be achieved from the sputtering process from silver nitrate powder.

4. References

[1] J. Credoua and T. Berthelot, J . Mater. Chem. B, **2**, 4767-4788 (2014).
[2] V. Kanikireddy et al., Int. J. Biol. Macromol. **164**, 963-975 (2020).
[3] S. Pal et al., ACS Omega, **2**, 3632−3639 (2017).
[4] A.D. Battaglin et al., Materials Research, **17**, 1410-1419, (2014).

Acknowledgments
Laptec (Unesp Sorocaba), for the use of the plasma reactor. LNNano (CNPEM), for the use of SEM and EDS. Suzano Papel e Celulose, for suppling nanocelulose suspension to the NC films manufacture.

*Corresponding author: adelgado@ufscar.br

VACUUM PRESSURE METROLOGY BY THE STATIC EXPANSION METHOD

Degasperi, F. T.[1], Arakawa, R.[2], Oliveira, J. S.[3], Batista, L. N.[3], Martarelli, K. C. R.[1], Oliveira, G. D. S.[1]
[1]*Faculdade de Tecnologia de São Paulo – FATEC SP – CEETEPS*
[2]*ETEC Prof. Horácio Augusto da Silveira – CEETEPS*
[3]*Laboratório de Pressão - LAPRE – INMETRO*

1. Introduction

A joint work between the *Laboratório de Tecnologia do Vácuo - LTV* of *FATEC-SP - CEETEPS* and the *Laboratório de Pressão* - LAPRE of the Instituto Nacional de Metrologia, Qualidade e Tecnologia - INMETRO, aims to improve a system that aims to be a standard vacuum primer in Brazil. Its operation uses the method of successive static expansion to make vacuum manometer metrology. With this, this project is of interest in the industrial area, but there is also the possibility of carrying out studies on metrology in vacuum and the interference that certain variables have on the measurement of pressure. In industrial processes, control over the variables that interact with the vacuum system becomes important, since a variation in pressure can influence the manufacture of a product, thus, metrological quality must be maintained with pressure sensors.

2. Experimental

The metrological system is composed of a set of vacuum chambers with several volumes determined with their measurement uncertainties, and the largest vacuum chamber is called the expansion vacuum chamber, as illustrated in figure 1. The concept of *Boyle-Mariotte* (equation 1) in the system. To carry out the measurements, the temperature is controlled through a conditioned environment, around 20 ºC. Thus, with the injection of molecular nitrogen gas - N_2 - in one of the vacuum chambers or in a combination between the volumes of the starting vacuum chambers, with a predetermined pressure p_1, with the volumes of the vacuum chambers well determined, this way In this way, it is possible to find the value of the final pressure p_2 of the vacuum system, after the expansion of the gas that was in the initial volume V_1 to the expansion chamber, with the final volume V_2, this volume being the sum of the volumes involved in the expansion . By integrating vacuum gauges, you can calibrate the vacuum gauges, using equation 1, with this you can calculate the percentage error of the standard that exists in the LTV, keeping the temperature constant

$$p1 \,.\, V1 = p2 \,.\, V2 \quad (1)$$

3. Results e Discussions

Using the vacuum gauges from *LAPRE – INMETRO*, which are MKS capacitive membrane pressure gauges of 1 torr, 100 torr and two of 1000 torr (with the 1000 torr gauges calibrated by the *Physikalisch-Technische Bundesanstalt – PTB - Germany*) and two gauges *LTV's* capacitive membrane system. A series of expansions were carried out and the results are shown in part in table 1. When analyzing the measurements, it is noted that for pressures from 10 torr to 100 torr (pressure range analyzed) the equipment has a relative error per turn from 0.5% to 5%. For pressures lower than 10 torr, the relative error starts to increase significantly. There were high values of relative error, mainly in the MKS gauges as it was found that there was a small gas leak in this part of the connection.

Fig. 1. *Vacuum system using the LTV static expansion method - FATEC-SP.*

Pressão Final			Análise de Dados			
				Erro (%)		
Brooks (torr)	MKS (1 torr)	MKS (100 torr)	Teórico (torr)	Brooks (torr)	MKS (1 torr)	MKS (100 torr)
50,60	-	-	49,99	1,22	#VALOR!	#VALOR!
50,70	-	50,43	50,07	1,26	#VALOR!	0,72
16,00	-	15,715	16,06	0,36	#VALOR!	2,14
10,70	-	10,38	10,97	2,47	#VALOR!	5,39
1,00	-	0,798	0,86	16,80	#VALOR!	6,80
1,02	0,98356	0,863	0,89	14,68	10,07	3,42
2,50	-	2,133	2,08	20,48	#VALOR!	2,78
80,70	-	80,38	81,38	0,84	#VALOR!	1,23
0,94	0,5316	0,424	0,80	17,60	33,33	46,83
1,00	0,585	0,477	0,69	44,58	15,42	31,04
0,60	0,18	0,0704	0,32	89,18	43,26	77,81

Tab. 1. *Table with the results of expansions.*

4. References

[1] Arakawa, R. *"Caracterização do Padrão Primário de Vácuo pelo Método de Expansão Estática."*124p. (2013).

*Corresponding author: ftd@fatecsp.br

PRESSURE FIELD AND ITS GRADIENT IN TUBE DEVICES IN HIGH VACUUM SYSTEMS

Degasperi, F. T., Ricotta, R. M.*
[1]*Faculdade de Tecnologia de São Paulo – FATEC SP – CEETEPS*

1. Introduction

High vacuum tube systems are widely used in particle accelerator arrays, storage rings, microwave amplifiers and others. This work presents the results of the analytical and numerical calculations of the modeling of the pressure field and its gradient of a system that consists of a composition formed by tubes of cylindrical and conical geometry. The modeling performed assumes that the transport of gases occurs in the molecular gas transport regime and that it can be considered a diffusive phenomenon. In the analysis, the natural specific degassing rate of the walls (outgassing), the specific conductance and the effective pumping speed at the pipe ends are considered in detail.

2. Experimental

Figure 1 shows the schematic of the vacuum system that consists of a sequence of three tubes of cylindrical, conic and cylindrical geometry. The modeling for obtaining the pressure fields and their gradients in the tubular geometry vacuum chamber starts from the identification that the transport of gases occurs in the molecular regime (free molecules) and is a diffusive process. In this way, to reach the solutions in the steady case, the boundary conditions and the initial condition are settled in details. Another hypothesis adopted explicitly is that in the high-vacuum and ultra-high vacuum tube systems the transport of gases is a diffusive process. The general differential equation of the diffusive process for obtaining the pressure field in the steady state is given by

$$c(x)d2p(x)dx2+ dc(x)dxdp(x)dx=-qx \quad (1)$$

where $c(x)$ is the conductance and qx is the function that represents the sources of gas present in the system. The functions $q(x)$ and $c(x)$ are constant for the cylindrical tube but for the conical tube they are dependent on the position x along the tube. Equation (1) is solved at each tube unit and the appropriate boundary conditions of pressure continuity and throughput are established at the pipe junction and at the ends, [1], [2].

3. Results and Discussions

The analytic results for the pressure field in each composition have already been evaluated and the boundary conditions have been applied. Figure 2 shows an overall view of the pressure field over the entire length of the tubes, by considering the case of larger diameter D = 8 cm and smaller diameter of d= 4 cm, equal tube lengths, L= 200 cm and realistic values of the outgassing rates. It is observed that the pressure variation is accentuated at the ends of the tubes, reaching decreasing values in the central region of the tube composition. This type of behavior is typical of all ends pumped vacuum systems and must be considered in all high and ultra high vacuum tube system designs to achieve the expected performance results.

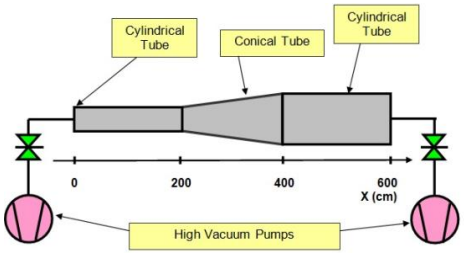

Fig. 1. *Vacuum system composition.*

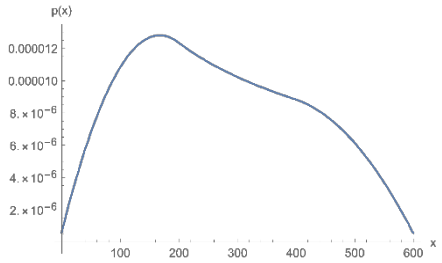

Fig. 2. *Pressure field as a function of the position.*

4. References

[1] F. T. Degasperi, R. M. Ricotta, Vacuum, **188C**, 1-30, (2021).
[2] F. T. Degasperi, R. M. Ricotta, High and Ultra-high Vacuum Pressure Profile and its Gradient of the Conic Tube, submitted to publication, (2022).

*Corresponding Author regina@fatecsp.br

METHODOLOGY FOR CHARACTERIZING NVG SYSTEMS

Duarte, C. B. da S.[1*], Damião, A. J.[1,2]
[1]*Instituto Tecnológico de Aeronáutica (ITA)*
[2]*Instituto de Estudos Avançados (IEAv)*

1. Introduction

Since the mid-1970s, Night Vision Goggles (NVG) have been increasingly used in military aviation [1] and other important surveillance and security tasks. Such devices allow flight at low altitudes, even at night, as they have intensifier tubes that amplify the effects of low light intensity [2]. The manufacturers do not always provide the technical data about the imaging sensors, allied to the fact that the conditions in which the data were taken are not provided. As a result, the identification of the capabilities and limitations of sensors in a given scenario is impaired. Due to the multiplicity of applications, a characterization is necessary for operational knowledge, allowing NVG operators to optimize and expand the use of the system by determining its capabilities, limitations, and the correct exploitation of its resources.

2. Theory

The spatial response of an electro-optical system, mainly concerning the resolution (perception) of details, considering the contrast between the elements of a scene, can be obtained by the Modulation Transfer Function (MTF) [3]. The main objective of this work is to present the development of a methodology to characterize an NVG system and obtain MTF data from the sensor so that it will be possible to identify the real potential of the system in its different applications. The methodology used in this work consists of assembling a standard optical system (camera plus lenses in the visible range of the electromagnetic spectrum) to be coupled to the NVG system under analysis. A known target is used as a standard image; The following images that the system will obtain will be analyzed and compared to the reference image concerning the degradation and other problems of the NVG system.

3. Result and Discussions

The satisfactory analysis of the degradation of the images obtained by the NVG system under study allowed the establishment of a methodology for characterizing the equipment (figure 1), thus enabling the analysis and future characterization of other devices of the same nature.

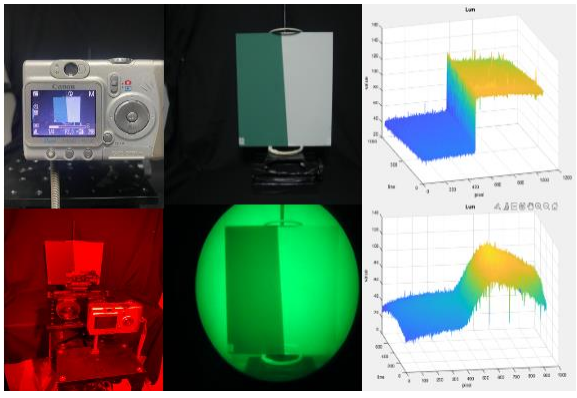

4. References

[1] Abel, D. H. *An image quality analysis of ANVIS-6 night vision goggles.* Wright-Patterson Air Force Base: Air Force Institute of Technology, (1994).
[2] Brickner, M. S. *Helicopter flights with night vision goggles:* human factors aspects. Moffett Field: NASA Ames Research Center (1989).
[3] Boreman, G. D. *Modulation transfer function in optical and electro-optical systems*. 110p. (2001).

Acknowledgments
To the Graduate Program in Operacional Applications at ITA (PPGAO/ITA).

*Corresponding author: charlesbruno_duarte@hotmail.com

CONVOLUTIONAL NEURAL NETWORK ASSESSMENT FOR PERSON DETECTION ON WATER USING INFRARED IMAGERY

Eick, F. B. L.[1]*, Andrade, R. M. de[2], Shiguemori, E. H.[3], Damião, A. J.[3]
[1]*Institute for Operational Applications, São José dos Campos - SP, Brazil*
[2]*National Institute for Space Research, São José dos Campos - SP, Brazil*
[3]*Institute for Advanced Studies, São José dos Campos - SP, Brazil*

1. Introduction

Maritime person-in-water search and rescue missions have to overcome challenges such as the homogeneity and mutability of the environment, the small area above the sea surface and the short time of survival. Thermal sensors allied with YOLOv4 [1], a convolutional neural network (CNN) based automatic object detection method, can help improve the chances of survival.

2. Experimental

A low-cost drone and sensor set was used to acquire real targets (persons and isolated life-vests) on LWIR thermal imagery to train, validate and generalize the YOLOv4 detection method. YOLOv4 Tiny [2], a scaled version of YOLOv4 suitable for limited processing capability, was also used. The influence of four training dataset compositions was evaluated regarding precision, recall and F1 score. The training datasets changed from simple (single height of acquisition) to complex (multiple heights including platform vertical and horizontal displacement). The estimated sensor's maximum distance of detection for human targets was used. An image thresholding technique was used for comparison on the same dataset.

3. Results and Discussions

The evaluated experiments presented higher recalls with more comprehensive datasets. Method's precision remained above 98% on all training datasets. Recall ranged from 19% to 79% considering images beyond the sensor's maximum detection distance and from 29% to 98% within this limit. The YOLOv4 Tiny method achieved slightly better recall with five times lower inference time (66 ms). Triangle [3] thresholding, the conventional technique chosen, did not perform well on the analyzed datasets.

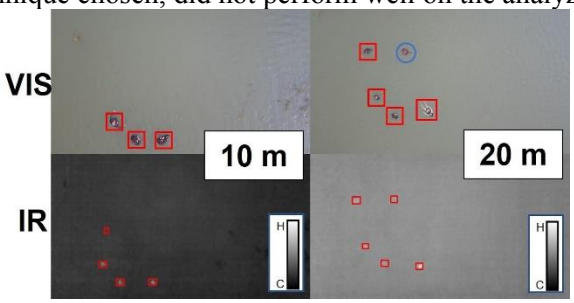

Fig. 1. *Composition of visible image (with ground truths) and thermal image (with detections).*

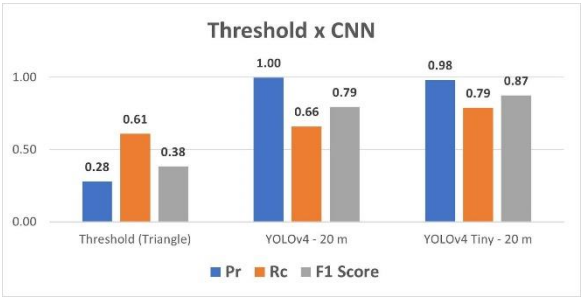

Fig. 2. *Results for the thresholding method against YOLOv4 and YOLOv4 tiny.*

4. References

[1] A. Bochkovskiy, C.-Y. Wang, and H.-Y. M. Liao, arXiv, (2020).
[2] C.-Y. Wang, A. Bochkovskiy, and H.-Y. M. Liao, CVPR, 13029-13038, (2021).
[3] G. W. Zack, W. E. Rogers, S. A. Latt, J Histochem Cytochem, 741-753, (1977).

Acknowledgments
Author Rafael Marinho de Andrade thanks the support of the Coordination for the Improvement of Higher Education Personnel (CAPES) – Financing code 88887.483839/2020-00.

*Corresponding author: eickfble@fab.mil.br

CHARACTERIZATION OF RETAINED AUSTENITE BY X-RAY DIFFRACTION IN A Z-TUFF PM TOOL STEEL

Eickhoff, L. M.[1], Neves, J. C. K. das[1*], Pintaude, G.[1]

[1]*Universidade Tecnológica Federal do Paraná*

1. Introduction

Sintered steels are produced by the powder metallurgy (PM) process, which roughly consists of powder production, proper mixing with additives, compacting, and sintering. The final microstructure is influenced by all these steps, and the product is usually referred to as PM steel. The use of PM to produce tool steels can reach more homogeneous microstructures than conventional metallurgy. It happens because the solidification of small particles during powder production is much less prone to segregate and form large carbides than the solidification of large sections, as in conventional steel making.

PM tool steels are submitted to the same hardening treatments as conventional steels, but due to their higher homogeneity, they exhibit quicker and more predictable responses and more isotropic properties [1]. Since austenite transformation to martensite is commonly incomplete in quenched tool steels, some level of retained austenite is present at room temperature [2] [3] after the process, which limits the hardness of quenched tool steels. Moreover, austenite can be further transformed into martensite, causing dimensional changes. In this context, this work aims to measure by X-ray diffraction the amount of retained austenite in a Z-Tuff PM tool steel (0.7% C – 7.5% Cr – 1.0 %V – 2.0% Mo – 1.5% Ni).

2. Experimental

Four samples of Z-Tuff PM steel were pre-heated at 450 ºC for 120 minutes, then submitted to a second pre-heating at 860 ºC for 20 minutes, fully austenitized for 20 minutes at 1040 ºC, and quenched. To be analyzed as-quenched, one sample(Q1040) was separated from the others. The remaining samples were tempered 1, 2, or 3 times at 560 ºC and named Q1040-1T560, Q1040-2T560, and Q1040-3T560, respectively.

X-ray diffraction (XRD) analyses were performed in a Shimadzu XRD-7000 diffractometer, following the procedures stated in ASTM E975-15 [4]. Vickers Hardness was accessed using an EMCO universal tester, and a Zeiss (EVO MA 15) scanning electron microscope (SEM) was used to characterize the microstructures.

3. Results and Discussions

XRD analyses revealed that most retained austenite was transformed in the first tempering cycle, which agrees with the observed hardness increase, as presented in Figure 1 for Q1040 and Q1040-1T560 samples. The second and third tempering steps led to additional hardness reduction.

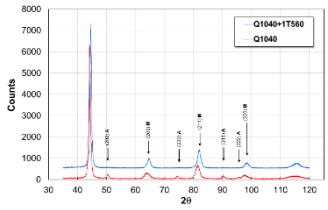

Fig. 1. *XDR patterns of Q1040 and Q1040-1T560 samples.*

4. References

[1] A. L. Silva and P.R. Mei. *Aços e ligas especiais*. 3. ed. Sumaré: Blucher (2010).

[2] J.A Cifuentes et al. *"Dimensional stability of bearing components made of steel SAE 52100 during tempering*"; XV Congresso Brasileiro de Engenharia e Ciência dos Materiais CBECIMAT, BRA (2002).

[3] H. B. Neto et al. "*Magnetic behavior of ABNT 4340 steel after quenching and tempering"*, 60th Annual Congress of ABM, BRA(2005).

[4] American Society for Testing and Materials, ASTM E975-15 (2022).

Acknowledgments

The authors thank ANGRA TECNOLOGIA EM MATERIAIS/Joinville-SC, Multi-User Center for Materials Characterization - CMCM of UTFPR-CT, and Francisco Arieta, Ph.D. Dörrenberg Edelstahl.

*Corresponding author: jkneves@utfpr.edu.br

GENERATION OF IRON OXIDES LAYERS IN ELECTRIC STEELS THROUGH PULSED BIPOLAR PLASMA

Fin, P.*[1], Recco, A. A. C. [1], Fontana, L. C. [1]
[1]*Universidade Estadual de Santa Catarina*

1. Introduction

Low carbon steel samples were oxidized by bipolar pulsed plasma, in order to obtain dielectric layers of oxides. The oxidation treatments through plasma, containing oxygen, were carried out with the samples arranged in two configurations in relation to the plasma: in cathodic potential (CP) and in floating potential (FP) [1]. The main characteristic of the treatment in cathodic potential is an intense ionic bombardment of the surface during the process, while the treatment in floating potential occurs with ionic bombardment of moderate intensity and in equilibrium with electronic bombardment. Furthermore, as the treatment is carried out with pulsed bipolar plasma, ionic and electronic bombardment occurs, interspersed, in both CP and FP configurations.

2. Experimental

Samples of AISI 1006 steel, semi-processed 0.4%-0.5%Si, 0.6 mm thick, were oxidized through plasma generated by ABiPPS (Asymmetric Bipolar Plasma Power Supply [2]. The samples were treated at different time and temperature, namely: 2.0h and 0.5h; 300°C (573K) and 500°C (773K). Prior to the treatment, the samples were polished (with alumina 1,0μm) and cleaned in ultrasound (with isopropanol) during 10 min. The final pressure into the vacuum chamber was 1,3 Pa, and the treatment was carried out in oxygen plasma (99.999%) at working pressure of 67 Pa.

3. Results and Discussions

ABiPPS pulsed bipolar plasma treatment allows a combination of parameters that increases the atomic mobility on the surface, which reduces residual stresses and enables the generation of oxide layers more adherent to the substrate. The oxidation results showed that there was the formation of the two crystalline phases magnetite and hematite, regardless of the oxidation conditions. The oxidation of samples showed growth of the homogeneous oxide layer, with thicknesses between 0.28∓0.04μm for the samples treated in CP and 0.23∓0.04μm for the samples treated in FP. Through the magnetic measurements made using the VSM technique, it was possible to verify that there was no degradation of the magnetic properties of the plates oxidized via plasma, which indicates that the oxide layer was restricted to the surface of the sample, without formation of a very thick oxygen diffusion layer.

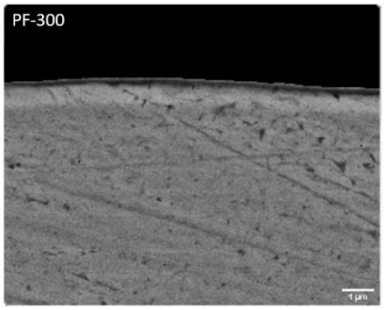

Fig. 1. *Images obtained through the BSE oxide layers cross section of the samples treated in floating potential.*

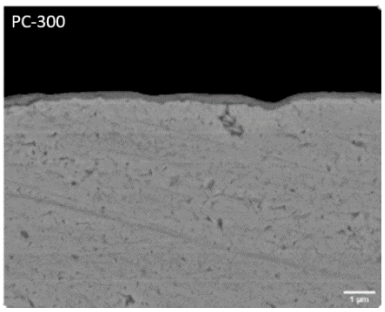

Fig. 2. *Images obtained through the BSE oxide layers cross section of the samples treated in cathodic potential.*

4. References

[1] FROMHOLD JR, A. T.; BAKER, John M. Journal of Applied Physics, **51,** 6377-6392, (1980).
[2] Scholtz J. S., Fontana L. C., Plasma Densification Method, Patent N° US 9,999,118 B2, Jun. 12, (2018).

Acknowledgments
This study was financed in part by the Coordenação de Aperfeiçoamento de Pessoas de Nível Superior- Brasil (CAPES)- Finance code 001.

*Corresponding author: paula.fin89@gmail.com

NICKEL OXIDE THIN FILMS GROWN BY HIPMS AT ROOM TEMPERATURE

Galindo, F. de O.[1], Oliveira, L. P. G. de[1], Cruz, E. C. R. da[1], Bortoleto, J. R. R.[1], Cruz, N. C. da[1] and Durrant, S. F.[1]

[1]*Institute of Science and Technology - Sorocaba Campus - ICTS/Unesp*

1. Introduction

Perovskite solar cells have attracted scholars due to their high efficiency, which has been rapidly improved since the development of the first solar cells in this category, with efficiency of 9.7% to the most recent certified by 22.7% [1]. This was only possible by improving crystal growth processes, modifications in the composition and electronic properties of perovskite film and highly efficient load carrier interface layers [2]. In this study was investigated the HTL (Hole Transport Layer), which is an active material and the role of absorbing photons and converting them into carriers of free charge, for this they must be transparent and have good electrical properties [3].

2. Experimental

The depositions followed the order: the deposition of a conductive and transparent layer of AZO (Zinc Oxide doped with Aluminum - Al2O3) on glass, and on the AZO layer a film of NiOx (Nickel Oxide) was deposited to act as a selective layer of load carriers. Therefore, it is necessary to investigate the optical properties of the layer as a function of the time variation (μs) of the pulse width of the pulsed DC source in HiPMS (High Pulsed Magnetron Sputtering) used for film deposition. This process was performed in a vacuum chamber, with a working pressure of 4 mTorr, using argon as precursor gas and oxygen in NiOx films, the voltage used in the source was 400V, and targets were positioned at a distance of 5 cm from the substrate

3. Results and Discussions

When performing the depositions of the NiOx films, it was possible to obtain films with thicknesses ranging from 224.6 ± 22.4 nm to 649.8 ± 33.2 nm, and, thus proving a variation in the deposition rate according to the variation of the pulse used during plasma. The average electrical resistivity of AZO films was 39.8 ± 3.9Ω, but NiO films have a nonconductive oxide behavior. The optical properties of the films are presented in Figure 1 and 2, the films shown in the figures have an average transmittance of around 80% in the visible region, for the reflectance the films with lower thickness presented a greater amount of interference fringes, due to the greater interaction of the light that passes through the film.

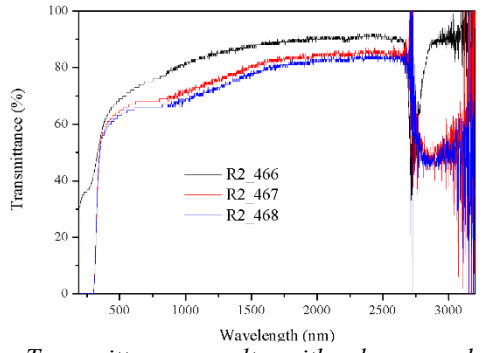

Fig 1. *Transmittance results with plasma pulse time variation in NiO_x samples.*

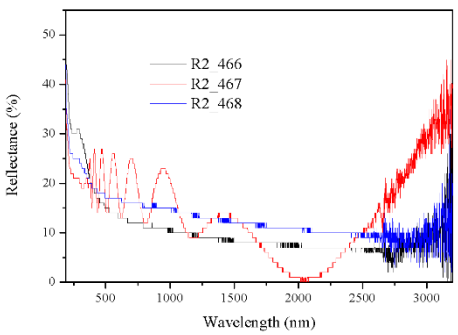

Fig 2. *Reflectance results with plasma pulse time variation in NiO_x samples.*

4. References

[1] Best Research-Cell Efficiencies, National Renewable Energy Laboratory, https://www.nrel.gov/pv/assets/images/efficiency-chart.png, (accessed: January 2018).
[2] B, Dongqin et al, Nature Energy., **1**, 1-5 (2016).
[3] S, Nanhai et al, Solar Energy Materials and Solar Cells., **94**, 2328-2331 (2010).

Corresponding author: felippe.oliveira@unesp.br

SYNTHESIS OF CU/NI-DOPED TITANIUM OXIDE CERAMIC COATINGS BY PEO PROCESS AND THEIR PHOTOCATALYTIC PERFORMANCE

Garcia, U. M.[1], Trivinho-Strixino, F.*[1]
[1] *Universidade Federal de São Carlos – UFSCar, campus Sorocaba, Sorocaba – SP*

1. Introduction

The evolution of large urban centers and the industry's constant evolution cause significant threats to the environment due to the potential for pollution caused by these centers. In recent years the concern with environmental preservation has increased, especially regarding water treatment [1]. The scientific community has increasingly studied oxide semiconductors for photocatalysis and degradation of pollutants, mainly due to their relatively low cost and reuse of the devices used [2]. Oxide doping can reduce energy loss and minimize the phenomenon of electron-hole recombination, enhancing the properties of the semiconductor, thus contributing to the development of new materials capable of degrading pollutants present in water.

2. Experimental

The samples of pure titanium grade 2 - Astm F67 were mechanically polished with sandpaper and degreased. The surface was subsequently treated by PEO plasma-assisted electrolytic oxidation, also known as micro-arc oxidation. Metallic salts containing Cu and Ni were added to the electrolyte for in situ doping of the oxide layer during the surface treatment. After the synthesis of the samples, photocatalysis tests were carried out under UV radiation to degrade the methylene blue solution and rhodamine B control molecules to investigate the photodegradation performance.

3. Results and Discussions

The Ni-doping level was higher when using a current density of 50 mA.com^{-2}, as shown in fig.1. However, the Cu-doping level was not detected using EDS analysis, showing the deposition of this metal on the negative cathode. There is a need for the complexation of metallic salt with the experimental electrolyte to produce negative-soluble anions using different complex salts dissolved in the electrolyte bath. This part of the experiments will be performed in future studies. For Ni-doping experiments, the electrolyte in the concentrations used provides a morphological architecture with grooves, as shown in fig.2.

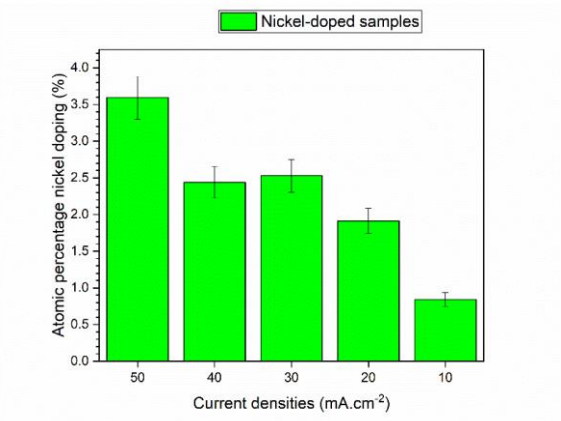

Fig. 1. *Graph of the percentage of nickel incorporated into the oxide layer, showing a significant increase as the current density increases.*

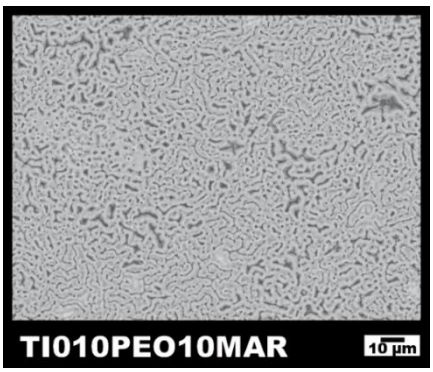

Fig. 2. *Top-view micrograph obtained by SEM of the TiO_2 oxide layer, doped with nickel, showing the elongated pores on the sample's surface.*

4. References

[1] P. Favia and R. D'Agostino, Surf. & Coat. Tech., **98**, 1102-1106, (1998).
[2] F. Parrino, et al. Catalysis Reviews, **61**, 163-213, (2019).

Acknowledgments
Capes, Fapesp, Cnpq, UFSCar, PPGCM .

*Corresponding author: fstrixino@ufscar.br

BACTERIA ANTI-ADHERENT SURFACES PRODUCED BY DBD PLASMAS

Getnet, T. G.[1,2]; Silva, G. F.[3]; Duarte, I. S.[3]; Kayama, M. E.[4]; Rangel, E. C.[1]; Cruz, N. C.[1*]
[1]*Laboratory of Technological Plasmas, São Paulo State University, Sorocaba, SP, Brazil.*
[2]*Department of Chemistry, Bahir Dar University, Bahir Dar, Ethiopia.*
[3]*Laboratory of Environmental Microbiology, Federal University of Sao Carlos, Sorocaba, SP, Brazil.*
[4]*Laboratory of Plasma and Applications, São Paulo State University, Guaratinguetá, SP, Brazil*

1. Introduction

The development of bacterial resistance is a major concern as there is not any antibiotic that is effective against all microorganisms [1]. Owing to that, the search for new agents to eradicate resistant microbes is a matter of public health. In this context, in this work it has been evaluated the possibility to deposit coatings from eugenol and carvacrol natural extracts on stainless steel plates using dielectric barrier discharges.

2. Experimental

The treatments have been performed in a homemade reactor fully described elsewhere [2]. Non-synthetic carvacrol and eugenol monomers were used as film precursor. The coatings have been characterized by SEM, FTIR and contact angle measurements. It has been evaluated the effect of the coatings on the adhesion and proliferation of Staphylococcus aureus, Pseudomonas aeruginosa, Escherichia coli, and Candida albicans.

3. Results and Discussions

As it can be observed in figure 1 which presents FTIR spectra of stainless steel plates coated with carvacrol films deposited with (a,b) and without (c,d) plasma exposure before (continuous line) and after exposure (dotted lines) to UV irradiation, the chemical structure of the coating produced exposing the monomer to the plasma is similar that one of the precursor. The figure also suggests that the plasma deposited film is much more stable than that obtained only with the immersion of the substrate in the oil. As it can be observed in figure 2 the coatings completely inhibited the adhesion of E. coli and decreases in 6 orders of magnitude the amount of adhered S. aureus in comparison with the as-received stainless steel.

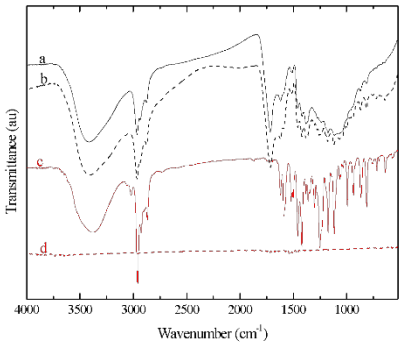

Fig. 1. *FTIR spectra of (a, b) direct coating of carvacrol and (c, d) carvacrol-derived film coated on steel substrate by DBD plasma. The dashed and solid lines are before and after exposing the films to UV-lamp, respectively.*

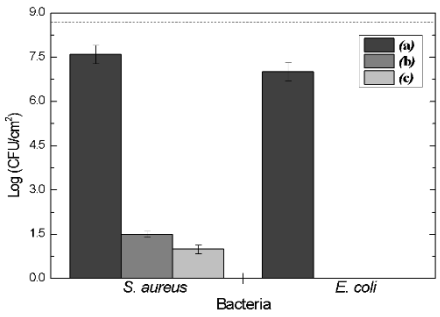

Fig. 2. *The concentration of S. aureus and E. coli on stainless-steel slides as-received (a), immersed for 45 min in liquid carvacrol (b), and coated with plasma deposited carvacrol film (c). The dotted line indicates the concentration of bacteria in the initial inoculum.*

4. References

[1] M. Gross, Antibiotics in crisis, Curr Biol. **23**, R1063-5 (2013).
[2] Getnet, Tsegaye G, et al., Thin Solid Films, **734**, 138833 (2021).

Acknowledgement
The authors thank the Brazilian funding agencies CNPq and FAPESP.

*Corresponding author: nilson.cruz@unesp.br

BETA-METASTABLE TI ALLOYS WITH LOW ELASTIC MODULUS FOR BIOMEDICAL APPLICATIONS

Grandini, C. R., FBSE*
UNESP - Univ Estadual Paulista, Laboratório de Anelasticidade e Biomateriais, 17.033-360, Bauru, SP, Brazil

1. Introduction

The beta-type Ti alloys are arguably the most versatile in the Ti family, and widely used for biomedical applications [1]. In order to design alloys combining superior mechanical characteristics with no cytotoxic effects, the first priority is to understand the microstructure at ambient temperature [2]. When the alloys are cooled rapidly enough from above the β-transus temperature, there is insufficient time for eutectoidal diffusion-controlled decomposition processes to occur, thus the high temperature phase transforms into martensite. For Ti alloys, the high temperature body-centred cubic (bcc) β phase transforms martensitically into a hexagonal close packed (hcp) α′ phase upon quenching, where α′ is crystallographically identical to the equilibrium α phase. On the other hand, the solid metastable β phase may transform, under external stress, into a distorted hexagonal structure designated α″ which has an orthorhombic unit cell. The α″ phase nucleates heterogeneously as thin laths at existing subgrain boundaries [3]. The phase stability of Ti alloys can be altered by the addition of β-stabilising elements of two types, isomorphous and eutectoid. In general, isomorphous β-stabilisers (such as Mo, V, W, Ta and Nb) decompose to form α+β phases with no intermetallic compounds being formed [4-6]. In this study, novel β-Ti metastable alloys with low elastic modulus are presented, aiming orthopedic or dental applications.

2. Experimental

The alloys were melted using an arc-furnace, with water-cooled copper crucible, non-consumable tungsten electrode and argon-controlled atmosphere. Then, the sample was subjected to homogenization heat treatment with a heating rate of 10°C/min up to 1000°C, in which remained at this temperature for 24 h with vacuum better than 10^{-6} Torr and then cooled slowly in the furnace. The alloys' structure was analyzed by X-ray diffraction with the diffractograms submitted to the Rietveld's structural refinement. The crystalline microstructure was obtained by optical and scanning electron microscopy. Selected mechanical properties (hardness and elastic modulus) were performed. The biocompatibility of the alloys were analyzed by indirect cytotoxic test.

3. Results and Discussion

Structural analysis showed a coexistence of α' (hexagonal compact), α" (orthorhombic) and β (body-centered cubic) phases. By means of the Rietveld's method, it was possible to quantify the fraction of these phases in the alloy and observed the variations in the lattice parameters caused by the addition of alloying elements. In the microstructural analysis, the presence of intra-grain needles was observed, characteristic of martensitic phases α' and α", distributed in the β metallic matrix, in agreement with the x-ray diffractogram. The hardness values were above the cp-Ti and Ti-6Al-4V alloy, whereby the solid solution hardening of the alloy. The hardness and elastic modulus of the alloy were modified according to the treatment performed, solution treatments induce the formation of metastable phases that have high hardness and elastic modulus values. In the indirect cytotoxicity test, no cytotoxic effects were observed on the produced alloys.

4. References

[1] S.S. Sidhu, H. Singh, M.A.-H. Gepreel, Materials Science and Engineering C, **121**, 111661, (2021).
[2] S.W. Lee et al., Materials Science and Engineering A, **802**, 140621 (2021).
[3] G.H. Zhao et al., Materials Science and Engineering A, **815**, 141229, (2021).
[4] G.C. Cardoso, M.A.R. Buzalaf, D.R.N. Correa, C.R. Grandini, Metals, **12**, 788, (2022).
[5] P.A.B. Kuroda, B.L.T. Pedroso, F.M.L. Pontes, C.R. Grandini, Metals, **11**, 1507, (2021).
[6] P.A.B. Kuroda et al., J Mater Sci: Mater Med, **31**, 19 (2020).

Acknowledgments
This research was supplied by Brazilian Agencies CAPES, CNPq, and FAPESP.

*Corresponding author: carlos.r.grandini@unesp.br

CARBON NANOTUBES FUNCIONALIZED BY ETCHING FOR USE IN CANCER PHOTOTHERMAL THERAPY USING LIGHT-EMITTING AT DIODE 660 NM.

Hergesel, K. G.[1*], Almeida, L. S. de[2], Nascimento, G. G.[1], Lima, A. D. R.[3], Ferrari, B. B.[3], Santos, L. M. B. dos[3], Oliveira, A. L. R.[3], Manfrinato, M. D.[1,2], Rossino, L. S.[1,2], Oliveira, E. C.[1]
[1] *Faculty Technology of Sorocaba – FATEC, CEETEPS-SP*
[2] *Federal University of São Carlos – UFSCar*
[3] *University of Campinas – UNICAMP*

1. Introduction

Multi-walled carbon nanotubes (MWCNT) are nanometer-scale particles that can cross the cell membrane. However, MWCNTs are hydrophobic and aggregate in contact with the aqueous medium. The present work uses the etching to change the surface of MWCNTs, making them more hydrophilic. We evaluated the uptake of etching MWCNTs by murine melanoma cells (B16F10) and the effect of photothermal therapy using 660 nm LED light.

2. Experimental

MWCNTs were treated by etching for 30 seconds and characterized by XPS, Raman, and TEM tests. For thermal ablation, B16F10 cells were incubated with MWCNTs-0 and MWCNT-F-30s. After 24 hours, cells were exposed to 660nm LED for 5 minutes for three consecutive days. The cytotoxicity by MTT was used to assess cell viability after photothermal therapy.

3. Results and Discussions

MWCNT-30s showed better dispersion in water when compared to MWCNT-0s (Figures 1A and 1D). Etching did not damage the structure of MWCNTs (Figures 1B, 1C, 1E, and 1F). However, the effect of LED ablation was not observed compared to the control.

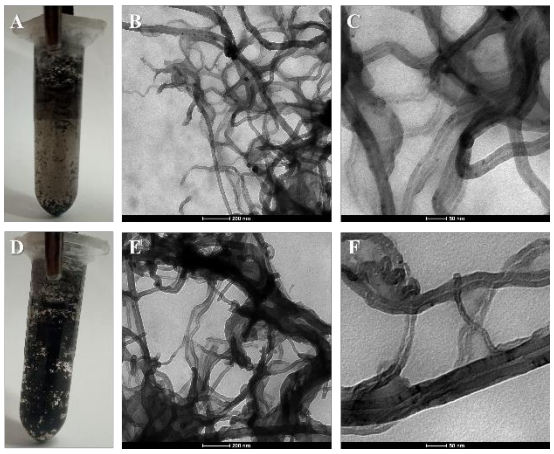

Fig. 1. ***A)*** *Dispersion test on MWCNT-0.* ***B)*** *MWCNT-0 TEM at 200 nm scale.* ***C)*** *TEM of MWCNT-0 with 50 nm scale.* ***D)*** *Dispersion test on MWCNT-30s.* ***E)*** *TEM in MWCNT-30s with 200 nm scale.* ***F)*** *TEM in MWCNT-30s with 50nm scale.*

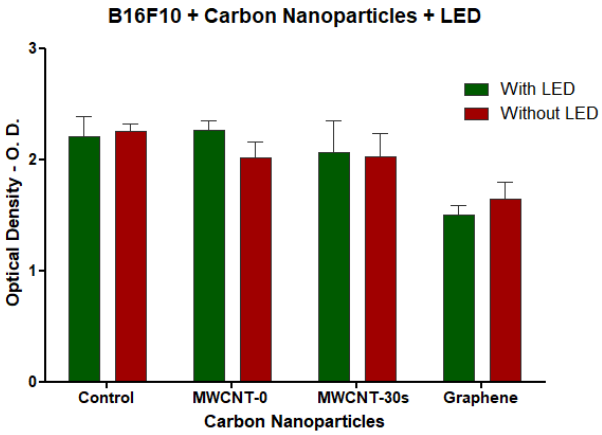

Fig. 2. *Treatment of the B16F10 cell line that internalized functionalized and non-functionalized nanotubes submitted to 660nm LED phototherapy.*

4. References

[1] D. Chudoba and K. Ludzik and M. Jazdzewska and S. Woloszczuk, International Journal of Molecular Sciences. **21**, 1-24 (2020).
[2] R. F. O. Paula and I. A. Rosa and I. F. M. Gafanhão and J. L. Fachi and A. M. G. Melero, A. O. Roque and V. O. Bolderini, L. B. Ferreira and S. P. Irazusta and H. J. Ceragioli and E. C. Oliveira. Nanomedicine: Nanotechnology, Biology and Medicine, **28**, 1-12, (2020).

Acknowledgments
We are grateful to FAPESP, CNPq and CPS for funding the project, also to the Unicamp Institute of Biology.

*Corresponding author: ka.hergesel@outlook.com

DESINFECTION OF N95 RESPIRATORS IN LOW PRESSURE PLASMA

Issaka, R. K.[1], Ribeiro, R. P.[1], Cruz, N. C.[1], Passeti, T.[2], Rangel, E. C.[1]
[1]*Science and Technology Institute of Sorocaba (ICTS), São Paulo State University (UNESP), 511 Três de Março Av., Sorocaba, 18087-180, SP, Brazil*
[2] *Biotechnology and Innovation in Health and Pharmacy Graduate Program, University Anhanguera at São Paulo (UNIAN-SP). Avenue: Raimundo Pereira de Magalhães, 3305. São Paulo, Brazil.*

1. Introduction

With the COVID 19 advent, the use of face respirators was expanded from hospitals and clinics to the daily life routines, increasing waste generation, causing lack of this device and raising its costs. Even in full conditions of use, respirators are discarded after the usage time indicated by the manufacturer has elapsed, once a cost-effective validated sterilization process that guarantee the functionality of the sterilized device does not exist[1]. In this sense, the purpose of this work is to evaluate possible routes of respirators' disinfection in low pressure plasmas using atmospheres containing pure citric acid or those in which citric acid is diluted with O_2, N_2 and Ar.

2. Experimental

Autoclaved Polypropylene's (PP) samples (1,0 cm x 2,0 cm), from N95 commercial respirators, were contaminated by contact, using *Saccharomyces cerevisiae (S. cerevisiae)*ATCC9763. Samples were then exposed to capacitively coupled plasma processes (13.56 MHz, 100 W) stablished from citric acid ($C_6H_8O_7$) alcoholic's solution (10% v/v). Treatments were conducted for 10 min in atmospheres of pure $C_6H_8O_7$ solution and diluting the citric acid solution with 50% of O_2 , with 25% O_2 + 25% Ar and with 25% O_2 + 25% N_2. The plasma was excited by the lowermost electrode. Base pressure was 2.7 Pa (2,0 X 10^{-2} Torr) and working pressure was 9.3 Pa (7,0 X 10^{-2} Torr). It was investigated the effect of the dilution compound (O_2, Ar or N_2) on the number of unities forming colonies (UFC). The wettability, chemical structure and morphology of the PP fabric, were also accessed to evaluate the condition of the fibers after the disinfection procedures.

3. Results and Discussions

All the plasma treatments decreased the UFC, with the reduction degree depending on the composition of plasma atmosphere (Fig. 1). The best result was obtained for pure citric acid treatments while the incorporation of O_2, Ar and N_2, reduced the process efficiency. Just slight changes were observed on the morphology, topography, chemical composition and molecular structure of the fibers. Water contact angle (Fig. 2), a property related to the material outermost layer chemistry and morphology, was not substantially altered, suggesting that the plasma procedures proposed here are harmful to microbiologic culture but not to the fibers.

TEST	GROWTH	RESULTS
Control	(+)	1,5 x 10^6 UFC/mL (± 1,00)
Control / PP	(+)	1,1 x 10^6 UFC/mL (± 0,29)
Citric acid	(-) fungistatic	1,5 x 10^2 UFC/mL (± 0,12)
O_2	(+)	3,0 x 10^4 UFC/mL (± 0,24)
O_2 + Ar	(+)	5,2 x 10^4 UFC/mL (± 0,53)
O_2 + N2	(+)	9,5 x 10^4 UFC/mL (± 0,73)

Fig. 1. *Units forming colonies (UFC) of PP contaminated with S. cerevisiae and treated with plasma composition atmosphere.*

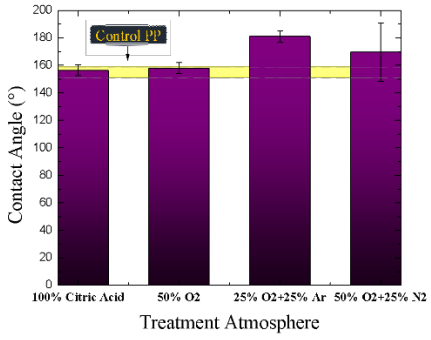

Fig. 2. *Water contact angle of PP fabric as a function of the plasma composition atmosphere.*

4. References

[1] J. C. Bailar and D. S. Burke. *"Reusability of Facemasks During an Influenza Pandemic",* National Academies Press, USA, (2006).

Acknowledgments
Authors thank to FAPESP (2017/21034-1) andCNPq (2021/1929) for financial support.

*Corresponding author: taniaaguiarpasseti@gmail.com

EFFECT OF CARBON NANOTUBE DEPOSITION THROUGH PULSED ELECTRICAL CURRENT IN WATER/CNT SOLUTION ON ELECTRICAL CONDUCTIVITY OF THE JUTE FIBRES

Iwasaki, K. M. K.[1]*, Pinto, L. M.[1], Fontana, L. C. [1] and Becker, D.[1]

[1]*Laboratory of Plasmas, Films and Surfaces Centre for Technological Sciences, UDESC, Joinville, Santa Catarina 89.219-70, Brazil*

1. Introduction

Natural fibres are composed predominantly of cellulose, hemicellulose, and lignin. Due to the cellulose and lignin presence, they have inherent electrical insulating properties [1]. According to Zhuang et. al [1], by depositing carbon nanotube on the jute fibres (JF) surface, it is possible to obtain an electrically conductive surface. Considering this fact, this preliminary study investigates the effect of the carbon nanotube (CNT) deposition through pulsed electrical current in water/CNT solution on the electrical conductivity of the jute fibres. Aiming to obtain an effective deposition, this process which is an adaption of the Electrophoresis Deposition Process (EDP) was performed using different conditions, such as pulse types and solution (medium) types.

2. Experimental

Table 1 summarizes the composition of each medium and pulses type adopted in the EDP. As shown, five mediums were prepared. For facilitate the medium identification it was used the following abbreviations. The MCNT abbreviation means that was insert MCNT (Multi-wall type with 95 %) purity on the medium. In other hand, H_2O represents deionized water and SDS represents Sodium Dodecyl Sulphate (anionic surfactant). Also, to represent the positive pulses it was adopted $2p^+$ and to identify positive and negative pulses it was used $2p^+2p^-$. JF analysed were extracted from woven fabric purchase from Castanhal Textile Company. As can see in Tab. 1, Sample 1 to 4 were submitted in the EDP, Sample 5 is the JF as received. The electrical and reactor configuration used was based on Dos Santos *et. al* [2] study. The $2p^+$ and $2p^+2p^-$ were generate in the Asymmetric Bipolar Plasma Power Supply (A.BiPPS). $2p^+$ was set around 800 V while $2p^-$ around -600 V. All the samples were submitted in the process at 30 min.

Tab 1. *EDP parameters such as pulse type and medium type of each sample.*

Sample	1	2	3	4	5*
Pulse type	$2p^+2p^-$	$2p^+$	$2p^+$	$2p^+2p^-$	-
Medium	MCNT+H_2O+SDS	MCNT + H_2O +SDS	MCNT + H_2O	MCNT + H_2O	-

* JF as received.

To perform the electrical characterisation, the samples were cut into short lengths to fill 1 cm2 of area. The thickness of the samples was around 0.0085 mm. The impedance values were measured using Potentiostat Gamry (1010e). Voltage amplitudes around 10 mV (rms) was applied during AC impedance spectroscopy. The frequencies ranged from 1 to 10^4 Hz.

3. Results and Discussions

It is expected to increase electrical conductivity in the samples submitted in EDP treatment with surfactant medium due to the effective dispersion of CNT.

4. References

[1] Zhuang, R. C., Doan, T. T. L., Liu, J. W., Zhang, J., Gao, S. L., & Mäder, E., Carbon, **49**, 2683-2692, (2011).
[2] dos Santos, V. F., Fontana, L. C., Sagás, J. C., Missner, M. E. P., & Becker, D., Journal of Applied Physics, **129**, 123302, (2021).

Acknowledgments
The authors would like to acknowledge the financial support for CNPq, FAPESC and PROMOP.

*Corresponding author: kelvin.iwasaki@edu.udesc.br

ROLE OF MOLECULAR SPECIES IN COLD ATMOSPHERIC ARGON PLASMA: A GLOBAL MODEL STUDY

Karnopp, J.[1]*, Sagás, J. C.[2], Pessoa, R. S.[1]
[1]*Instituto Tecnológico de Aeronáutica – São José dos Campos*
[2]*Universiade do Estado de Santa Catarina - Joinville*

1. Introduction

Cold atmospheric pressure argon plasma is widely used for a variety of applications in materials science, medicine, and engineering. Plasma chemistry is affected by the gas pressure. For low pressure, the main species present in discharge volume are argon in ground state (Ar), argon ion (Ar^+), and excited (Ar^r, Ar^p) and metastable (Ar^m) atoms. However, at high pressures, other species become relevant in the plasma chemistry as highly excited and molecular species. Some studies include molecular ion or dimer (Ar_2^+) and molecular metastable or excimer (Ar_2^m) at atmospheric pressure in plasma model, but a few experimental information was obtained [1]. The plasma modelling is essential to understand the plasma chemistry and the influence of process parameters, such as gas flow and applied power. In this work, a (zero dimensional) global model [2] for atmospheric argon plasma was developed for study how the species Ar_2^+ and Ar_2^m affect the plasma chemistry.

2. Methodology

In this model, two cases were studied. In the case 1, only atomic species were considered, Ar, Ar^+, Ar^r, Ar^p and Ar^m. In the case 2, Ar_2^+ and Ar_2^m were included in the model. The reaction set includes electrons impact reactions, heavy species reactions and three body reactions. The Maxwell-Boltzmann distribution was considered for electrons. The simulations were performed for atmospheric pressure and absorbed power range of 1 W to 30 W. The software Comsol Multiphysics 6.0 was used to solve the problem.

3. Results and Discussions

Figure 1(a) shows the electron temperature for both cases as function of absorbed power. The electron temperature does not change significantly with power increases. The presence of Ar_2^+ and Ar_2^m species in plasma increases electron temperature and approaches experimental values [3]. The electron and ion densities increase with the absorbed power as observed experimentally (Fig. 1(b)). For case 2, the electron and atomic ion density are lower than for case 1. In case 2, two ionic species are considered, Ar^+ and Ar_2^+, and the density of molecular ion is higher than that of atomic ions.

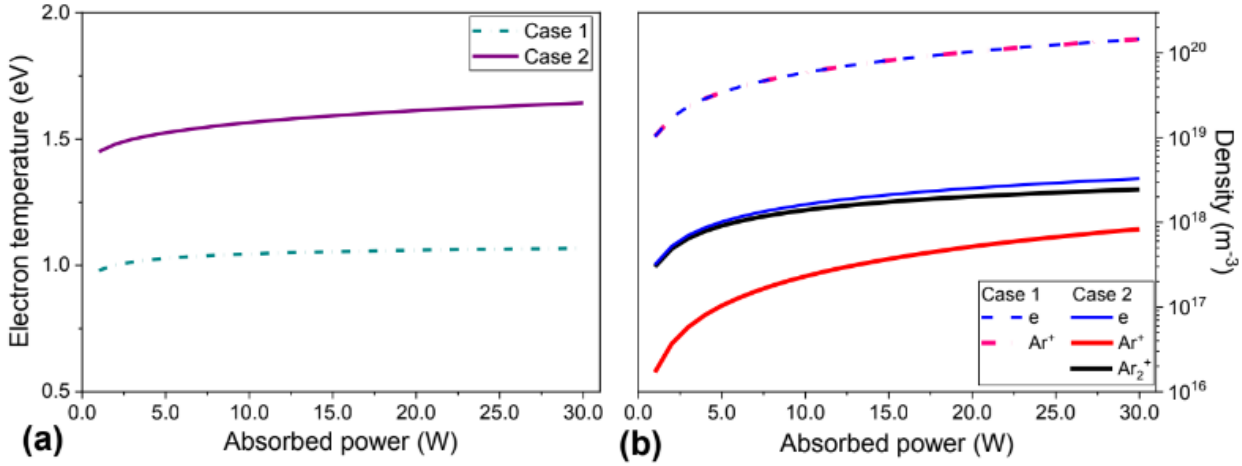

Fig. 1. *Electron temperature (a) and density of electrons and ions (b) for cases 1 and 2 as function of absorbed power.*

4. References

[1] J. Golda et al., Plasma Processes Polym. **17,** e1900216, (2019).
[2] L. L. Alves, A. Bogaerts, V. Guerra, M. M. Turner, Plasma Sources Sci. Technol., **27,** 023002, (2018).
[3] G. Nayak. et al., J. Appl. Phys. **128**, 243302, (2020).

Acknowledgments
Júlia Karnopp thanks CAPES (Finance Code 001) for the scholarship.
*Corresponding author: julia_karnopp@outlook.com

REDUCING ZINC OXIDE DEGRADATION EFFECT ON POLY (ACID LACTIC) MATRIX BY PLASMA SURFACE TREATMENT

Klok, L. A.[1]*, Steffen, T. T.[1], Sabedra, H. R.[1], Fontana, L. C.[1], Becker, D.[1], Marega, F. M.[2], Harb, S. V.[2], Cunha, D. A.[2], Pessan, L. A.[2], Costa, L. C.[2]

[1] *Center for Technological Sciences, UDESC, Joinville, Santa Catarina, Brazil*

[2] *Federal University of São Carlos, São Carlos, São Paulo, Brazil*

1. Introduction

Poly (acid lactic)/zinc oxide (PLA/ZnO) nanocomposite is a promising material for producing scaffolds used in bone regeneration. One challenge on this application, however, regards to ZnO degradation effect on PLA matrix, which can be overcome by ZnO functionalization [1]. Therefore, this work proposes the treatment of ZnO surface by plasma, using liquid lactic acid (LA) as a functionalization agent, to reduces the nanoparticles effect on the PLA degradation.

2. Experimental

The solid ZnO was manually mixed with LA in a mass proportion of 30:70. The sample was treated in a cylindrical (h=2 cm, Ø=6 cm) homemade reactor, configured as capacitively coupled plasma (Fig.1). A radio frequency source, set as 35 W power supply was used, conducted by 5 minutes. After treatment, the sample was washed with distilled water to remove unreacted molecules, following a method described by Steffen et al. [2]. The nanocomposite processing was performed with 10 % in mass of ZnO particles, in a mixing chamber coupled with a Haake torque rheometer, model Rheomix 600p (CCDM/UFSCar), with counter-rotating and semi-interpenetrating roller-type rotors at 175 ºC. Mixing and dispersion occurred for 5 minutes at a rotation of 60 rpm.

3. Results and Discussions

Figure 2 shows torque results for pure PLA, nanocomposites with pristine ZnO (PLA_ZnO) and treated ZnO (PLA_t_ZnO). For PLA_ZnO sample the viscosity is reduced in comparison to pure polymer, indicating that ZnO addition contributes to the degradation of the PLA matrix, which agrees to the literature. For PLA_t_ZnO sample, it can be observed that torque curve is closer to the one of pure PLA. After 5 minutes of mixture at 175 °C, the torque value was recorded as 6,2 Nm for pure PLA, 0,2 Nm for PLA_ZnO and 2,7 Nm for PLA_t_ZnO. Regarding to torque value of pure PLA, that corresponds to a variation of 97 % (PLA_ZnO) and 56 % (PLA_t_ZnO). It suggests that plasma functionalization of ZnO with LA reduces the effects of ZnO on PLA matrix degradation.

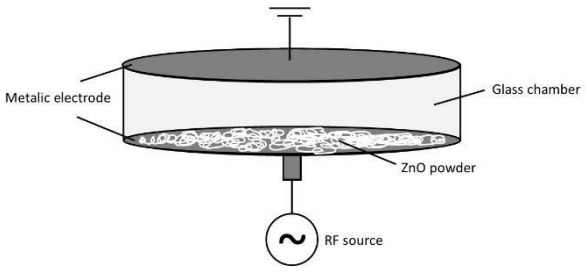

Fig. 1. *Schematic representation of plasma reactor used to treat ZnO powder sample.*

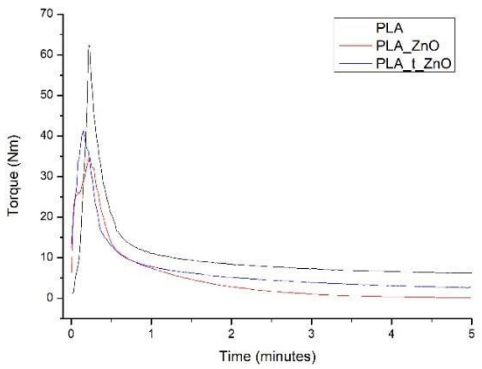

Fig. 2. *Torque curves of pure PLA, PLA_ZnO and PLA_t_ZnO samples.*

4. References

[1] I. Armentano, et al. Polym. Degrad. Stab, **95**, 2126-2146, (2010).

[2] T. T. Steffen, et al. Appl. Surf. Sci, **491**, 405-410, (2019).

Acknowledgments

This work was supported in part by FAPESC [project 2020TR1450] and by FAPESP [project 2019/27415-2].

*Corresponding author: laryssaklok@gmail.com

SURFACE TREATMENT OF POLYPROPYLENE USING A CONICAL APPJ-LIKE

Kodaira, F.V.P.*, Leal, B.H.S, Tavares, T.F., Kostov, K. G.
São Paulo State University (UNESP), School of Engineering, Guaratinguetá, SP, Brazil.

1. Introduction

The development of new atmospheric pressure plasma sources is increasing every year to overcome previous limitations, adapt them for new applications, and optimize existing ones. In this work a funnel-shaped atmospheric pressure plasma jet (APPJ) was used to overcome some limitations of previous devices, such as parallel plate DBD and traditional APPJs for material treatment. Both the DBD and the normal APPJs have a limitation for the treatment of materials, the first needs to operate with very small distances between the plates, no more than a few millimeters, and although efficient for the treatment of large areas, it is unfeasible for the treatment of thick and irregular samples, while the second can act freely on the surface of any sample regardless of geometry, however it acts in a very small region, a few times larger than the size of the plasma plume, which does not exceed a few millimeters, this makes the treatment of large areas costly in time and resources [1–3]. The conical APPJ proposed in this work tries to overcome these cited difficulties of the previous devices. Having a large output (75 mm) it can treat a much larger surface area than traditional APPJs, while not having close parallel plates allows greater freedom as to the geometry of the sample.

2. Experimental

The plasma device consists in a glass funnel with Ø75mm nozzle and 70mm in height, a pin-to-plate pair of electrodes with the plate electrode covered by glass which also serves as sample holder. A pulsed voltage at 25KHz in burst mode with 2ms period and 12 cycles was applied to the needle-shaped electrode, the discharge power was around 7W. 50x20x1mm samples of Polypropylene (PP) were treated for 60, 180, and 300s. The wettability (by water contact angle (WCA)) and their molecular structure (by FTIR) were measured. Both faces of the polymers were measured, as it was observed that the treatment occurs on both the side facing up and the side facing the sample holder.

3. Results and Discussions

The discharge power was around 7W, measured by the VxQ Lissajous figure method.[2]

The FTIR showed the presence of oxygen groups (C=O at 1720 cm^{-1}) on the top side of the samples and nitrogen groups (amide around 1650 cm^{-1}) on the bottom side, the presence of those groups increased with the treatment time. The WCA decreased on both faces, on the top face from 95 to around 80 degrees for 1 minute of treatment and 70 degrees for 5 minutes of treatment, on the bottom face it decreased to 50 degrees for 1 minute of treatment and 20 degrees for 5 minutes of treatment. Despite the lower reduction of the WCA in comparison with the bottom face of the sample, the top face presented more homogeneous values along its surface.

4. References

[1] J. Winter, R. Brandenburg, K.D. Weltmann, Plasma Sources Sci Technol, **24**, 1-11, (2015).
[2] T.S.M. Mui, R.P. Mota, A. Quade, L.R. de O. Hein, K.G. Kostov, Surf Coat Technol, **352**, 338-347, (2018).
[3] M.J. Shenton, G.C. Stevens, J Phys D Appl Phys, **34**, 2761–2768 (2001).

*Corresponding author: kodaira.felipe@gmail.com

APPLICATION OF FUNNEL-SHAPED COLD PLASMA JETS FOR PIGMENTATION ENHANCEMENT OF COMMERCIAL TEXTILES.

Leal, B. H. S.*, Kodaira, F. V. P., Kostov, K. G.
Universidade Estadual Paulista (UNESP), Faculdade de Engenharia de Guaratinguetá (FEG), Guaratinguetá, SP, Brazil

1. Introduction

The ironing of warp fabric after weaving is a very common practice in the textile industry, it increases the tensile and friction resistance of the fabric, however the ironing hinders pigmentation processes. To better adapt the fabric for pigmentation, chemical reagents are often used in aqueous media, which often produce residues that are harmful to the environment. With the advance of the environmental concern new strategies and treatments are being developed, one of them is the plasma treatment, which, different from the usual, besides allowing a better acceptance of the pigment on the fabric, has a low impact [1]. The atmospheric plasma jets (APPJs) have been gaining more and more space in the industry because they do not require vacuum systems, which are usually expensive, and often are not limited to the region of the reactor, which allows the treatment of long surfaces. However, APPJs must be operated at high voltages, in the kV range, which makes the production of power supplies more expensive. In addition, the volume of plasma generated is relatively short, often limited to a point plume of a few millimeters, which makes the homogeneous treatment of large surfaces difficult. The funnel-shaped jet is a reactor with a considerable output (64 mm diameter), which allows it to treat a large region homogeneously.

2. Experimental

The funnel-shaped reactor is composed of a glass funnel with 64mm outlet, two electrodes one needle-shaped attached to the smallest opening of the funnel and the other flat circular positioned below the dielectric barrier of the system and grounded, a glass plate 6mm thick. The high voltage source was associated with a function generator and an oscilloscope, which also made measurements of the system's current and transposed charge through auxiliary circuits associated with the grounded electrode [2]. To perform the study, samples of commercial fabrics with dimensions of 25mm x 50mm were treated, the materials chosen for the treatment were 100% Cotton and 67%Polyester 33% Cotton fabrics. The samples were treated at different exposure times and subjected to capillarity tests with a solution of methylene blue in distilled water [3]. The mass absorbed by the samples were compared with that of an untreated control sample, in addition the height of the solution absorbed by capillarity was characterized.

3. Results and Discussions

The height of the absorbed column and the mass absorbed by the materials increased significantly according to the treatment time, thus indicating that the treatment was able to superficially alter the samples. In addition, according the evaluation of the treatment regarding the absorption time, it was possible to indicate that both materials reached absorption saturation within 20 min of exposure to the solution.

4. References

[1] Poll, H. U., U. Schladitz, and S. Schreiter. Surface and Coatings Technology **142,** 489-493, (2001).
[2] Mui, Taiana She Mir, et al. Surface and Coatings Technology **352**, 338-347, (2018).
[3] Ferrero, F. Polymer testing **22.5,** 571-578, (2003).

Acknowledgments
The authors would like to acknowledge CAPES for the financial support in Brazil.

*Corresponding author: silva.leal@unesp.br

UV-VIS SPECTROSCOPY AS A TOOL FOR DETECTION OF LONG-LIVED REACTIVE SPECIES IN PLASMA-ACTIVATED LIQUIDS

Lima, L. G. de*, Marcondes, M. S., Neto, B. D. B., Júnior, W. C., Pessoa, R. S.
Laboratório de Plasmas e Processos (LPP), Departamento de Física, Instituto Tecnológico de Aeronáutica – São José dos Campos

1. Introduction

Plasma-activated water (PAW) or plasma-activated liquid (PAL) is generated by activating cold plasma at ambient pressure. The activation process produces long-life reactive species in water or liquid, such as reactive oxygen and nitrogen species (RONS), namely nitrite (NO_2^-), nitrate (NO_3^-), nitrous acid (HNO_2), ozone (O_3), and hydrogen peroxide (H_2O_2). With this, PAW plays an important role for multidisciplinary branches of science and gains prominence due to its applicability in medicine, dentistry, agriculture and food sciences [1,2]. Moreover, with the significant increase in applications of PAW and PAL, it is necessary to understand which RONS can be formed and how they are formed, in addition to the quantification of their concentrations that may vary from application to application. For example, for inactivation of bacteria and fungi it is necessary to increase concentrations of H_2O_2 and O_3, in the case of agricultural applications, higher concentrations of nitrate and nitrite are desired [2]. Therefore, the present work uses UV-VIS optical absorption spectroscopy to detect RONS in different activated liquids.

2. Experimental

For this study, different types of liquids were used as targets, namely tap water, filtered water, distilled water, deionized water, and saline solution. Cold plasma at ambient pressure was generated by a gliding arc discharge of the direct vortex flow reactor [2]. The target liquids were placed in Petri dishes and positioned 0.5 cm from plasma, activated at times of 1.0, 2.0, 3.0, 4.0, 5.0, 10.0, 15.0, 20.0, 25.0, 30.0, 40.0, 50.0, and 60.0 minutes. Before and after activation, the physical-chemical parameters were measured, such as pH, oxidation-reduction potential (ORP), TDS (total dissolved solids) and electrical conductivity (σ). Finally, UV-VIS spectra were obtained with the aid of UV-VIS optical absorption spectroscopy. The spectra were deconvoluted with the aid of gaussians and the peaks of NO_2^-, NO_3^-, HNO_2, O_3, and H_2O_2 were identified with the help of the literature [3].

3. Results and Discussions

For all activated liquids we obtained a reduction of the initial pH in the first minutes of activation, and in 3.0 min a pH of approximately 3.5 was reached for all liquids. After 60.0 min of activation the liquids reached pH values of the order of 2.5. It was evident the dependence of ORP with pH, where there was a directly proportional increase with the reduction of pH. In contrast, conductivity increased with increased TDS. Deconvoluted UV-VIS spectra show that from the third minute of activation the appearance of HNO_2 already begins, which is evidenced between 320 and 400 nm. For all liquids, the species of NO_3^- was the one with the highest concentration, being approximately 50% for all. In contrast, the saline solution presented 39% of NO_3^-, and two new species HCl (~1%) and HOCl (~1%) appeared, probably due to the saline solution containing NaCl in its composition. Therefore, UV-VIS optical absorption spectroscopy proved to be efficient in detecting and quantifying the concentration of long-life reactive species in PAW and PAL.

4. References

[1] Milhan, N.V.M. et al. Int. J. Mol. Sci. **23**, 4131, (2022).
[2] Chiappim et al. Water, **13**, 1480, (2021).
[3] Jan Birkmann, et al. Water Practice and Technology 1, **13**, 879–892, (2018).

*Corresponding author: luanlgl@outlook.com

ABRASIVE WEAR IN WHITE CAST IRON HIGH CHROMIUM

Lopes, M. A. [1,2], Araújo, R. M. R. [1,3], Florêncio, O. [4]*
[1]*Mackenzie Presbyterian University, CEP 01302-907, São Paulo-SP, BR.*
[2]*Weir Minerals, CEP 13213-085, Jundiaí-SP, BR.*
[3]*Institute for Technological Research, CEP 05508-901, São Paulo-SP, BR.*
[4]*Federal University of São Carlos, CEP 18052-780, Sorocaba-SP. BR*

1. Introduction

White cast iron high chromium have been widely used in applications where large losses of materials occur through abrasion, for example in the cement industry and in the mining industry..

2. Experimental

In metal casting, in the heat transfer process during solidification, the cooling rates, the solidification times and the thermal profiles in the metal and in the mold are fundamental parameters, the knowledge of which is important for the final control of the part. A silica sand mold with step profile in different thicknesses was used, allowing solidification with different rates of heat extraction and different types of refinements in the microstructure of the metal alloy [1]. The abrasion wear test with a rubber wheel will be carried out in the abrasometer equipment belonging to the Laboratory of Surface Phenomena of USP (LFS/USP).

3. Results and Discussions

Figure 1 shows the influence of the cooling rate on the refinement of the microstructure, where the sample 1, for having a smaller thickness (4.00 ± 0.02 mm), solidifies faster and, the sample 4, for having a greater thickness (22.00 ± 0.02 mm), solidifies more slowly, resulting in larger austenite dendrites and, consequently, larger free distances between carbide eutectic regions. This work analyze the influence of microstructure refinement on wear resistance, so it was necessary to calculate the spacing between eutectic regions of carbides, in order to correlate with the variation of mass loss of the specimen and thus determine the abrasive wear curve. The finest microstructures were for the less thick specimens and the coarser microstructures on the thicker samples. The abrasive wear decreased with increasing mean free spacing between eutectic carbide regions (Figure 2). The abrasion wear test was carried out according to the ASTM technical standard - G65.

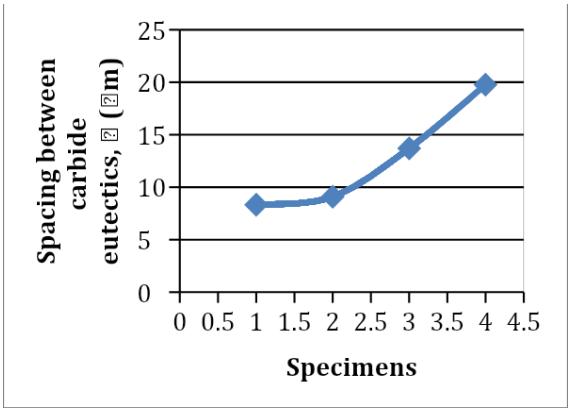

Fig. 1. Variation of the spacing between carbide eutectic.

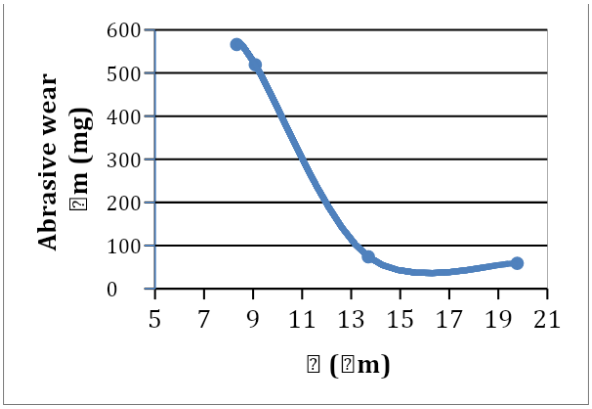

Fig. 2. Abrasive wear curve

4. Reference

[1] American Society for Testing and Materials. **ASTM-G65**, (2015).

*Corresponding author: odila@df.ufscar.br

EFFECT OF HEAT TREATMENTS ON TI-10MO-XMN ALLOYS (X = 0, 2, 4, 6 AND 8 %P) FOR BIOMEDICAL APPLICATIONS

Lourenço, M. L.[1]*, Grandini, C. R.[1]
[1]*UNESP – Univ. Estadual Paulista, Laboratório de Anelasticidade e Biomateriais, 17.033-360, Bauru, SP*

1. Introduction

With improved quality of life, people are living longer and better. In this sense, life expectancy has increased, increasing the number of the elderly population in the world. There was a need for prostheses and implants to have a longer useful life without causing harm to the patient [1]. Therefore, studies have increased in development of new materials. Targeting β-type Ti alloys are alloys with a low modulus of elasticity [2]. The objective of this work was to study the influence of heat treatments on the structure and microstructure, as well as some selected mechanical properties of Ti-10Mo-xMn alloys (x = 0, 2, 4, 6, 8).

2. Experimental part

The alloys were melted in an arc furnace. The chemical analysis of the samples was performed by EDS measurements, chemical mapping, and density with the Archimedes method. After melting, the ingots underwent a 10-6 Torr vacuum homogenization heat treatment (TT), followed by hot rolling and subsequent annealing TT. From there, some aging TTs were performed with a temperature below the β-transus temperature: the TT varied in time (1, 3, and 6 h) and temperature (300, 450, and 600 ºC) with rapid cooling with water [4]. In each condition, structural characterization was performed using X-ray diffraction with Rietveld analysis. For the microstructural characterization, optical and scanning electron microscopy measurements were used. The microhardness and elastic modulus of the alloys in question were also analyzed.

3. Results and Discussion

The alloys showed good homogeneity, with no segregation of alloying elements and chemical composition close to the nominal value, proving the ideal stoichiometry of the ingots. The structural characterization showed the predominance of the beta phase in all conditions studied, which was corroborated by the images obtained in the optical micrographs and scanning electron micrographs. The alloys were β-metastable, with a low modulus of elasticity, and sensitive to the treatments performed, which were associated with previous results of biocompatibility, showed promising results to be used as a biomaterial.

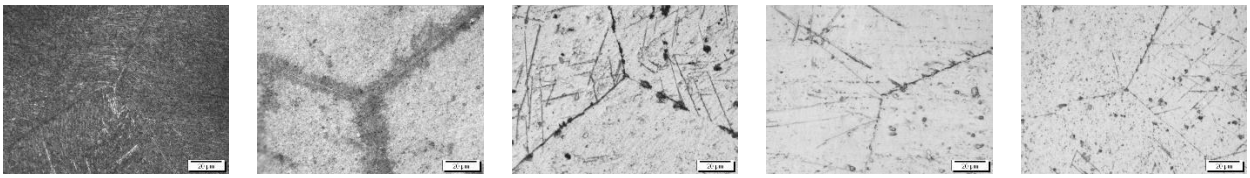

(a) Ti-10Mo (b) Ti-10Mo-2Mn (c) Ti-10Mo-4Mn (d) Ti-10Mo-6Mn (e) Ti-10Mo-8Mn

Fig. 1. *Optical micrographs of the alloys at 1000x magnification, after TT annealing.*

4. References

[1] C.-T. Wu, et al, Materialia, **21**, 101313, (2022).
[2] S.S. Sidhu, H. Singh, M.A.-H. Gepreel, Materials Science and Engineering: C, **121**, 111661, (2021).
[3] H. Li, Q. Cai, S. Li, H. Xu, Journal of Materials Research and Technology, **16**, 588-598, (2022).
[4] M.L. Lourenço, F.M.L. Pontes, C.R. Grandini, Metals, **12**, 527, (2022).

Acknowledgment
The authors thank CAPES, CNPq, and FAPESP for their financial support.

*Corresponding author: mariana.lourenco@unesp.br

DEVELOPMENT OF A HYBRID JOINT BETWEEN THE AA2024-T3 TREATED BY PLASMA ELECTROLYTIC OXIDATION (PEO) WITH PEI/GLASS FIBER LAMINATE

Lucas, R. R.[1]*, Marques, L.F.B.[1], Mota, R.P.[1]
[1]*Department of Physics, School of Engineering, São Paulo State University (UNESP), Av. Dr. Ariberto Pereira da Cunha, 333, Pedregulho, 12516-410, Guaratinguetá, SP, Brazil.*

1. Introduction

Among the methods of joining dissimilar materials, welding bonding is one of the most promising, due to its good cost vs. benefit ratio [1]. To improve surface adhesion, several techniques are employed, a recent technique in the literature is plasma electrolytic oxidation (PEO), that in addition to improving the tribological properties of light alloys, such as aluminum, improves chemical properties and increases the surface area with typical microstructures of the process, which ensure a mechanical locking with the polymer matrix of the composite [2, 3].

2. Experimental

In this study the AA2024-T3 aluminum alloy was used based on the ASTM D1002:10. Treated by the PEO method, with a voltage of 380V (DC) and varying the time in 120, 210 and 380 seconds, with alkaline electrolyte based on Na_2SiO_3 (15 g/L) and with addition of Na_3PO_4 (1.5 g/L). After the anodizing process, the treated alloy was subjected to oxy fuel welding (OFW) along with a sheet of thermoplastic composite material, with the distance from the torch nozzle to the samples in 30 mm and heating time in 100 seconds. To evaluate the shear strength of the hybrid joint, a mechanical testing machine of the brand Shimadzu AG-X was used, based on ASTM D-1002:2010, with a displacement of 1.5 mm/min and a load module of 50kN.

3. Results and Discussions

It was observed that the hybrid joint presented shear strength values of 1.7 to 4.1 MPa, as shown in Figure 1, with good mechanical anchoring between the polymer matrix and the oxide PEO coating, but in some points, compared to other joining methods such as adhesive joining (up to 30 MPa), the welding joining process needs to have optimized parameters, it is observed that the oxide coating rupture demonstrating its fragility, due to Si concentrations in the coating, favoring its fracture [3] as shown in Figure 2.

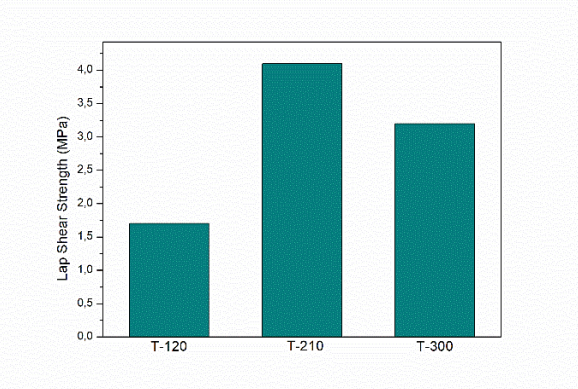

Fig. 1. *Hybrid AA2024 T3/PEI Fiberglass Joint Shear Strength*

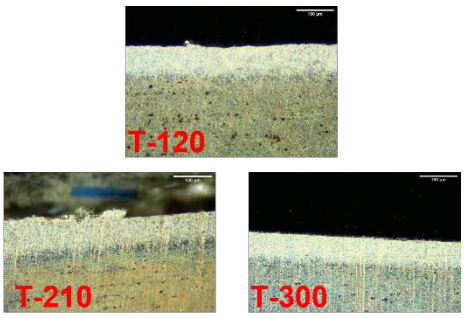

Fig. 2. *PEO-treated alloy cross section microscopy*

4. References

[1] Oliveira, V. S. et al., Welding Journal, **100**, 142-149, (2021).
[2] Lucas, R.R. et al., MRS Communications, **12,** 266–271 (2022).
[3] Shore, D. et al., Surface And Coatings Technology, **428**, 127898 (2021).

*Corresponding author: rr.lucas@unesp.br

MECHANICAL PROPERTIES OF BULK METALLIC GLASSES BASED IN ZIRCONIUM ALLOYS

Lustosa, C. J. R.[1*], Marques, P. W. B.[2], Almeida, A.[3], Vilar, R.[3], Florêncio, O.[4]
[1] *Mackenzie Presbyterian University, CEP 01302-907, São Paulo-SP, BR.*
[2] *Federal University of São Carlos, CEP 13565-905, São Carlos-SP, BR.*
[3] *Instituto Superior Técnico, CeFEMA-Center of Physics and Engineering od Advanced Materials, Universidade de Lisboa, 1049-001, Lisboa, PT*
[4] *Federal University of São Carlos, CEP 18052-780, Sorocaba-SP. BR.*

1. Introduction

Bulk metallic glasses (BMG) are materials with absence of atomic structural order (amorphous). Their properties are very different from those of their crystalline counterparts of the same composition, showing high resistance to compression, higher elasticity, and absence of ductile-brittle transition.

2. Experimental

This work presents a study of the mechanical properties of BMG with two compositions ZrAlCu and ZrAlCuEr alloys, produced by arc furnace melting. The structural characterization has been done by X-ray diffraction (Rigaku Miniflex II diffractometer). The microstructural characterization was performed by scanning electron microscopy (Jeol JSM-6510 microscope), with an attached EDS (Energy Dispersive X Ray Spectrometer) module for elemental microanalysis. The mechanical properties (elastic modulus and indentation hardness) were evaluated by indentation tests (Shimadzu ultramicroindenter, model DUH-211S).

3. Results and Discussion

Optical microscopy observation of the cast samples confirms the respective integrity, and the absence of defects like cracks or pores formed in the fabrication process. The XRD analysis of the $Cu_{47.75}Zr_{47.75}Al_{4.5}$ alloy shows that it is only partially amorphous, while the $Cu_{47.5}Zr_{45.5}Al_5Er_2$ alloy presents absence of crystalline phases. The values of elastic modulus (E) and indentation hardness (H_i) measured in both alloys are presented in the tables below. The results show a higher standard deviation percentage for the CuZrAl alloy (35% in elastic modulus and 24% in hardness) than for the ZrAlCuEr alloy (standard deviation percentage of 16% in elastic modulus and 17% in hardness), indicating a lower homogeneity of the former sample. This behavior has been previously observed and attributed to the formation of microalloys inside the amorphous arrangement, caused by the hybridization of the orbitals of the Cu-Al atoms that form densely packed regions surrounded by weakly packed regions [1]. Furthermore, there are interactions between Cu-Zr atoms which tend to form nanocrystals with martensitic structure within the amorphous matrix [2, 3]. These two mechanisms may be responsible for the high variation in the elastic modulus observed for the $Cu_{47.75}Zr_{47.75}Al_{4.5}$ alloy. However, in the $Cu_{47.5}Zr_{45.5}Al_5Er_2$ alloy, the presence of erbium absorbs oxygen from the material, causing less variation among regions of densely/weakly packed structures, which results in the greater amorphization degree of this alloy.

E [GPa]	53.2	34.3	88.2	91.5	55.2	65.7	56.6	41.4	49.2	35.7	**57 ± 20**
Hi [GPa]	5.2	4.1	8.0	8.7	5.6	6.8	6.0	5.0	5.8	4.4	**5.9 ± 1.4**

Elastic modulus (E) and indentation hardness (H_i) of the $Cu_{47.75}Zr_{47.75}Al_{4.5}$ alloy

E [GPa]	45.0	57.4	51.2	42.1	63.3	62.8	62.3	**54.9 ± 8.8**
Hi [GPa]	4.3	5.7	5.6	4.9	7.3	6.8	5.9	**5.8 ± 1.0**

Elastic modulus (E) and indentation hardness (H_i) of the $Cu_{47.5}Zr_{45.5}Al_5Er_2$ alloy

4. References

[1] Y. Q. Cheng; E. Ma; H. W. Sheng, Physical Review Letters, **102**, 245501, (2009).
[2] E. M. Carvalho and I. R. Harris, Journal of Materials Science, **15**, 1224-1230, (1980).
[3] A Moreno-Gobbi; P. S. Silva; A. Maso; P.W.B. Marques; O. Florêncio; L. G. Sarasua, Materials Today Communications, **26**, 102125, (2021).

Acknowledgments:
FAPESP/BR (grants #2013/13378-1, #2013/05987-8 and #2017/08913-6), CAPES/BR

*Corresponding author: cicerojunior15@hotmail.com

CONTACT FATIGUE ASSESSMENT OF NITRIDED AISI 321 STEEL

Manfrinato, M. D.[1,2*], Rossino, L. S.[1,2], Kliauga, A. M.[2], Morón, R. C.[3], Escobar-Hernández, J.[4], Rodríguez-Castro, G. A.[4]

[1]*Faculdade de Tecnologia do Estado de São Paulo (Fatec Sorocaba), CEETEPS, Sorocaba-SP*
[2]*Universidade Federal de São Carlos, PPGCM, UFSCar Campus Sorocaba, Sorocaba-SP*
[3]*Tecnológico Nacional de México Campus Tlalnepantla, Av., Instituto Tecnológico, S/N. Col. La Comunidad, Tlalnepantla de Baz 54070, Estado de México, Mexico*
[4]*Instituto Politécnico Nacional, SEPI ESIME Zacatenco, Grupo Ingeniería de Superficies, U.P. Adolfo López Mateos, Zacatenco, Ciudad de México 07738, Mexico*

1. Introduction

Austenitic stainless steels are used in diverse industries due to their excellent corrosion resistance. However, its low surface hardness restricts their applications [1]. Thus, plasma nitriding at low temperature has been used to increase surface hardness and fatigue properties without reducing its corrosion resistance [2]. On the other hand, standing contact fatigue (SCF) relates to the plastic deformation at the surface of the material produced by the dry and frictionless Hertzian stress contact between two bodies, whose magnitude is under the yield stress; it can be studied by repeatedly impacting a spherical counterbody on a plane surface [3]. Initially, a critical load is obtained by constant load tests; then, subcritical dynamic tests are performed for layer integrity appraisal. In this work, the SCF behavior of plasma nitrided AISI 321 steel was studied.

2. Experimental

The thermochemical treatments were conducted in AISI 321 steel circular specimens of 25.4 × 7 mm. Nitriding was performed at a pressure of 266.6 Pa, with a total gas flow of 1000 sccm (75% N_2 and 25% H_2); temperatures were established at 400 and 500 ◦C for 6 h, resulting in samples identified as N400 °C and N500 °C. For the SCF tests, an MTS Acumen electrodynamic machine was used, impacting a 3 mm diameter Al_2O_3 ball. First, static loads between 100 and 1000 N were applied, establishing a critical load of 300 N, related to the presence of circumferential cracks in N400 °C. Next, dynamic tests from 10^3 to 10^5 cycles were performed, applying three subcritical loads (40%, 50% and 60%) in both layers. After the tests, the samples were analyzed by optical microscopy and profilometry.

3. Results and Discussions

The composition of N400 °C is expanded austenite (S) and white layer, whereas in N500 °C, the decomposition of S into chromium nitride and iron nitride occurs, resulting in a mixture of CrN, (FexN) and white layer. The contact fatigue results show that increasing treatment temperature worsened the integrity of the layer in both static and dynamic tests. In static tests, show the Figure 1, N400°C only presented circumferential cracks, even at the highest load. In contrast, for N500°C layer, besides circumferential cracks, gross spallations occurred, evidencing a more fragile layer. In the dynamic tests, show the Figure 2, this trend prevailed, the N400°C layer presented a better standing contact fatigue behavior over N500°C, attributed to a more ductile nature.

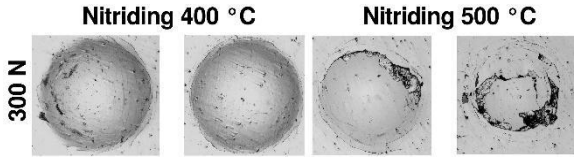

Fig. 1. *Static load tests with 300 N in nitrided samples.*

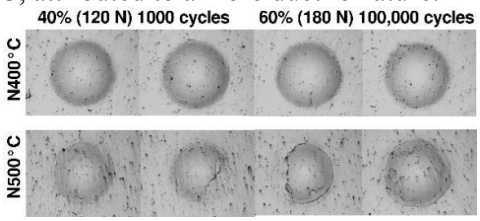

Fig. 2. *Extreme ends conditions of the dynamic tests conducted in nitrided samples.*

4. References

[1] C.E. Pinedo, A.P. Tschiptschin, Int. Heat Treat. Surf. Eng., **5**, 73–77, (2011).
[2] F. Borgioli, E. Galvanetto, T. Bacci, Corros. Sci., **136,** 352–365, (2018).
[3] B. Alfredsson, M. Olsson, Fatigue Fract. Eng. Mater. Struct., **22**, 225–237, (1999).

Acknowledgments
R. C. Moron wants to acknowledge Cátedra COMECYT EDOMEX fellowship.
*Corresponding author: marcos.manfrinato@fatec.sp.gov.br

MA-ACTIVATED DEIONIZED WATER CONSERVATION AT A LOW TEMPERATURE

Marcondes, M. S.*, Lima, L. G. de, Neto, B. D. B., Júnior, W. C., Pessoa, R. S.
Laboratório de Plasmas e Processos (LPP), Departamento de Física, Instituto Tecnológico de Aeronáutica – São José dos Campos

1. Introduction

Plasma has been studied and applied in several areas, emphasizing health, dentistry, and agriculture [1]. Plasma activation of water results in plasma-activated water (PAW), an acidic solution rich in long-lived reactive species, such as reactive oxygen and nitrogen species (RONS), namely, nitrite (NO2-), nitrate (NO3-), nitrous acid (HNO2), ozone (O3), and hydrogen peroxide (H2O2) [1, 2]. These RONS have the property of inactivating microorganisms of great clinical importance and being essential for agriculture. However, it was observed that the acidity and RONS concentrations in the PAW stored at room temperature undergo drastic changes in short time intervals. Consequently, PAW loses its antimicrobial effectiveness, thus reducing the interest in large-scale production and use. The present work aims, with the help of a multiparameter, to measure the physicochemical parameters, such as pH, total dissolved solids (TDS), and conductivity, and with the aid of UV-VIS optical absorption spectroscopy to obtain spectra UV-Vis to monitor long-lived reactive species, which will be quantified to study the conservation of PAW properties at low temperature after several thawing, namely thermal thawing, natural thawing and microwave thawing [2].

2. Methodology

For this study, 40 mL of deionized water (DI) was activated by cold plasma at ambient pressure, which was generated by a gliding arc discharge of the direct vortex flow reactor (FVFR) type [2]. DI water was placed in a Petri dish and positioned 0.5 cm from the plasma, being activated for 60.0 minutes. After this activation time, the PAW was characterized by a multiparameter meter (Model Combo 5, Akso, São Leopoldo, RS, Brazil) to measure pH, TDS, and conductivity by UV-VIS optical absorption spectroscopy for the detection of RONS. Three equal volumes were separated and stored in a standard freezer at -30ºC temperature. During 15 consecutive days, these volumes were thawed, characterized, and refrozen. After each thawing, the physicochemical parameters and the UV-Vis spectra were measured to monitor the parameters. Finally, the UV-Vis spectra were deconvoluted with the aid of Gaussians, and the peaks of the RONS, namely, NO2-, NO3-, HNO2, O3, and H2O2 were identified using the literature [2].

3. Results and Discussions

After 15 thawings were performed on different days, it was possible to verify that the pH values in the samples thawed through thermal heating and naturally did not have significant changes in their pH throughout the research about the day of activation. In contrast, the sample melted via microwave reduced its pH compared to the day of activation. In natural thawing, the pH on the day of activation was recorded at 2.5 and on the last day at 2.75. The thermally thawed sample had the pH on the day of activation at 2.7 and the previous day at 2.66. In the microwave-thawed sample, the pH on the day of activation was 2.86, and on the last day, it was 2.53. The values of TDS and conductivity fluctuated with the thawing. The sample thawed via microwave had TDS at 424ppm and conductivity at 642µS on the activation day and TDS at 2.31ppt and conductivity at 3.51mS on the last day. The natural thawing sample had TDS at 465ppm and conductivity at 714µS on the activation day and TDS at 1.94ppt and conductivity at 2.95mS

4. References

[1] N. Milhan, W. Chiappim, A. Sampaio, M. Vegian, R. Pessoa, C. Koga-Ito, International Journal of Molecular Science., **23**, 4131, (2022).
[2] W. Chiappim, A. Sampaio, F. Miranda, M. Fraga, G. Petraconi, A. da Silva Sobrinho, K. Kostov, C. Koga-Ito, R. Pessoa, Water, **13**, 1480, (2021).

*Corresponding author: marcondes.micaela5@gmail.com

PROCESSING OF PEO-COATINGS DECORATED WITH TA OXIDES IN LOW CARBON STEEL SAE 1020 TARGETING BIOMEDICAL APPLICATIONS

Marcuz, N.[1], Rangel, E. C.[2], Cruz, N. C. da[2], Correa, D. R. N.[3]
[1]*FATec – Faculdade de Tecnologia de Sorocaba, Sorocaba (SP), Brazil*
[2]*UNESP - Univ. Estadual Paulista, Laboratório de Plasmas Tecnológicos, Sorocaba (SP), Brazil*
[3]*IFSP - Instituto Federal de Educação, Ciência e Tecnologia de São Paulo, Sorocaba (SP), Brazil*

1. Introduction

Low carbon steel SAE 1020 is extensively used in modern society for several engineered devices, in particular for construction and machine parts, such as rings, axis, columns, and gears. The metal has good ductility, hardness, and wear resistance, besides its low cost. Tantalum (Ta) is a transition element from the group V from the periodic table. The element is chemically inert at room temperature, possessing biocompatibility and osseointegrative ability when in contact with bone tissues, which have attracted the attention of the orthopedic and dental industries. In the present study, low carbon steel SAE 1020 samples were submitted to PEO treatment in a Ta-rich electrolyte. Then, the phase and chemical composition, topography, wettability, and corrosion properties of the surface were evaluated in terms of the applied potential, targeting to the use as implantable material.

2. Experimental

Low carbon steel SAE 1020 samples (20 x 20 x 5 mm) were preliminarily polished with SiC waterproof papers (until #1200 mesh) and ultrasonically cleaned in acetone for 5 min. PEO treatment was performed in a pulsed power source (MAO-30, Plasma Tech. Ltd.), with voltages in the range 200-300 V, frequency of 1 kHz, duty cycle of 60%, for 10 min. The electrolyte was composed of an aqueous solution with 2 $g.L^{-1}$ KOH and 10 $g.L^{-1}$ TaOH. The surfaces were characterized by SEM/EDS, XRD, FTIR, profilometry, and wettability. The applicability in the biomedical area were assessed by corrosion test in aqueous 0.9% NaCl solution, with an Ag/AgCl as reference electrode, and Pt wire as counter electrode. The corrosion properties were acquired with open circuit potential, potentiodynamic polarization, and electrochemical impedance spectroscopy measurements.

3. Results and Discussions

The samples' morphology changed from porous to crater-like with the voltage rising, exhibiting distinct current values (Fig. 1). The Fe_3O_4 oxide was the majority component of the coatings, being the Ta incorporated in the coatings as a trace. The PEO-treated surfaces were rougher, more hydrophilic, and had improved corrosion properties than the untreated sample. The sample treated at 200 V exhibited the best combination of properties for potential use as low cost biomedical materials.

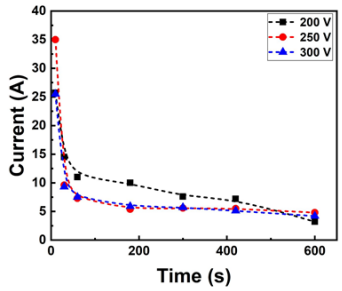

Fig. 1. *Current x time curves of the PEO-treatments.*

4. References

[1] R. F. Antonio et al., Surface and Coatings Technology, **357**, 698-705 (2019).
[2] C. Martinez et al., Materials, **11**, 17, (2018).

Acknowledgments
Financial support: FAPESP, CNPq, and CAPES.

*Corresponding author: diego.correa@ifsp.edu.br

EFFECT OF PLASMA-ENHANCED CHEMICAL VAPOR DEPOSTION ON LYSOZYME AND ITS ANTIMICROBIAL PROPERTIES

Miranda, L. F. B.[1]*, Souza, J. G. S.[2], Rangel, E. C.[3], Barão, V. A. R.[1]
[1]*University of Campinas (UNICAMP), Piracicaba Dental School, Piracicaba, São Paulo*
[2]*Guarulhos University, Guarulhos, São Paulo / Dentistry Science School (Faculdade de Ciências Odontológicas - FCO), Montes Claros, Minas Gerais*
[3]*São Paulo State University (UNESP), Institute of Science and Technology, Sorocaba, São Paulo*

1. Introduction

Superhydrophobic coating on titanium surface deposited by Plasma-Enhanced Chemical Vapor Deposition (PECVD) reduces the bacterial attachment and the number of pathogen bacteria in the biofilm grown in its surface [1]. Although it is a promising strategy to reduce implant loss, the coating does not inactivate attached bacteria which could reduce the potential of the biofilm growth and of infection incidence. The addition of an agent with antimicrobial properties, as lysozyme [2], to the coating could overcome this limitation. However, it requires that lysozyme is functional active after exposure the plasma process conducted for deposition of the superhydrophobic film, matter investigated here.

2. Experimental

Hen egg-white lysozyme lyophilized powder (EC 3.2.1.17) was placed in a pressure-resistant autoclavable glass bottle (uncapped) inside of a stainless-steel reactor chamber, which contains two parallel-plate horizontal circular electrodes. The chamber was evacuated to a background pressure of $\approx 2.0 \times 10^{-2}$ Torr. An atmosphere containing 50% O_2, 30% Ar, and 20% hexamethyldisiloxane was created inside the chamber at a working pressure of 5.0×10^{-1} Torr. In the lower, electrode, a radiofrequency (13.56 MHz) with an output power of 150 W was applied and plasma was generated for 30 min. To study the lysozyme antimicrobial effect after exposition to PECVD, Gram-positive *Streptococcus mutans* UA159 was cultured in BHI medium containing glucose 1% without lysozyme (control) or with 1 mg/mL of pristine lysozyme (LZM) or lysozyme exposed to PECVD (LZM-PECVD) (n=6/group). The absorbance (600 nm) of the bacterial suspension was measured hourly up to 7 h to obtain the bacterial growth curve. In the end, the suspensions were diluted and placed in BHI agar plates for colony-forming units (CFU) count to evaluate bacterial viability. Data were analyzed by one-way and two-way ANOVA and Tukey's test (α=0.05).

3. Results and Discussions

Both LZM and LZM-PECVD were able to reduce the absorbance values in comparison with the control group ($p<0.05$), indicating lower microbial density and bacterial viability. Bacterial viability reduction was confirmed by CFU/mL data, in which the concentration of planktonic bacteria in the LZM-PECVD group ($6.0\times10^{10} \pm 1.4\times10^{10}$) was similar to LZM ($6.5\times10^{10} \pm 1.7\times10^{10}$) ($p>0.05$), but significantly lower than the control ($1.1\times10^{11} \pm 4.1\times10^{10}$) ($p<0.05$), showing the maintenance of lysozyme antimicrobial property after its exposition to PECVD. Therefore, it can be concluded that the exposition of lysozyme to Plasma-Enhanced Chemical Vapor Deposition does not affect its antimicrobial properties compared with pristine lysozyme.

4. References

[1] J.G.S. Souza, M. Bertolini, R.C. Costa, J.M. Cordeiro, B.E. Nagay, A.B. de Almeida, B. Retamal-Valdes, F.H. Nociti, M. Feres, E.C. Rangel, V.A.R. Barão, ACS Appl. Mater. Interfaces, **12**, 10118-10129, (2020).
[2] D.M. Chipman, N. Sharon, Science, **165**, 454-465, (1969).

Acknowledgments
This study is partially supported by the São Paulo Research Foundation (2020/05231-4 to V.A.R.B), the Conselho Nacional de Desenvolvimento Científico e Tecnológico – Brazil (CNPq) (#304853/2018-60 to V.A.R.B), and the Coordenação de Aperfeiçoamento de Pessoal de Nível Superior (Grant/Award Number: 001).

*Corresponding author: luisfbmiranda@gmail.com

AGEING EFFECTS ON PLASMA POLYMERS FROM ETHYLENEDIAMINE/C_2H_2 AND 2-METHYL-2-OXAZOLINE FOR BIOMEDICAL APPLICATIONS

Moreira Júnior, P. W. P.[1]*, Kodaira, F. V. P.[1], Mota, R. P.[1]
[1]*UNESP – Univ. Estadual Paulista, Av. Dr. Ariberto Pereira da Cunha, 333 - Guaratinguetá, SP, Brazil.*

1. Introduction

2-metil-2-oxazoline plasma polymers (pp-Oxazoline) and ethylenediamine plasma polymers (pp-EDA) are known by its biocompatibility and functionalities when in contact with the human body. As remarkable properties they present non-fouling and pinhole-free surfaces that are friendly to appropriated proteins for human cells proliferation [1]. Furthermore, pp-Oxazoline are alternative polymers to PEO and PEG, besides holding the same biocompatibility of these materials, they are also more resistant to biological degradation [2]. Thin films of pp-EDA are nitrogen rich materials and may present amine and amide (when oxidized) groups on its structures [3]. As main property, the pp-EDA is able to improve human cell adhesion and proliferation on its surfaces. Our earlier studies showed pp-EDA are unstable in aqueous media, however mixing C_2H_2 with EDA precursor promotes better stability for these materials whereas retain nitrogen groups. This new class of materials has been substantially investigated on the last decade and the study of ageing effects on their properties is essential for further applications where storage and carrying processes are involved.

2. Experimental

In this work pp-Oxazoline and pp-EDA were deposited by PECVD process under low pressure conditions in a standard stainless steel reactor chamber with parallel plates electrode configuration. The discharges were performed at 100 mTorr and 200 mTorr of total pressure and excited by a RF power supply operating at 13.56MHz and 5W and 30W of power. The samples were storage in a room where temperature and humidity were controlled. The storage time was up to 5 months and the measurements of thin films properties were performed monthly. To investigate the ageing effects on samples due storage process, water contact angle (WCA) and energy surface (ES) measurements were employed as well as Fourier transformed infrared spectroscopy (FTIR).

3. Results and Discussions

Overall, both pp-EDA and pp-Oxazoline thin films showed hydrophilic character regardless the deposition parameters, however the ageing effect for each sample is distinct, being more significant for pp-EDA. FTIR measurements showed significant amounts of amine groups in pp-EDA and amide and carboxyl groups on pp-Oxazoline. The presence and relative amount of these groups on thin films are of high importance for their applications and promote the hydrophilicity observed with WCA measurements. Furthermore, FTIR spectra indicate the oxidation process over the storage time, which is correlated to changes in WCA character and thin films stability in aqueous media.

4. References

[1] Xiang, L. N. et. al. Chinese chemical letters, **24**, 597 – 600, (2013).
[2] Ramiasa, M. N. et al. Chem. Commun, **51** 4279 – 4282 (2015).
[3] Testrich, H., et al. Mat. Sci. and Eng. C, **33**, 3875 – 3880, (2013).

Acknowledgments
The authors would like to acknowledge CAPES and FAPESP for the financial support.

*Corresponding author: pedro_kcond28@hotmail.com

EVALUATION OF CORROSION RESISTANCE OF ZIRCONIA COATING ON TI-6AL-4V ALLOY BY ELECTROLYTIC PLASMA OXIDATION (PEO)

Nanuh[1], A.C.; Rangel[2], E.C.; Correa[3], D.R.N.; Cruz[2], N.C.
[1]*UNISO – Univ de Sorocaba, Sorocaba, Brazil*
[2]*UNESP – Univ Estadual Paulista, Laboratório de Plasmas Tecnológicos, Sorocaba, Brazil*
[3]*IFSP – Câmpus Sorocaba, Advanced Metallic Materials Group, Sorocaba (SP), Brazil*

1. Introduction

The plasma electrolytic oxidation (PEO) is a surface modification technique that uses conventional electrolysis, being applied mainly in valve metals, such as Al, Mg, Ti, Ta, and Zr. The technique has been widely used to modify surfaces, since it provides the formation of a porous oxide layer, strongly bonded to the substrate, with excellent durability, chemical stability, and high hardness [1]. In this study, the electrochemical properties of PEO-treated Ti-6Al-4V alloys in a ZrO_2-rich electrolyte were evaluated for biomedical applications.

2. Experimental

Disk-shaped samples of Ti-6Al-4V (ASTM F136), with dimensions of ϕ10 mm x 3 mm, was used as substrate. The electrolyte was composed of 0.08 mol.L^{-1} of zirconium oxide (ZrO_2) and 0.04 mol.L^{-1} of potassium hydroxide (KOH). The PEO treatments were performed in a system consisting of a pulsed voltage source (MAO-30), a water-cooled stainless steel tank, and a suspended electrode. The surface treatments were carried out at voltages between 375 V and 500 V. To evaluate the corrosion behavior of the samples, it was performed electrochemical impedance spectroscopy (EIS), potentiodynamic polarization (PDP), and open circuit potential (OCP). The measurements were carried out in NaCl 0,9% solution, with a three-electrode system consisting of a platinum counter electrode, an Ag/AgCl reference electrode and a coated sample as the working electrode inserted into a Teflon mask, with an exposed area of 26.42 mm^2. The polarization curves were acquired in the potential range from – 1000 to 2000 mV with a scanning rate of 1 mV/s at the open circuit potential during 3.600 s.

3. Results and Discussions

Figure 1 shows the OCP variation of the bare Ti-6Al-4V sample after PEO treatment at 500 V and 375 V during 3.600 s. Comparing the curves, it is possible to verify that the surface coating caused the OCP to move to more positive values, which indicates a nobler behavior of the PEO-treated samples. Figure 2 presents the PDP curves, where it is possible to verify that the coating shifted the curves to more positive corrosion potentials, indicating a greater corrosion resistance [2].

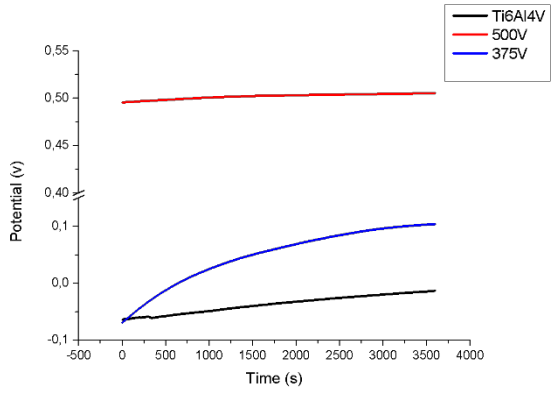

Fig. 1 *OCP curves.*

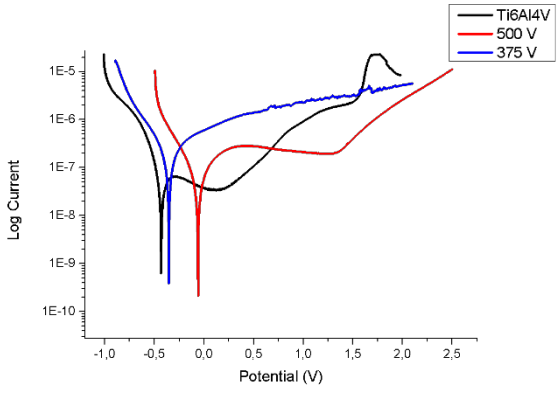

Fig. 2. *Potentiodynamic polarization curves.*

4. References

[1] T. W. Clyne and S. C. Troughton. International materials reviews **64**, 127-162, (2019).
[2] A. Fattah-alhosseini, M. Molaei and K. Babaei. Surfaces and Interfaces **21**,100659, (2020).

Acknowledgments
The authors thank the Brazilian funding agencies CNPq and FAPESP.

*Corresponding author: aline_cristines@hotmail.com

TEMPORAL EVOLUTION OF PHYSICOCHEMICAL PARAMETERS IN PLASMA ACTIVATED LIQUIDS (PAL) BY GLIDING ARC PLASMA

Neto, B. D. B.[1,2]*, Lima, L. G. de[2,3], Chaves, J. P. M.[2], Karnopp, J.[2], Marcondes, M. S.[2,3], Chiappim, W.[2], Pereira, A. L. de J.[2], Pessoa, R. S.[2]

[1]*IFSP – Instituto Federal de Educação, Ciência e Tecnologia de São Paulo, Campus São José dos Campos*
[2]*ITA – Instituto Tecnológico de Aeronáutica, São José dos Campos*
[3]*Universidade Anhembi Morumbi, São José dos Campos*

1. Introduction

The interest in Plasma Activated Liquids (PAL) has been increasing over the years, due to its wide and efficient application as a decontaminating agent [1,2]. Among the numerous plasma techniques, Gliding Arc Plasma is widely used due to its low cost and high activation efficiency [2]. Thus, the present work aims to optimize the activation of different liquids (tap water, filtered water, distilled water, deionized water, and saline solution), using the Gliding Arc Plasma technology.

2. Experimental

The activation of liquids by plasma was made using an atmospheric Gliding Arc Plasma. In this work, a continuous compressed airflow of 5 L/min was used, considering the composition of humid air as 79% N_2, 20% O_2, and 1% H_2O, applying a voltage of 2 kV through a high-voltage supply. The activation of the liquid was performed in a volume of 40 mL placed in a Petri dish at 3 mm from the plasma plume. In order to evaluate the temporal evolution of physicochemical parameters, activation ranged from 1 to 60 min (with intervals adopted as 1, 2, 3, 4, 5, 10, 15, 20, 25, 30, 40, 50, and 60 minutes), and the characterization of the physicochemical parameters of the liquids, as well as Hydrogenic Potential (pH), conductivity (σ), Total Dissolved Particles (TDS) and Oxidation-Reduction Potential (ORP) obtained by a multiparameter meter and the obtaining their optical absorption spectra using the UV-vis spectrophotometry technique.

3. Results and Discussion

The study of the temporal evolution allowed the analysis of the behavior of the different physicochemical parameters, in addition to evaluating the variation of the volume of the liquid with the activation time, allowing the study of the volumetric variation as a function of the plasma dosage. The pH values of activated liquids tend to decrease with temporal evolution, to reach a plateau, in which the buffering capacity of the liquid is reached. The TDS increases significantly, as plasma activation promotes a large increase in the number of species that are dissolved in the liquid, directly influencing the increase in conductivity and ORP. The conductivity showed a large increase, as the number of ions present in solution, which are responsible for electrical conduction in aqueous solution, increases significantly due to TDS. On the other hand, the ORP is directly related to the increase in the concentration of Reactive Oxygen and Nitrogen Species (RONS), with oxygen being responsible for the increase in the redox potential of the solution, and as seen previously, the increase in RONS is directly linked to the increase in TDS. The optical absorption spectra allowed a qualitative analysis regarding the concentration of species present in the liquids, in agreement with the physical-chemical parameters obtained. The volumetric variation was observed for all liquids and was observed its decreases as a function of the plasma dosage, which refers to how much energy is accumulated by the plasma in each time interval.

4. References

[1] W. Chiappim, A. G. Sampaio, F. Miranda, M. Fraga, G. Petraconi, A. S. Sobrinho, K. Kostov, C. Koga-Ito and R. Pessoa, Water, **13**, 1480, (2021).
[2] C. M. Du, J. Wang, L. Zhang, H. X. Li, H. Liu and Y. Xiong, New Journal of Physics, **14**, 073510, (2012).

Acknowledgments
FAPESP for granting the scientific initiation scholarship (2021/03620-6). To ITA for providing the infrastructure used during the execution of the project. And to the entire LPP – ITA team for their support.

*Corresponding author: botan.bdn@gmail.com

IN VITRO EVALUATION OF EXPOSURE OF TUMORAL CELLS TO SOLUTIONS TREATED WITH COLD ATMOSPHERIC PLASMA

Neves, D. V. das[1], Hersegel, K. G.[1], Nascimento, G. G.[1], Lima, D. de M.[1], Proença, J. P. de[2], Gonçalves, T. M.[2], Cruz, N. C. da[2], Oliveira, E. C. de[1].

[1] *Immunocell - Laboratório de Imunologia e Imunoterapia de Tumores - Faculdade de Tecnologia de Sorocaba (FATEC So), CEETEPS, Sorocaba-SP*

[2] *Laboratório de Plasmas Tecnológicos, Unesp- Instituto de Ciência e Tecnologia de Sorocaba-SP*

1. Introduction

Several studies have highlighted Cold Atmospheric Plasmas (CAP), i.e ionized gases at room temperature, as a promising tool for cancer treatment. CAPs have demonstrated antitumoral effect when applied to incorporate reactive especies in different types of solutions or applied directly on tumors [1]. Melanoma is a one of most aggressive skin neoplasms and it incidence has continuously grown in the world. In this study, we have used CAPs to incorporate in water solutions, reactive species that can interfere in in vitro cell survival.

2. Experimental

Saline 0,9% (NaCl) and Ringer Lactate (Ri-Lac) solutions were exposed to plasmas for different durations (30, 45 and 60 minutes). Murine melanoma cells lineage (B16F10) were distributed in 96 well plate at concentration of $1x10^5$ cell/mL and, after accession, cells were exposed to solutions treated with plasma for 30, 60 and 120 minutes. Finishing the treatment times, the solutions were replaced by culture medium (DMEM supplemented with 10% bovine fetal serum, 2% Glutamine e 1% Antibiotic) and incubate for 24 hours. Cellular viability was evaluated using MTT method.

3. Results and Discussions

Figures 1 and 2 demonstrate the reduction of B16F10 cells viability *in vitro,* when exposed to NaCl and Ri-Lac solutions treated with CAP. However, this reduction was also observed in control solution. The largest reduction was observed in NaCl solutions.

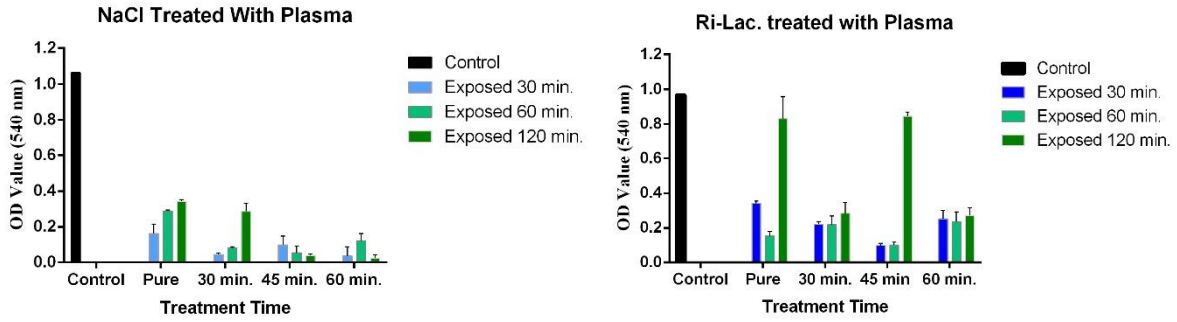

4. References

[1] Yan, D., Xu, W., Yao, X. et al. Sci Rep, **8**, 15418, (2018).
[2] Alimohammadi, Mina et al. Biomolecules, **10**, 1011, (2020).

Acknowledgments
CNPq and *Fapesp* for the financial support.

*Corresponding author: diegoverduino@hotmail.com.

DEVELOPMENT OF A SOFTWARE TO DESIGN ULTRA-HARD METAL ALLOYS

Nonato, R. B. P.[1], Restivo, T. A. G.[2]
[1]*Federal Institute of Santa Catarina (IFSC, campus Xanxerê)*
[2]*University of Sorocaba (UNISO)*

1. Introduction

Wear resistance is a requirement in parts like bearings, cutting tools, etc., which demand longer lifespans. Consequently, ultra-hard metal alloys (UHMAs) are commonly employed to resist longer working cycles. One of the applied approaches to design UHMAs is the parametric [1,2]. This approach consists in the calculation of a set of parameters and evaluation of criteria that, theoretically, leads to stable solid solutions.

2. Experimental

Based on this approach, a software developed by the authors, called DIAMOY, employs twenty parameters and five criteria to compose the alloy design process. DIAMOY was coded in Microsoft Visual Basic 6.0® and turned into a Windows® application.

3. Results and Discussions

The results from the software were compared to two UHMAs from [3] with a maximum relative error of 1.923% for one UHMA, and 3.183% for the other UHMA. The expected contributions of this software are: (a) the organization of the parameters and criteria into a single application, thus facilitating the design process; (b) operation in a more practical manner; (c) portability, as it can be executed in any Windows®-based device.

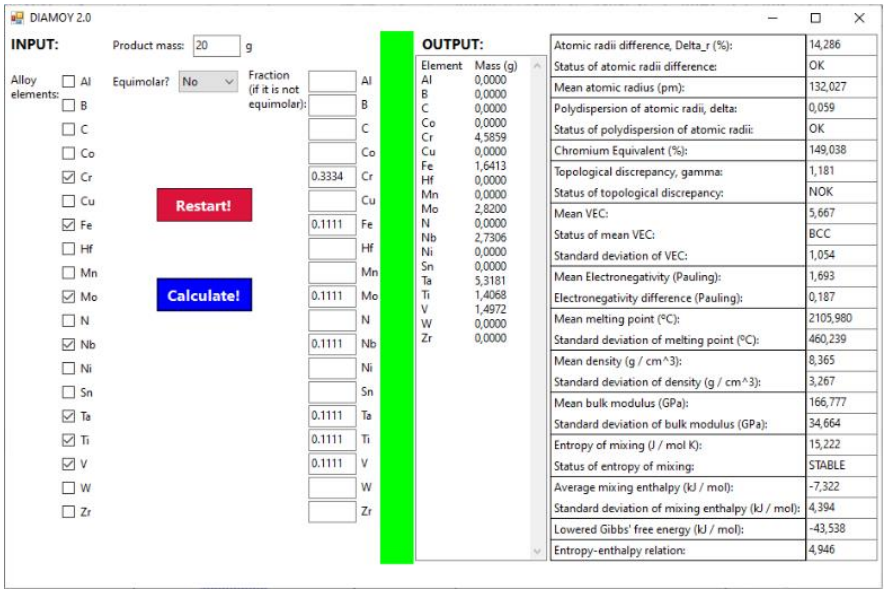

Tab. 1. *Screen showing DIAMOY calculation for non-equimolar 20 g of $Cr_3FeMoNbTaTiV$ alloy*

4. References

[1] A. Tazuddin, K. Biswas, N.P. Gurao, Materials Science & Engineering A, **657**, 224-233, (2016).
[2] A. Tazuddin, N.P. Gurao, K. Biswas, **697**, 434-442, (2017).
[3] T.A.G. Restivo, G.M.G. Restivo, **36**, 1316-1327, (2021).

Acknowledgments
The authors acknowledge the congress organizing committee, FAPESP council for funding through project 2020/09736-3. Also Catalisa ICT/SEBRAE/CNPq29083-128, and CNPq-Universal 408406/2021-6.

*Corresponding author: raphaelbasilio@gmail.com

DEVELOPMENT OF ULTRA-HARD METAL ALLOYS

Nonato, R. B. P.[1]*, Figueira, R. C. R.[2], Ferreira, O. A.[2], Padovani, C.[2], Belchior, A.[2], Aranha, N.[2], and Restivo, T. A. G.[2]
[1]*Federal Institute of Santa Catarina (IFSC, campus Xanxerê)*
[2]*University of Sorocaba (UNISO)*

1. Introduction

Many materials were designed by researches in order to solve the most diverse problems. When the wear resistance is a requirement, the demand is for harder materials. Therefore, one of the solutions is to employ ultra-hard metal alloys (UHMAs), e.g. special steels/superalloys. In what concerns hardness, the conventional metal alloys may reach values of 1100 HV (Vickers hardness, kgf/mm^2), e.g. the M40-series high-speed steel (HSS) [1]. Boronized, nitrided, and carburized alloys may reach up to 1900 HV [2], while their ceramic phases lead to brittle behavior. The present work proposes new metallic alloys which are harder than current materials.

2. Experimental

Firstly, the alloys denominated 4, 4.1, 5, 6, and FN22 were theoretically designed based on lattice occupancy project (LOP). After the design, for each alloy, element powders were mixed to obtain homogeneity. The powder mass was then compacted to achieve a cohesive metallic pellet form. This form was posteriorly molten at a plasma arc furnace into ingots. Vickers hardness measurements (2 N load) are performed to compare with other samples from literature.

3. Results and Discussions

The samples molten from a pellet form and posteriorly cast into ingots present 1 to 3 BCC phases, which indicates that the LOP project was validated. The values of Vickers hardness are shown in Tab. 1, where mean and maximum values can be compared to distinct results obtained from the literature. It is found that the hardness increasing of alloys 4 and 5 after carburizing is dramatic, bringing these materials closer to covalent ceramics in this regard. The high hardness of the proposed alloys is thus revalidated, proving that they are the hardest metallic materials ever made. Moreover, reasonable toughness close to 11 MPa.m$^{1/2}$ were measured by Palmkvist radial cracks method. Therefore these combined results tend to uncover the Holly Grail of Metallurgy.

Alloy	HV mean (kgf/mm2)	HV max (kgf/mm2)
4 pallet	1028	1163
4.1 pallet annealed 1000°C/ 1h	1374	1400
5 plate	1125	1179
6 pallet	1222	1343
4 plate	970	1227
4 annealed 1200°C/3h	1125	1247
4 carburized 1150°C/4h	2222	2577
5 carburized 1200°C/3h	1099	1378
5 carburized 1150°C/4h	1843	2130
FN22 annealed 1200°C/3h	615	679
FN22 annealed 1200°C/4h	757	848
FN22 carburized	921	1284

Tab. 1. *Vickers hardness (HV) for the designed alloys under distinct conditions*

4. References

[1] D. H. Dennis *"Properties and Selection: Irons, Steels, and High-Performance Alloys in ASM Handbook"*, vol.1, ASM International, USA, (1993).
[2] Klaus, M.Z. *"Properties and Selection: Nonferrous Alloys and Special-Purpose Materials in ASM Handbook"*, vol.2, ASM International, USA, (1993).

Acknowledgments
The authors acknowledge the congress organizing committee, FAPESP council for funding through project 2020/09736-3. Also Catalisa ICT/SEBRAE/CNPq29083-128, and CNPq-Universal 408406/2021-6.

*Corresponding author: raphaelbasilio@gmail.com

CHARACTERIZATION OF STRONTIUM TITANATE (001) SURFACE BY X-RAY PHOTOELECTRON DIFFRACTION

Pancotti, A.[1], Siervo, A.[2], Landers, R.[2], and Nascente, P. A. P.[3]*
[1] *Federal University of Jatai, Special Academic Unit for Exact and Technological Sciences, Jatai, GO, Brazil*
[2] *State University of Campinas, "Gleb Wataghin" Institute of Physics, Campinas, SP, Brazil*
[3] *Federal University of Sao Carlos, Department of Materials Engineering, Sao Carlos, SP, Brazil*

1. Introduction

The perovskite ceramic strontium titanate ($SrTiO_3$ or STO) has attracted considerable attention as very promising material for catalytic, photocatalytic, electronic, magnetic, and spintronic applications due to its low cost and high chemical stability [1, 2]. The (001) surface has been the most investigated one and several different surface reconstructions have been reported [3]. In this study, we report on the growth, composition, and structural characterization of $SrTiO_3$ (001) surface by X-ray photoelectron spectroscopy (XPS), low energy electron diffraction (LEED), and X-ray photoelectron diffraction (XPD).

2. Experimental

The surface analysis system was equipped with LEED optics, a conventional Al κα X-ray source, a high-resolution electron analyzer, an ion gun for *in-situ* sample cleaning, and a two-axis sample manipulator capable of heating the samples from RT up to 1400 K. The samples were cleaned *in-situ* by alternating cycles of oxygen exposure and annealing at 940 K, then the samples were annealed at 1200 K in UHV for 40 minutes. The base pressure was kept below 2.7×10^{-8} Pa during the experiments. Multiple scattering calculation of diffraction (MSCD) was used to simulate the experimental XPD results.

3. Results and Discussions

The high-resolution Sr 3d, Ti 2p, and O 1s XPS spectra taken at grazing emission are consistent with Sr^{2+}, Ti^{4+}, and O^{2-} ions in the SrTiO3 perovskite structure, with minor peaks corresponding to surface SrO. Annealing the $SrTiO_3$ (001) sample at different temperatures gives rise to different reconstructions; the sample that was annealed at 600 °C presented a (1 × 1) LEED pattern, and at 900 °C, a (5 × 5)-R26.6° (Rt5) pattern. Fig. 1 depicts a model for the $SrTiO_3$ (001) surface. Fig. 2 displays the simulated XPD patterns for a Rt5 reconstruction of the $SrTiO_3$ (001) surface, and the best results indicate the coexistence of 40% SrO and 60%TiO_2 terminations on the $SrTiO_3$ (001) surface [3].

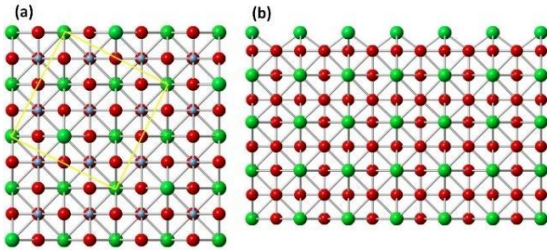

Fig. 1. *(a) top view and (b) side view of SrO- and/or TiO_2-terminated reconstruction for the $SrTiO_3$ (001) surface. The blue atoms represent Ti, the red atoms, O, and the green atoms, Sr.*

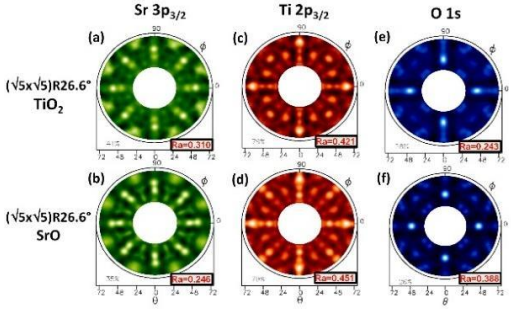

Fig. 2. *Simulated XPD patterns for a Rt5 reconstruction for the Sr $3p_{3/2}$ emitter: (a) TiO_2 and (b) SrO terminations; for the Ti $2p_{3/2}$ emitter: (c) TiO_2 and (d) SrO terminations; for the O 1s emitter: (e) TiO_2 and (f) SrO terminations.*

4. References

[1] M. Plaza *et al.*, J. Am. Chem. Soc., **138**, 7816-7819 (2016).
[2] J.-Y. Baek *et al*., J. Mater. Sci. Technol., **42**, 28-37, (2020).
[3] A. Pancotti *et al*., Surf. Sci., **715**, 121937, (2022).

Acknowledgments
This work was supported by FAPESP (proposals 2017/18574-4 and 2017/25983-8), CNPq (grants 310774/2020-9 (AP), 304119/2019-9 (AS), and 302450/2017-3 (PAPN), and CNPEM/LNLS.

*Corresponding author: nascente@ufscar.br

NFLUENCE OF PH ON THE EFFICIENCY OF GRAPHENE DEPOSITION IN POLYESTER TEXTILES USING PULSED ELECTRICAL DISCHARGE IN AQUEOUS MEDIUM

Pazda, V. C. H.[1]*, Hamester, M. R. R.[2], Becker, D.[1], Fontana, L. C.[1]
[1]*Laboratory of Plasmas, Films and Surfaces, Santa Catarina State University (UDESC), Joinville, Brazil*
[2]*Textile Industrial, Diklatex*

1. Introduction

The so-called smart textiles include textiles with antimicrobial, water-repellent and self-cleaning functions, among others; these characteristics can be obtained by incorporating nanoparticles into textile fibers [1]. Graphene has great potential due to its excellent thermal and electrical conductivities, high mechanical strength and flexibility [2]. The present work investigates the influence of pH (hydrogenonic potential) on the efficiency of graphene deposition in Polyester textiles, using pulsed electrical discharge in aqueous solution.

2. Experimental

The Assimetric Bipolar Plasma Power Suply (ABiPPS) was used to generate the pulsed electrical discharge, it was developed at UDESC-CCT and is available at the Laboratory of Plasmas, Films and Surfaces/ CCT. The reactor used was of the home made type; two electrodes made of pure titanium were attached to the lid, one polarized and one grounded. A stainless steel grid fixed to the polarized electrode was used, where the textile samples were fixed. Electronic cables with clamps were connected to the electrodes, for the passage of electrical discharge to occur; in addition, an oscilloscope was used to monitor the voltage and current of the system. The electrical discharge operated in positive voltage of 500V in a period of 20 minutes, for both samples. The same was used in aqueous solution with the presence of graphene at a pH of 1.9 and later of 6.5.

3. Results and Discussions

The manual washing process of the samples was carried out after passing through the electrical discharge. In the sample from the solution with pH of 1.9, the graphene deposition did not occur; in the first wash the particles came off the textile, proving that they were weakly fixed. In the sample from the solution with a pH of 6.5, deposition occurred, so that the textile was able to retain the graphene particles in the manual washing; such behaviors are illustrated in figures 1 and 2. Therefore, it is observed that the deposition efficiency depends on the pH of the solution.

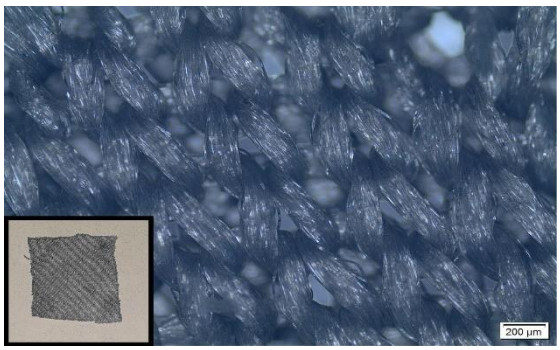

Fig. 1. *Polyester textile sample; pulsed electrical discharge in solution with a pH of 1.9.*

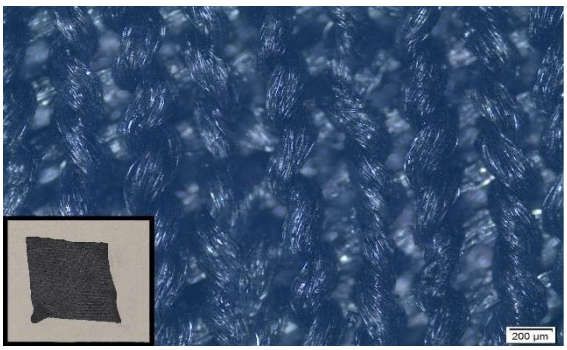

Fig. 2. *Polyester textile sample; pulsed electrical discharge in solution with a pH of 6.5.*

4. References

[1] SANTOS, Vanessa Fischer dos. Deposição de nanopartículas de TiO2 em tecidos de Algodão e Poliamida utilizando Descarga Elétrica Pulsada em Meio Líquido. Joinville, 2021.
[2] DOMINONI, Elisa Héllen Segundo. Mecanismo de Esfoliação de Grafite por Aplicação de Tensão em Fase Líquida. Joinville, 2021.

Acknowledgments
This research was supported by FAPESC 2021TR1283.

*Corresponding author: veronicacpazda@outlook.com

THE TARGET DISTANCE INFLUENCE ON THE POWER OF A TRANSFERRED COLD ATMOSPHERIC PRESSURE PLASMA JET

Petroski, K. A.*, Nascimento, F. do, Kostov, K. G.
São Paulo State University (UNESP), School of Engineering, Guaratinguetá-SP

1. Introduction

When a plasma discharge interacts with atmospheric air, it is possible to generate reactive oxygen and nitrogen species as well as light emissions e.g. UV light. Some of these species have biological effects such as destruction of bacteria and improvement of mechanisms involved in wound healing. The transferred cold atmospheric pressure plasma jet, in addition to being able to provide those species and UV light, allows easy handling and then a certain distance is maintained from the target [1]. This is accomplished by producing a discharge in a DBD system in a noble gas flow, then using a flexible plastic tube and a copper wire connected to the system both the gas flow and voltage are transferred to the other end of the tube where it produces a plasma jet. In this work the behavior of the power was investigated with the variation of the distance of the target in relation to the exit of the tube.

2. Experimental

A homemade transferred cold atmospheric plasma jet been driven with a sinusoidal voltage of 25 kHz in bust mode with a period of 1.7 ms and 15 oscillation cycles as shown in the figure 1 was applied. The plasma jet was produced with a constant power input and Argon flow rate of 2.0 l/min, and the tube output was directed to a metallic target. The current measurement was made by using a resistor of 47.0 ohm positioned after the target. The data was obtained using a tube 100.0 cm long and for 8 different distances from the target.

3. Results and Discussions

As it is presented in figure 2, as the target is moved away, the power decreases. This probably happens because for greater distances the interaction of the plasma with the atmospheric air increases, therefore greater is the energy dissipation in vibrational and rotational modes of molecules such as nitrogen and oxygen.

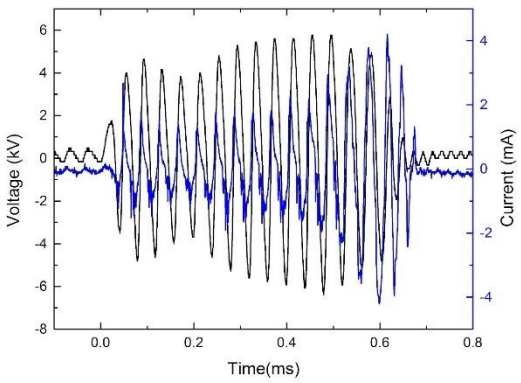

Fig. 1. *Current and voltage signal measured in the system*

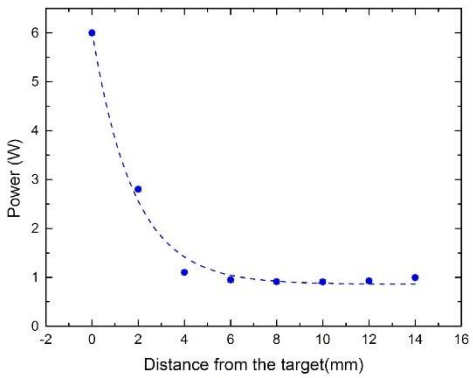

Fig. 2. *Power measured at the target for 8 different distances from the target.*

4. References

[1] K. G. Kostov, M. Machida, V. Prysiazhnyi, and R. Y. Honda, Plasma Sources, Sci. Technol., **24**, 025038 (2015).

Acknowledgments
This work was supported by CAPES - Finance Code 001 and FAPESP (grant 2019/05856-7).

*Corresponding author: kleber.a.petroski@unesp.br

CO_2 SENSORS AND MINIBIOREACTORS APPLIED ON RESEARCH AND TEACHING

Pichi Jr, W.[1*], Shimahara, A. I.[1], Silva, M. L. P. da[1,2]
[1]*Faculty of Technology of São Paulo, CPS, Brazil*
[2]*School of Engineering, USP, Brazil*

1. Introduction

Nowadays, sustainability is pursuit on every production process. One important step to achieve such goal is the development of bioreactors, mainly automated ones in order to assure reproducibility and parameters optimization. Therefore, such automation will require online sensors and procedures to evaluate velocity parameters. In addition, low cost miniaturized bioreactors are fundamental for undergraduate teaching and graduate research in the engineering schools. Thus, the aim of this work is the development of CO_2 sensors and minibioreactors useful for teaching and research.

2. Experimental

Simulation of the proposed bioreactor [1] and the corresponding automation for pH, temperature and luminosity [2] were described elsewhere. This work deals with CO_2 control (T6615, Amphenol advanced sensors), bioreactor fluidics determination and sample pretreatment. CO_2 sensors required an electric circuit and an acquisition system for data analysis whereas bioreactor fluidics was determined using tracers; thus, these two steps assured an operational device. Sample pretreatment (before bioreactor use) was meant for undergraduate teaching and uses as setup sealed petri dishes and air compressor, as reactant sugar cane and baker's yeast (*Saccharomyces cerevisiae*). The main tested parameters were concentration and aeration.

3. Results and Discussions

CO_2 optical sensors can be easily coupled to acquisition systems (Fig. 1) and presents high sensitivity and quick response (Fig. 2) to propelled air. CO_2 concentration inside the reactor can be tested using lit cigarettes as tracers. CO_2 concentration as a function of time (Fig. 3) shows unexpected variations, mainly due to bubble formation although two sensors positioned on different positions showed the same behavior, i.e., indicating system reproducibility. The minireactor (Fig.4), 20 cm length, was made in PVC except for inlet and outlet, which uses acrylics and allows verify fluidic behavior. Mixing inside the system does not require moving parts. Therefore, this small low cost system offers several advantages not only on research but also in teaching.

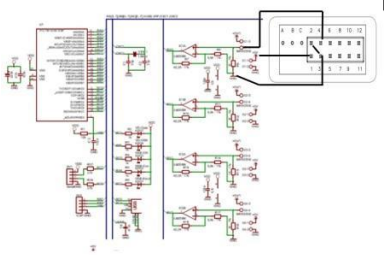

Fig. 1. *CO_2 sensors electrical scheme.*

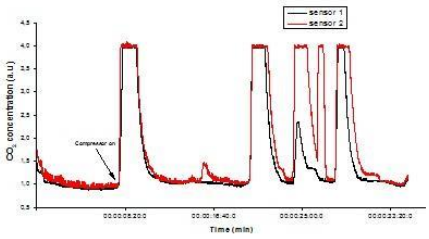

Fig. 2. *CO_2 sensors response for propelled air.*

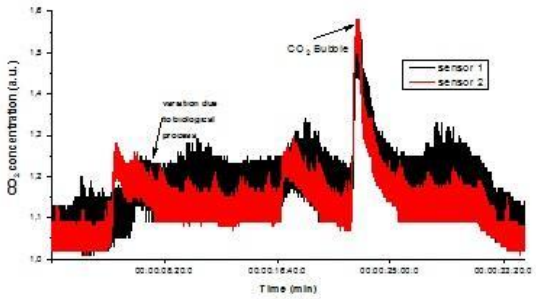

Fig. 3. *CO_2 detection as a function of time.*

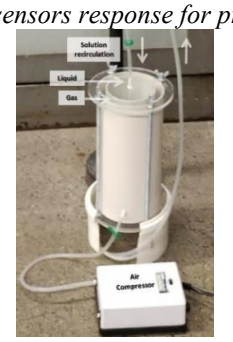

Fig. 4. *Minireactor photo.*

4. References

[1] L. A. da Silva, T. M. de Faria, D. T. de Oliveira, M. L. P. Silva, BT FATEC-SP, **52**, 16 (2021).
[2] T. M. de Faria, L. A. da Silva, D. T. de Oliveira, M. L. P. Silva, BT FATEC-SP, **52**, 15 (2021).
*Corresponding author: jrww01@gmail.com

DEVELOPMENT OF TI-(10-X)AL-XV (X=0,2, AND 4 WT%) ALLOYS FOR USE SINGLE-AXIS KNEE PROSTHESES

Pinto, B. O.[1*], Torrento, J. E.[1], Grandini, C. R.[1], Correa, D. R. N[2].
[1]*UNESP – Univ. Estadual Paulista, Laboratory of Anelasticity and Biomaterials, Bauru (SP), Brazil*
[2]*IFSP – Câmpus Sorocaba, Advanced Metallic Materials Group, Sorocaba (SP), Brazil*

1. Introduction

Biomaterials, in general, are biocompatible with tissues or organs of the body. The Ti-Al-V alloy is a strong candidate for the manufacture of knee prostheses, as studies prove its excellent performance compared to pure titanium [1]. For its manufacture, metals are the most used due to fatigue, fracture, corrosion, and resistance when subjected to firm loads of compression and tensile volume [2]. The main objective of this work is to develop a material that replaces stainless steel for use in light and resistant monocentric knee prostheses based on titanium, aluminum, and vanadium, at a lower cost for elderly patients.

2. Experimental

Commercially pure metals were cut and separated in mass proportion. Then they were ultra-fluoric cleaning solutions in nitric acid. The alloy samples were cast by an arc melting furnace with an inert argon atmosphere, a copper crucible, and a non-consumable tungsten electrode cooled in water. The EDS technique coupled with a scanning electron microscope was used for physicochemical characterization to measure the chemical composition. The Archimedes principle collected the density values. X-ray diffraction measurements were performed using the powder method to analyze the phase composition. For microstructural analysis, optical and scanning electron microscopy were employed.

3. Results and Discussions

The technical composition of EDS proved the correct distribution of the elements during the melting process, corroborating a theoretical theory and confirming the excellent quality of the prepared samples. Radiographic results show lamellar structures with a predominant alpha matrix. Optical and scanning microscopy was performed by α, α+β phases. O. With the addition, more significant of Al with α-stabilizing function, consequently increasing the V (mail β-stabilizing), the alloy becomes lighter, mainly when the pure materiality α-stabilizing is more and, currently, used in prosthetics.

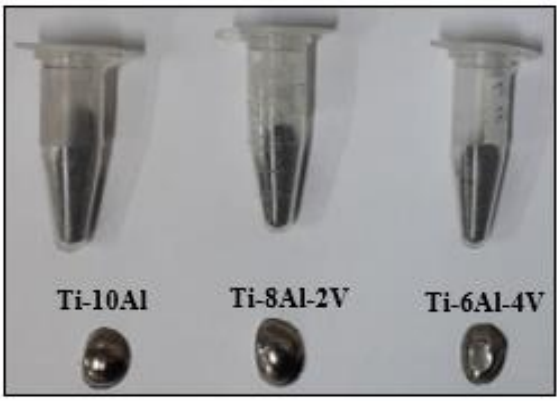

Fig. 1. *Photography of the as-cast samples.*

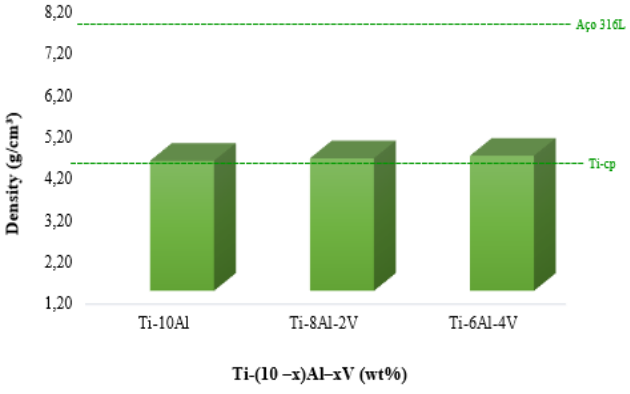

Fig. 2. *Density values.*

4. References

[1] D.R.N, Correa et al, Materials Letters, **179**, 118-121, (2016).
[2] I.R, Ramos, et al, Materials Research, **24** (suppl 1), (2021).

Acknowledgments
The authors thank FAPESP and CNPq for the financial support.

* Corresponding author: bruna.oliveira-pinto@unesp.br

SYNTHESIS OF TANTALUM-DOPED IRON OXIDE COATINGS ON AISI 304 STEEL WITH PLASMA ELECTROLYTIC OXIDATION FOR USE WITH BIOMATERAL

Proença, J. P.[1,2*], Correa, D. R. N.[2]; Cruz[1], N.C.; Rangel[1], E.C.
[1]*UNESP – Univ Estadual Paulista, Laboratório de Plasmas Tecnológicos, Sorocaba, Brazil*
[2]*IFSP – Câmpus Sorocaba, Advanced Metallic Materials Group, Sorocaba (SP), Brazil*

1. Introduction

Among the austenitic stainless steels, the AISI 304 has been widely used in the medical and dental fields, due to its high mechanical strength and biotolerability by the human body. However, its use as implants requires greater corrosion resistance, so that the material does not release hazardous ions or debris, causing a rejection of the implant through inflammation or necrosis. One way to increase this corrosion resistance is by adding a surface coating of ceramic oxides, which act against intergranular corrosion [1]. Through the process of plasma electrolytic oxidation (PEO), it is possible to create an oxide layer on the metal surface strongly adhered to. Considering the recent biofunctional properties discovered in tantalum oxide [2,3], such as biocompatibility, bioactivity, and corrosion resistance, its use as coatings in PEO can give 304 stainless steel a greater potential for use as metallic biomaterials.

2. Experimental

The PEO treatment was carried out in a stainless steel reactor with internal water cooling. The samples were placed at a negative potential (anode), while the stainless steel chamber was kept at a positive potential (cathode). The surface treatments were carried out with a pulsed voltage source, with voltages of 200 V, a frequency of 1000 Hz, and a duty cycle of 60%, for 10 min. The electrolyte was varied, consisting of an aqueous solution of 2 g/L, 2.5 g/L, and 3 g/L of potassium hydroxide (KOH), and tantalum hydroxide (TaOH) in the proportions of 10 g/L, 30 g/L, and 50 g/L. The treatments were carried out in triplicate, to ensure good reproducibility of results. Then, morphology, phase proportion, and chemical composition were evaluated by SEM/EDS and XRD measurements.

3. Results and Discussions

During the first minute of treatment, it is possible to see in Fig. 1 a current increase due to the KOH electrolyte. After that, an exponential decrease of the current proves that an oxide layer is formed on the substrate surface, which hinders the passage of current and favors the appearance of micro-arcs. SEM/EDS results indicated that the oxide layer was porous, with some amount of Ta oxide incorporated into the coating. The XRD pattern exhibited just an amorphous phase composition. XPS analyzes were also performed to characterize the surface species and their evolution, confirming the presence of Ta_2O_5 in the coatings.

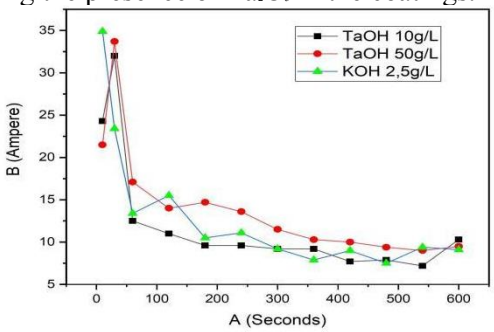

Fig. 1. *Graph of current variation (B) over time (A).*

4. References

[1] Manam, N. S. et al., Journal of Alloys and Compounds, **701**, 698–715, (2017).
[2] Antonio, R. F. Tese (Doutorado) – Universidade Estadual Paulista. Faculdade de Ciências. Bauru, (2016).
[3] Zeliang D. et al., Ceramics International, **47**, (2021).

Acknowledgments
The authors thank the Brazilian funding agencies CNPq and FAPESP.

*Corresponding author: joao.proenca@unesp.br

NATURAL RUBBER MODIFIED WITH HYALURONIC ACID FOR SKIN LESION APPLICATIONS

Quevedo, B. V.[1,3]*, Silva, L. C. S. C. da[3], Motta, A.C.[3], Komatsu, D.[2,3], Rezende, M. de L.[2], Duek, E. A. de R.[1,3]
[1]*Federal University of São Carlos – 18052-780, Sorocaba, Brazil.*
[2]*Faculty of Technology of Sorocaba – 18013-280, Sorocaba, Brazil.*
[3]*Pontifical Catholic University of São Paulo – 18030-070, Sorocaba, Brazil.*

1. Introduction

Studies show that biopolymers such as natural rubber (NR) and hyaluronic acid (HA) are of great interest to the biomedical area, because in addition to being biocompatible with the body, they can act in tissue repair [1]. However, individually they have certain limitations that must be improved. Thus, this work aims to modify the NR through grafting with HA, forming a new biomaterial with hybrid properties that can be applied in the future as a dermal dressing [2]. Thus, the material obtained was analyzed by spectroscopic techniques and esterification reactions were observed, which suggest a chemical interaction between both chemical structures.

2. Experimental

NR is epoxidized (ENR) by addition of formic acid and hydrogen peroxide. For the grafting process, 30% HA was added to the reaction, which was heated to reflux at 40°C at different times (3, 4 and 5 hours). The material was poured into a Teflon mold and oven dried at 35°C. After drying, it was washed with distilled water. The samples are submitted to Fourier Transform Infrared Spectroscopy (FT-IR) and Nuclear Magnetic Resonance (^{1}H NMR).

3. Results and Discussions

It was observed through FT-IR analysis, Fig. 1, that the sample subjected to 5 hours of reaction showed the appearance of a new band at 1774 cm^{-1}, which may be associated with the C=O stretching of the ester, which suggests grafting by esterification between the chemical groups of ENR and HA [1]. This corroborates the result presented in the 1H NMR spectrum, Fig. 2. that in addition to presenting signals referring to the protons of the epoxidized isoprene unit and protons present in the N-acetylglucosamine group of HA [1], it also presented a signal at 2.1 ppm(c), which was associated with the protons present in esters, which reinforces the grafting reaction [3]. Spectroscopic analyzes suggest indications that the HA was grafted onto the chemical structure of the ENR, thus synthesizing a new hybrid biomaterial.

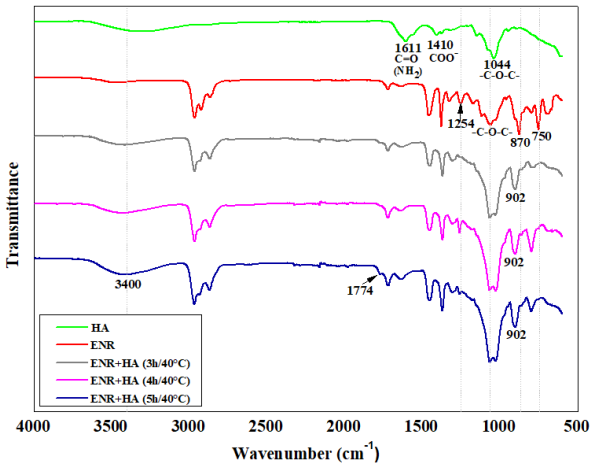

Fig. 1. *FT-IR of HA, ENR and ENR(g)HA.*

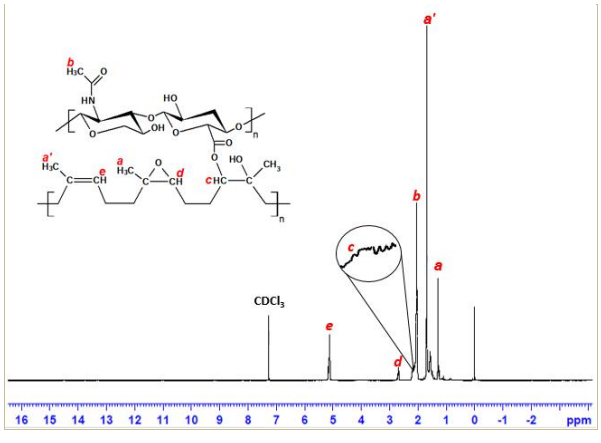

Fig. 2. *^{1}H NMR spectrum and possible chemical structure of the ENR grafted with HA (5h/40°C).*

4. References

[1] Lee, H. Y., et al., Colloids Surf. B, **174**, 308-315, (2019).
[2] Venkatanarasimhan, S., Dhamodharan D., Polym. Bull. **72**, 2311-2330, (2015).
[3] Pongsathit, S., Pattamaprom C., Int. j. radiat. phys. chem., **144**, 13- 20, (2018).

Acknowledgments
Coordenação de Aperfeiçoamento de Pessoal de Nível Superior – Brasil (CAPES).
*Corresponding author: brunaqueved@gmail.com

PROPOSED MECHANISM FOR THE FORMATION OF $SIO_XC_YH_Z$-TIO_X NANOCOMPOSITE THIN FILMS BY PECVD USING DATA FROM IRRAS, PM-IRRAS, AND XPS

Ribeiro, R. P.[1*], Cruz, N. C.[1], Rangel, E. C.[1]
[1]*Science and Technology Institute of Sorocaba (ICTS), São Paulo State University (UNESP), 511 Av. Três de Março, Sorocaba, 18087-180, Brazil*

1. Introduction

Recently, there has been an increase in the interest in the scientific community for the production of nanocomposite thin films combining liquid and gas phase processes. This is experienced by creating an aerosol of nanoparticles from a colloidal solution or by directly injecting the colloidal solution into the gas phase system, most processes being done at atmospheric pressure. However, these methods have disadvantages compared to low-pressure plasmas with low ion energy and a very small mean free path, which limits the possibility of deposition of dense films and may limit homogeneity [1]. An alternative for this is the creation of nanoparticles in the low-pressure plasma itself, using the PECVD methodology for nanocomposite film deposition. Therefore, the purpose of this work was to develop multifunctional Si-based nanocomposite films containing TiO_2 particles. For this, the PECVD methodology was used from the liquid mixture of titanium tetraisopropoxide compounds, TIPT, hexamethyldisiloxane, HMDSO, in addition to argon and oxygen gases. Using a combination of IRRAS, PM-IRRAS and XPS, in addition to research in the literature, an attempt was made to delineate a reaction mechanism that justifies the formation of chemical bonds observed in the deposited films.

2. Experimental

Thin films were deposited onto aluminum thin film mirror plates and glass plates from atmospheres containing titanium tetraisopropoxide (TTIP), hexamethyldisiloxane (HMDSO), Ar and O_2. The total pressure in the chamber and the deposition time were fixed at 133 Pa and 1800 s, respectively. The proportion of O_2 was varied from 0 to 90%, while the proportion of the mixture TTIP, HMDSO and Ar (carrier gas) was varied in the opposite direction. The plasma was excited by applying 25 W of RF signal (13.56 MHz) to the upper electrode, while the lower electrode (sample holder) remained grounded. The molecular structure of the films obtained was analyzed using IRRAS, PM-IRRAS and XPS.

3. Results and Discussions

Combining the results obtained by the IRRAS, PM-IRRAS, and XPS techniques, together with the binding energies and fragmentation mechanisms of the monomers reported in the literature, it was possible to delineate possible routes of formation of the chemical bonds observed in the thin films deposited with different proportions of oxygen.

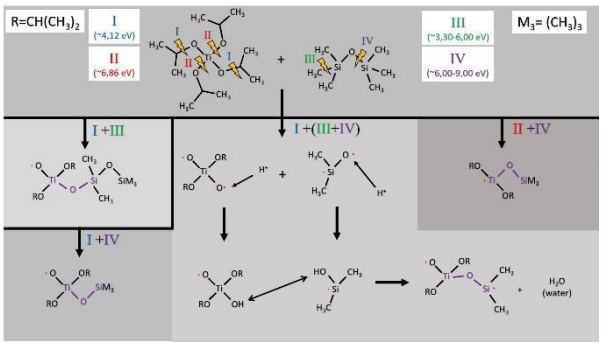

Fig. 1. *Possible mechanisms for creating Ti-O-Si bonds.*

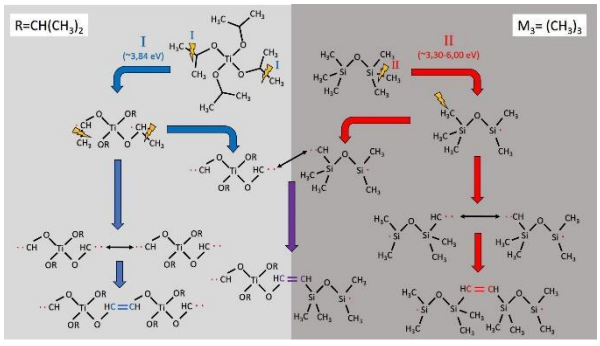

Fig. 2. *Possible mechanisms for the formation of C=C bonds.*

4. References

[1] Mitronika et al., SN Appl. Sci., **3**, 665, (2021).

Acknowledgments

Authors would like to thank CAPES (1766917- RPR) and FAPESP (2017/21034-1) for their support.

*Corresponding author: rafael-parra.ribeiro@unesp.br

STUDY OF THE EFFECT OF TEMPERING TEMPERATURE AND CARBON ADDITION EFFECT ON THE PROPERTIES OF THE SAE 8640 STEEL SUBMITTED TO PLASMA NITRIDING

Rossino, L. S.[1,2]*, Coan, K. S.[1], Antônio Junior, C. A.[2], Silva, F. L. F.[2], Almeida, L. S.[2], Danelon, M. R.[2], Manfrinato, M. D.[1,2]

[1]*Faculdade de Tecnologia do Estado de São Paulo (Fatec Sorocaba), CEETEPS, Sorocaba-SP*

[2]*Universidade Federal de São Carlos, PPGCM, UFSCar Campus Sorocaba, Sorocaba-SP*

1. Introduction

Plasma nitriding and nitrocarburizing are thermochemical treatments in which the temperature and composition of the treatment environment may improve the surface properties of the metal but influences or impair the properties of the substrate [1]. The objective of this work is to verify the simultaneous effect of the nitriding temperature (Nit) on the formation of the layer and the softening of the substrate, as well as the effect of carbon (nitrocarburization - NC) on the effectiveness of the plasma treatment of 8640 steel.

2. Experimental

The quenching studied metal was subjected to 6 series of treatments: tempering at fixed temperature with subsequent nitriding at different temperatures (T+R450+Nit), tempering at different temperatures and subsequent nitriding at a fixed temperature (T+R+Nit450), tempering carried out together with nitriding at different temperatures (T+Nit), nitrocarburizing and tempering carried out together (T+NC) and nitrocarburizing at different temperatures in the material quenched and tempered at different temperatures (T+R450+NC and T+R+NC450). The material with and without treatment was characterized by metallography, hardness test, and abrasive microwear test. The results of the plasma treated materials were compared to the as received metal (MB), quenched, and tempered (T+R), and nitrided as received material (MB+Nit).

3. Results and Discussions

It was observed that the performance of the surface treatment generates microstructural changes and a decrease in the hardness of the substrate compared to the tempering treatment carried out in a conventional furnace. The nitrocarburization treatment is more effective in maintaining the substrate characteristics achieved in the tempering treatment performed in a conventional furnace. The temperature of the nitriding or nitrocarburizing treatment has a relevant influence on the hardness of the substrate, but the tempering temperature performed before the surface treatment did not show a significant influence on the surface properties of the material subjected to thermochemical treatments carried out at fixed temperature. However, the kind of processing influences the formation of the layer. For example, T+N or T+NC showed the formation of a composite layer at 250°C, which was not observed in the other processing conditions. All thermochemical treatment conditions provided higher hardness compared to MB and T+R material, emphasizing that nitrocarburizing produced layers with maximum hardness, greater total thickness compared to nitrided samples and greater wear resistance compared to untreated material, quenched, and tempered material and nitrided material.

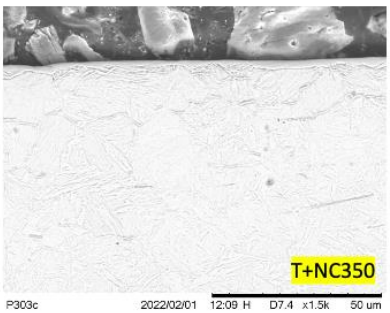

Fig. 1. *Micrography of T+NC350 sample.*

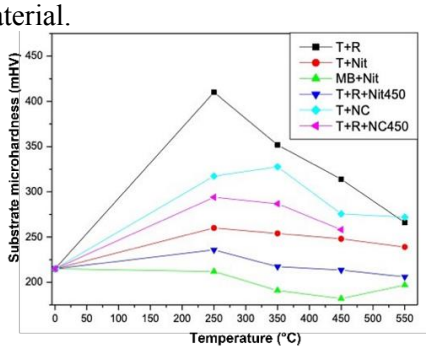

Fig. 2. *Microhardness result to different treatment conditions.*

4. References

[1] S. P. Bruhl et al., Industrial Lubrication and Trioblogy, **68**, 125-133, (2016).

Acknowledgments

We would like to thank CEETEPS and CNPq (163608/2020-2).

*Corresponding author: luciana.rossino@fatec.sp.gov.br

EVALUATION OF DLC FILM DEPOSITION ON THE CUTTING TOOL SUBMITTED TO THE DRY DRILLING PROCESS IN THERMOSETTING POLYMER

Rozatti, M. P.[1], Oliveira, J. J. de[1], Danelon, M. R.[2], Rossino, L. S.[1], Toti, F. de A.[1]
[1]*Faculty of Technology of Sorocaba – Fatec-So*
[2]*University of São Carlos – Ufscar - So*

1. Introduction

The academic and industrial sectors are looking forward the development and application of materials that attend design needs considering the manufacturing process, costs and environment impact of a determined product. In this context, the use of polymers is increasing depending on, for example, the mechanical properties per unit of mass. In the dry drilling process of these materials, the heat generation can raise the process temperature and exceed the glass transition temperature (Tg) or material degradation temperature, combined with this, the cutting tool wears out prematurely, which may affect the machined surface integrity. The application of heat treatment in the cutting tool is a variable to be studied in the process of improving the machinability of polymers [1]. In the cutting tool market, there are no specific tools for machining polymers, where the main difficulty is chip control and the cutting tools available are only for metal machining [2]. The present work aims to evaluate the wear performance of the high-speed steel drill cutting tool subjected to surface heat treatment by DLC (Diamond like-carbon) film deposition in the dry drilling of thermoset polymer.

2. Experimental

The initial procedure was to remove atmospheric pressure from inside the reactor. Then, the surface of two 6 mm diameter high speed steel (HSS) cutting tools were cleaned (Sputtering) with a mixture of gases in the proportion of 80% Argon – 20% Hydrogen. The deposition of the DLC film was performed by PECVD using a pulsed DC source at LabTES – Laboratory of Surface Technology and Engineering, at Fatec-Sorocaba. For this, a support was designed and manufactured to guarantee the deposition of the film on the entire surface of the cutting edges.

3. Results and Discussions

The DLC treatment was performed, and the vertical position of the tools provided the deposition of the film evenly over the entire surface of the cutting edges, as shown in Figure 1. Then, 06 holes were made in the thermoset polymer phenolic Celeron, in the center machining tool EMCO Concept Mill with Sinumerik 840D control. The cutting parameters used were: Vc of 40 m/min; feed rate of 143 mm/min and 2123 rpm. In the initial evaluation it was possible to verify that the DLC film supported the temperature of the process. However, new treatments will be performed, and the number of drillings will be increased to 50. Figure 2 shows the drilling process completed in the Celeron polymer.

Fig. 1. *DLC film deposition.*

Fig. 2. *Drill and drilling finished in Celeron polymer.*

4. References

[1] Chabbi, A. et al., International journal of advanced manufacturing technology, **91**, 2267-2290, (2017).
[2] Jagtap, T.U., Hemant, A.M. International Journal of Engineering and General Science, **3**, 2091–2730, (2015).

Acknowledgments
The team from the Surface Technology and Engineering Laboratory - LabTES.

*Corresponding author: francisco.toti01@fatec.sp.gov.br

EFFECTS OF LOW-TEMPERATURE PLASMA TREATMENT ON SUGARCANE BAGASSE-BIOCHAR

Santacruz-Salas, A. P.[1*]; Antunes, M. L. P.[1], Rosa, A. H.[1]; Rangel, E. C.[1].
[1]*São Paulo State University (UNESP), Institute of Science and Technology of Sorocaba, S.P., Brazil*

1. Introduction

Biochar made from agricultural residues is a viable alternative to address problems related to water pollution [1]. Therefore, it is interesting to improve its properties using different techniques, such as low-temperature plasma functionalization. A method that consists of producing energetic electrons, ions, and active radicals that enhance the porous structure of the sorbent and increase the number of functional groups on the surface [2]. For this reason, in the present study, biochar made from sugarcane bagasse was treated by a low-temperature plasma process with SF6 as a working gas and the physical and chemical effects caused by the modification were evaluated.

2. Experimental

For the preparation of biochar, the sugarcane bagasse was subjected to a pyrolysis process, with a heating rate of 5°C/min until it reached 300°C and this temperature was maintained for 2 h.
Plasma modification was performed using a stainless steel reactor. A certain amount (1g) of the sample was placed on reactor plate on the lower electrode and the system was evacuated at a background pressure of 2.2 Pa. SF6 gas was administered at a pressure of 12 Pa, producing a working pressure of 14.2 Pa. The applied power was 300W, 13.56 MHz and the working times were 2, 30, and 60 min.

3. Results and Discussions

The FTIR results show similar characteristics among all spectra (Figure 1), however it is possible to observe the presence of some bands, mainly in the biochar treated for 60 min, such as the band located in the 1040 cm-1 which is related to the C-F stretching vibration [3]. In conclusion, the results indicate the formation of small structures within the material that do not affect the main structure.

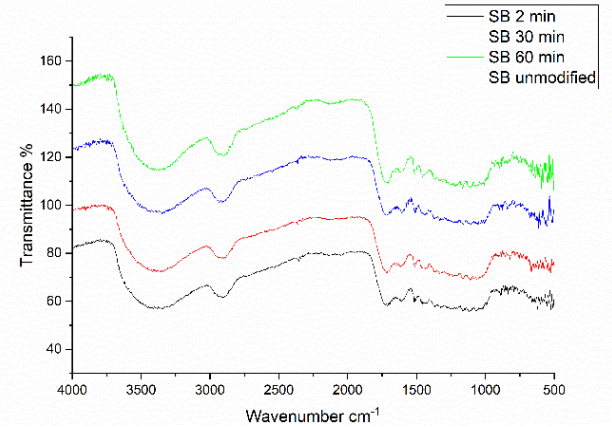

Fig 1. *The FT-IR spectra of Biochars*

4. References

[1] W.-H. Chen *et al.*, *Process Safety and Environmental Protection*, **160**, 704-733, (2022).
[2] T. Wang *et al.*, *Chemical Engineering Journal*, **331**, 536-544, (2018).
[3] Q. Zhang *et al., Journal of Alloys and Compound,* **901**, 163657 (2022).

Acknowledgments
This work was supported by the government of Nariño (Colombia) and The Center for Basic and Applied Interdisciplinary Studies Foundation – CEIBA through the project "Bécate Nariño."

*Corresponding author: paola.santacruz@unesp.br

EVALUATION OF THE SPATIAL RESOLUTION OF CAMERAS FOR REMOTE SENSING APPLICATIONS IN THE VISIBLE SPECTRUM AND NEAR-INFRARED

Santos, J. dos[1]*, Castro, R. M. de[2], Damião, A. J.[1,2]
[1]*Departamento de Ciência e Tecnologia Aeroespacial – Instituto Tecnológico de Aeronáutica – São José dos Campos (SP), Brasil*
[2]*Instituto de Estudos Avançados – São José dos Campos (SP), Brasil*

1. Introduction

The use of an electro-optical sensor to obtain information remotely has greatly impacted different areas of knowledge. Highlighting the suborbital performance levels, the use of photographic cameras coupled with drones has allowed the sensing of a region in a more accessible way. However, to guarantee the accuracy of the collected data, it is necessary to know the responses extracted from the sensor properly; therefore, its calibration is essential. In the case of electro-optical imaging sensors, their spatial resolution is an important feature to be evaluated. It consists of the detector's ability to distinguish the radiation variations in the target, that is, the ability to identify the contrasts of the observed region [1]. Thus, this work aimed to evaluate the Flir Duo and Parrot Sequoia cameras concerning their spatial characteristics to obtain reliable quantitative data in the visible and near-infrared spectrum range.

2. Experimental

The Slanted Edge method was adopted among the spatial calibration methods established by the ISO 12233 standard [2]. In this method, the sensor captures an image of a target with a contrast of colors, which will generate different digital levels in the sensor, and, from the amplitude of the signal measured by the sensor, a modulation transfer function (MTF) can be obtained. This curve indicates the relative efficiency of the sensor in observing target details. Therefore, to carry out calibrations and spatial characterizations using this method, it was necessary to produce targets to be imaged. The next steps were: a FieldSpec spectroradiometer was used to evaluate the targets radiometrically; a goniometer was used to control the positioning of the camera and allow angular variations of its sight every 15°, in addition to ensuring that the sensor observes the target from a central point. Finally, a Matlab software plug-in routine was used to generate the MTF of the images collected by the cameras.

3. Results and Discussions

The collection of radiometric data without angular variations, with the view of the sensor perpendicular to the target, allowed us to determine that the target has a diffuse reflection. However, from the increase of the spectroradiometer's viewing angle, it was noticed that the light reflection occurred in a specular way. Flir Duo camera visible range images are generated in JPG format only and show an MTF curve above the maximum normalized value. The images obtained by the Sequoia Parrot camera were saved in TIFF format and presented an expected MTF curve. However, when evaluating the digital levels of the images, it was found that they did not have a normal distribution, having several points of the image with the values maximum digital level of the camera. With this work, it was possible to observe that the automatic gain of control of the cameras, although it helps visualize the image, negatively influences the calibration of the same. In addition, the images generated in JPG format showed an increase in signal strength in the region of contrast between the color, generating an MTF curve with incorrect behavior. It will still be necessary to evaluate the influence of angular variations on the spatial calibration of these cameras.

4. References

[1] J. R. Schott "*Remote Sensing: the image chain approach*", 2nd edition, Oxford University Press, USA, (2007).
[2] ISO. "*ISO 12233:2017: Photography – electronic still Picture imaging – resolution and spatial frequency responses*", (2017).

*Corresponding author: jeannsant@hotmail.com

DEVELOPMENT OF PLASMA BORIDING USING SOLID PASTE ON 304 STAINLESS STEEL

Santos, O. A. de M. R.[1]*, Silva, F. L. F. da[2], Almeida, L. S. de[2], Manfrinato, M. D.[1,2], Rossino, L. S.[1,2]
[1]*Faculdade de Tecnologia do Estado de São Paulo (Fatec Sorocaba), CEETEPS, Sorocaba-SP*
[2]*Universidade Federal de São Carlos, PPGCM, UFSCar Campus Sorocaba, Sorocaba-SP*

1. Introduction

The boriding process is a thermochemical treatment with prominence in the current scenario of material research due to the excellent properties obtained through this treatment, aiming the industrial and aerospace area [1]. Plasma treatment using solid paste as a boriding agent has proved to be an interesting alternative due to the low treatment temperature, time, and the use of a non-toxic gas. The objective of this work is to develop the plasma boriding treatment using solid paste in 304 stainless steel.

2. Experimental

The solid paste composed of EKABOR®, sodium tetraborate, and ethyl alcohol was sprayed using a pressure gun connected to a compressor onto the polished and cleaned surface of the 304 stainless steel. Plasma surface treatment was carried out using 20% Ar, 40% H_2, and 40% N_2 at a pressure of 2 torr for 4 hours at 600°C, 650°C, and 700°C. The results were observed by metallographic analysis.

3. Results and Discussions

The spraying methodology to deposit the solid paste presented good adhesion and uniformity over the sample surface. It is possible to observe the formation of a boride layer on the surface of the treated material, proven by the EDS analysis (Table 1), in that the increase in the treatment temperature increased the thickness of the formed layer, as observed in Figure 1. The layer formation occurred at a temperature lower than that reported in the literature [2], emphasizing the effectiveness of this treatment configuration. These boriding plasma surface treatment using solid paste was carried out using an alumina plate to isolate the sample of the cathode electrode, avoiding arcs, and overheating on the treated material.

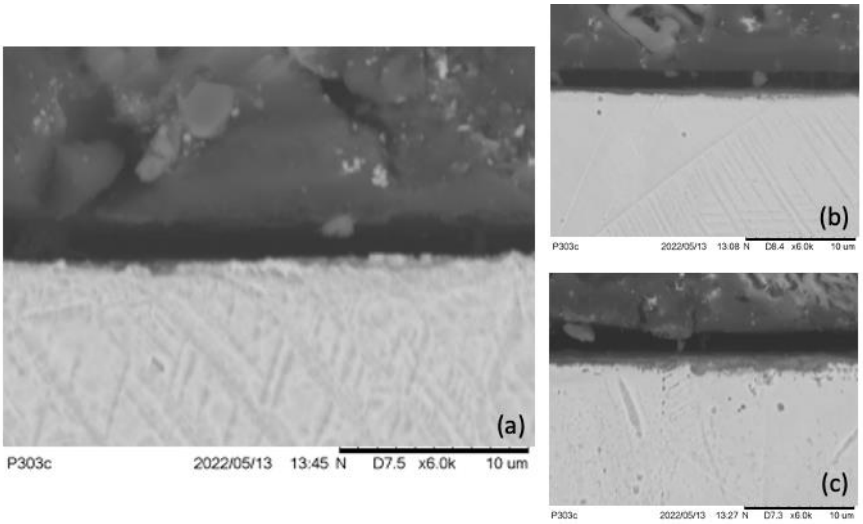

Fig. 1. *Micrography obtained for the plasma boriding treatment using solid paste at (a) 600°C, (b) 650°C, and (c) 700°C.*

wt% of boron element		
	Surface	Substrate
600°C	7.9	3.4
650°C	5.4	
700°C	8.6	

Tab. 1. *Chemical characterization of the layer produced for the plasma boriding treatment using solid paste obtained by SEM/EDS*

4. References

[1] E. R. Cabeo et al., Surf. & Coat. Tech., **116-119**, 229-233, (1999).
[2] M. Keddam et al., Trans Indian Inst Met, **70**, 1377-1385, (1980).

Acknowledgments
We would like to thank Fapesp (2021/05995-7).

*Corresponding author: otavioaugusto_mrs@hotmail.com

CARBON NANOTUBES PRODUCED BY PECVD ARE LESS TOXIC THAN THOSE PRODUCED BY CVD METHOD

Serenvices, K.[1*], Irazusta, S. P.[1,2], Almeida, L. S. de[3], Rossino, L. S.[1,3]
[1] *Faculdade de Tecnologia de Sorocaba – José Crespo Gonzales, CEETEPS-SP, Brasil*
[2]*Programa de Mestrado Profissional em Gestão e Tecnologia dos Sistemas Produtivos-CEETEPS, SP, Brasil*
[3]*Programa de Pós Graduação em Ciências dos Materiais – UFSCar- Sorocaba, SP, Brasil*

1. Introduction

The almost infinite possibilities of nanotechnology applications have motivated studies in several scientific areas [1]. Research aimed at developing nanotechnology seeks to master the manipulation of matter at atomic and molecular levels in order to introduce them into industrial products and processes, which generate billions of dollars in investment [1,2]. One of the most promising are carbon nanotubes (CNT), which have high mechanical strength, high capillarity and excellent optical and electronic properties, which give them several applications [1,2]. However, due to the same characteristics of NTCs, this growing production and application may have impacts on the environment, and there is no consensus about its possible impacts on ecosystems [3]. The aim was evaluate these possible impact in a aquatic bioindicator.

2. Experimental

The aquatic toxicity test used algae of the species *Raphidocelis subcapitata* according to the Environmental Protection Series EPS 1/RM/25, 2007 standard. CNTs produced by PECVD and a commercial CNT, brand HELIX, produced by CVD method, at concentrations of 0,1; 0,5; 1,0; 5,0; 10,0; 20,0; 40,0; 60,0; 80,0; 100,0mg/L were tested. Both samples were inoculated in microtiter plates, after 72h absorbance was measured at wavelengths of 620 and 650nm, and 3 replicates of each concentration were manually analyzed using a Neubauer Chamber. Lastly EC50 (concentration that causes 50% of mortality) were calculated.

3. Results and Discussions

Although the opacity of carbon nanotubes influences the absorbance analyses, by manually counting the samples, it was demonstrated that the PECVD CNTs are less toxic than the CVD CNTs, the EC50 was 9,316mg/L and 33,8µg/L respectively. However, despite the lower inhibition rate, cells were found to be cleaved and fully covered by the PECVD fabricated CNTs.

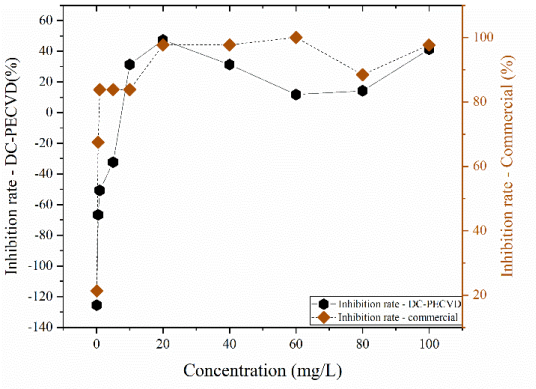

Fig. 1. *Comparative chart between inhibition of the samples*

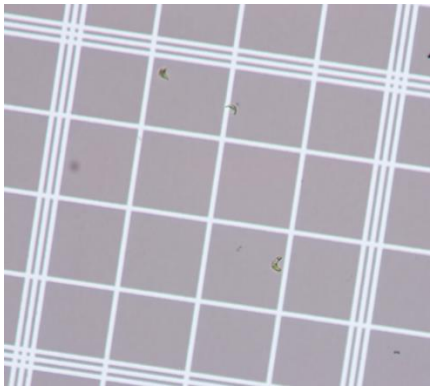

Fig. 2. *Initial presence of cleaved cells, in 10mg/L rate PECVD Samples.*

4. References

[1] S. F. Ferreira *et al*., Quím. Nova., **32,** 1860-1870, (2009).
[2] M. Herbst *et al*., Quím. Nova., **27**, 986-992, (2004).
[3] M. P. Paschoalino. Quím. Nova., **33**, 421-430, (2010).

*Corresponding author: kazys.serevincis@fatec.sp.gov.br

ELECTROSPUN FIBERS OF PVP AND ALOE VERA - SOLVENT INFLUENCE

Silva, A. N. R. da[1,2*], Assunção B. S.[2]
[1]*LSI-PSI EPUSP São Paulo Brazil*
[2]*FATEC-SP São Paulo Brazil*

1. Introduction

Electrospun nanofiber membranes find applications in several areas, such as filter, immobilization of enzymes or drug delivery. For drug delivery, it is important to understand the interaction between the polymer and the active principle added to the solution and how it is incorporated into the fiber during the electrospinning [1,2]. Therefore, the objective of this work is to study the interaction between solvents, polyvinylpyrrolidone (PVP) and aloe vera in order to stablish their influence in the electrospinning of membranes and respective properties.

2. Experimental Procedure

Solution with 1,8g PVP and 0,1g aloe vera with different solvents (ethanol, isopropanol and distilled water) were prepared. The electrospinning setup were described in previous works [1]. Any solution prepared with water or water mixtures presents lower viscosity compared with organic solution (IPA and ethanol), pure or mixed. As aloe vera is soluble in water, but poorly soluble in alcohol, water presence in the organic solvent mixtures facilitates the dissolution of aloe vera. Therefore, whereas alcohol entangled the polymer molecule, water creates hydrogen bonds with aloe vera and alcohol molecules, which means that interaction between polymer and the active principle is achieved by secondary interaction.

3. Results and Discussion

SEM (Figure 1) images show beads in fibers electrospun from the alcohol solutions that is due to the low solubility of aloe vera in alcohol, which also creates precipitate in most samples. Thus, the fiber morphology can be attributed to the aloe vera particulate presence. The Raman analysis presents fluorescence at the baseline, so it may have a highly stressed arrangement which can be attributed to the action of the electric field during the electrospinning [1]. The aloe vera components (polysaccharides) and the carbonyl of the PVP [2] can form hydrogen bridges with the solvents especially water. The bands at 1360 and 1560 cm^{-1} are poorly resolved in samples with water and best observed in organic solvents. While the first band may be due to CH the second may indicate OH or C=O, since no interaction is expected between the vinyl structure and the polar radicals of PVP it is more likely that the band at 1560 cm^{-1} is due to aloe vera.

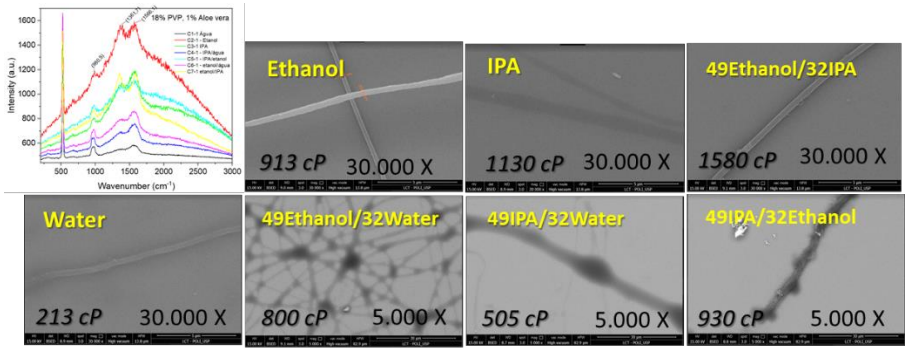

Figure 1: *Raman spectra and SEM images from electrospun fibers. Inside the images are the solution viscosity values and solvent composition.*

Thus, the organic solvents, due to their size and less polar region, allow the PVP in the fiber to have low interaction with the aloe vera and due to the high polarity and small size of the water, the interaction of the aloe vera with the polar regions of the PVP may be facilitated. The results suggest that the use of alcohol solvent is the best way to obtain PVP fibers with aloe vera.

4. References

[1] SILVA, A. N. R. et al. Materials Research, **8**, 105-108, (2005).
[2] FURLAN, R. et al. Proceedings of 31st SBMicro, 1-4, (2016).

Acknowledgments
To LCI-FATEC-SP, LSI-EPUSP and CNPq for the PIBIC scholarship.
*Corresponding author: neilde@lsi.usp.br

COMPARATIVE STUDY OF PLASMA AND SOLID BORIDING PROCESS OF THE TI6AL4V

Silva, F. L. F. da[2]*, Almeida, L. S. de[2], Santos, O. A. de M. R[1], Manfrinato, M. D.[1,2], Rossino, L. S.[1,2]
Faculdade de Tecnologia do Estado de São Paulo (Fatec Sorocaba), CEETEPS, Sorocaba-SP [2]Universidade Federal de São Carlos, PPGCM, UFSCar Campus Sorocaba, Sorocaba-SP

1. Introduction

Boriding is a thermochemical treatment that introduces boron into the material, aiming to improve the surface of the treated substrate. This treatment can be carried out by solid, liquid, gas, and plasma processes. Solid boriding is the most viable method because of its low cost and easy handling, covering the material with the powdered boring agent and raising the temperature in an oven. Plasma boriding using solid paste is one alternative to toxic boriding gas agents, such as BF_3 (boron trifluoride), B_2H_6 (diborane) or BCl_3 (boron trichloride). Ti6Al4V (Titanium, 6% Aluminum and 4% Vanadium) is used in the aeronautical and biomedical industry, however, surface treatment is extremely important to improve the mechanical and biological properties of the material [1,2]. The objective of this work is to introduce boron through solid and plasma boriding to compare the surface properties obtained by these processes.

2. Experimental

In the solid boriding process, the samples were covered with the boriding agent with Ekabor, and the temperature treatment carried out at 750ºC, 850ºC, and 950ºC for 6 hours. For plasma boriding process, the solid paste was produced with 70% Borax ($Na_2B_4O_7$) as a boriding agent and 30% Silicon Carbide (SiC) as the reaction stabilizer. The samples were covered with the paste and placed in the reactor, with 40% N_2 (nitrogen), 40% H_2
(hydrogen) and 20% Ar (argon), generating the plasma at 650ºC for 4 hours. Analyzes were performed by SEM (Scanning Electronic Microscope) and XRD (X-Ray Diffraction).

3. Results and Discussions

It was identified that oxides were formed in the solid process, with the presence of pores in the layer observed through SEM and the presence of TiO_2 (titanium dioxide) through XRD. The presence of oxygen is due to the high affinity of this element with titanium, and in this process, oxygen is a problem in the diffusion of boron in the substrate. At temperatures of 850ºC and 950ºC, the layer was obtained even with the presence of pores, and the desired phases TiB (titanium boride) and TiB_2 (titanium diboride) were also identified. In plasma boriding process, the formed layer presented the TiB and TiB_2 phases, without the presence of oxygen, as the process was carried out in a controlled atmosphere. In the plasma process, the formed layer is homogeneous without pores, and viable compared to the time and temperature that are lower by the direct interaction of the ions generated in the plasma with the paste, helping in the efficient diffusion of boron.

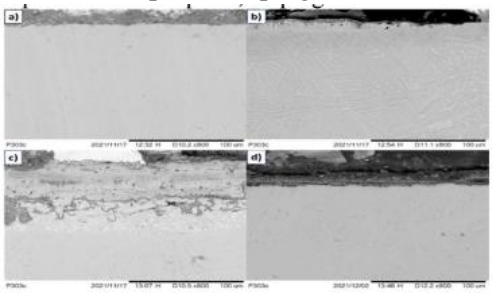

Fig. 1. *SEM, Solid Boriding: a) 750ºC, b) 850ºC, c) 950ºC and Plasma Boriding: d) 650ºC.*

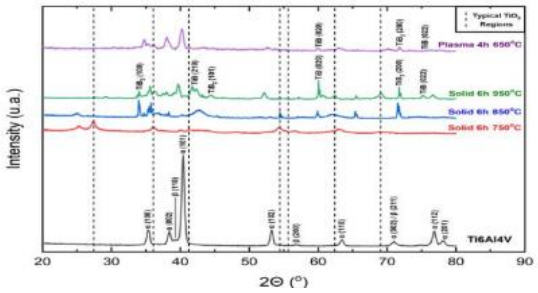

Fig. 2. *XRD of Ti6Al4V boride in solid and plasma method.*

4. References

[1] Küper, A. et al. Surface and Coatings Technology, **130**, 87– 94, (2000).
[2] Makuch, N. et al. Thin Solid Films, **626**, 25–37, (2017).

Acknowledgments
We would like to thank CAPES (001).

*Corresponding author: felipelopesfsilva@gmail.com

SYNTHESIS AND MECHANICAL CHARACTERIZATION OF GRADED TIN FILMS

Silva, F. C. da[1,2]*, Cozza, R. C.[1,3], Miscione, J. M. C.[2], Sagás, J. C.[4], Fontana, L. C.[4], Schön C. G.[2]
[1] *CEETEPS – Centro Estadual de Educação Tecnológica "Paula Souza" - Brazil*
[2] *Universidade de São Paulo, Department of Metallurgical and Materials Engineering - Brazil*
[3] *Centro Universitário FEI – Fundação Educacional Inaciana "Padre Sabóia de Medeiros" - Brazil*
[4] *Laboratory of Plasmas, Films and Surfaces, Universidade do Estado de Santa Catarina- Brazil*

1. Introduction

Ceramic hard films as titanium nitride (TiN) have been used in the last decades to enhance wear resistance and increase mechanical properties of surfaces. TiN stands out due to its excellent mechanical, optical, electrical properties and corrosion resistance [1]. Among many variations of the physical vapor deposition methods for the production of TiN films, grid assisted magnetron sputtering technique (GAMS) produces highly homogeneous films with nanograins due to the grid inserted between target and substrate [2]. The aim of this work is to synthesize and characterize mechanical graded and homogeneous TiN films by GAMS.

2. Experimental

Homogeneous and graded TiN films were deposited onto commercially AA1100 sheet in the "dog bone" geometry. The total deposition time was fixed at 30 min and DC substrate bias was set to -40 V for both conditions. Grazing incidence x-ray diffraction mode (GIXRD) experiments were carried out in the θ-2θ configuration. To determine mechanical properties (hardness and elastic modulus), nanoindentation tests were performed using instrumented indentation with a Berkovich tip and 5 mN load.

3. Results and Discussions

Figure 1 shows GIXRD patterns of homogeneous(a) and graded (b) TiN- GAMS films. For the graded TiN, the preferred orientation of the film showed a predominant (111) peak compared with homogeneous TiN film which exhibits (200) preferred orientation. According to Table 1, average values of reduced elastic modulus (E_r) and hardness (H) for homogeneous and graded TiN are similar. However, standard deviation for E_r is higher for the graded TiN film. This behavior occurs due to non-stoichiometric composition through thickness for graded TiN that creates thickness-variable properties compared to that of conventional homogeneous TiN film. Thus, synthesizing of graded TiN- GAMS is viable and presents gradient and thick-dependent properties which could be interesting for engineering applications.

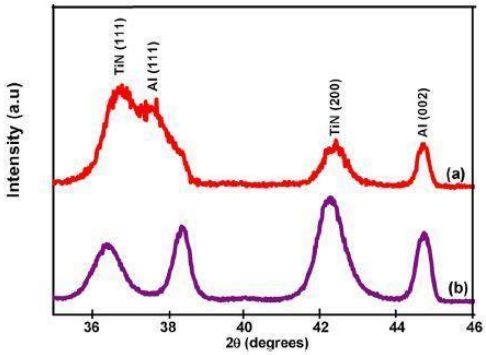

Fig. 1. *GIXRD diffraction pattern (15°) for: (a) graded TiN; (b) homogeneous TiN.[1]*

Condition	E_r [GPa]	H [GPa]
Homogeneous	207.1 ± 4.8	21.3 ± 1.0
Graded	203.2 ± 11.6	19.9 ± 2.0

Tab. 1 *Hardness and elastic modulus by nanoindentation tests for TiN films*

4. References

[1] F.C. Silva *et al*, Int. J. Hydrogen Energy, **45**, 33993-34010 (2020).
[2] F.C. da Silva *et al,* SN Appl. Sci.,**2**, 865 (2020),

*Corresponding author: felipe.carneiro01@fatec.sp.gov.br, felipecarneiro@usp.br

WEAR PROPERTIES OF AISI 4340 STEEL TREATED BY NITRIDING, DLC FILM AND DUPLEX COATING

Silva Filho, E. A.[1]*, Danelon, M. R.[1], Antônio Júnior, C. A.[1], Manfrinato, M. D.[1,2], Rossino, L. S.[1,2]
[1]*Universidade Federal de São Carlos, PPGCM, UFSCar Campus Sorocaba, Sorocaba-SP*
[2]*Faculdade de Tecnologia do Estado de São Paulo (Fatec Sorocaba), CEETEPS, Sorocaba-SP*

1. Introduction

DLC (Diamond-Like Carbon) film is an amorphous thin film composed by sp^3 and sp^2 bonds that has shown remarkable mechanical properties improvements to materials, such as low friction coefficient and high hardness and wear resistance. Nitriding is a thermochemical treatment which consists in the formation of a ceramic layer on the surface of the material and the diffusion of nitrogen in the matrix of the steel which improves wear, corrosion, and fatigue resistance. With the intention of combining nitriding and DLC film properties, duplex treatments have become an excellent alternative [1]. The purpose of this work is to compare the wear behavior of AISI 4340 steel treated by nitriding, coated by DLC film and duplex treatment.

2. Experimental

Plasma treatments were carried out by a Pulsed-DC power supply. Before every treatment, an ablation treatment with gas mixture of 80%Ar/20%H_2 was performed for 1h. DLC film deposition was performed using PECVD technique, but before the amorphous carbon film deposition, an organosilicon film was deposited to improve the film adhesion on the surface, with a gas mixture of 70%HMDSO/30%Ar for 15min. For the DLC film deposition a gas mixture of 90%CH_4/10%Ar was used, with gas flow of 30sccm for 2h. For nitriding treatment, the gas mixture utilized was 80%N_2/20%H_2 and gas flow of 500sccm for 5h. The duplex treatment parameters combined of both treatments. Micro-abrasive wear tests by fixed ball were performed with an 8N load in two different conditions. First, the samples were submitted to tests using 120,300,600,900,1200,1500 and 1800 seconds, at the same spot, only varying the time. At the second condition, the tests were performed only for 600s.

3. Results and Discussions

It is noted that all treatments improved the wear resistance of the samples. As shown in Figures 1 and 2, the duplex sample presented the highest wear resistance for both the 600s and the progressive 1800s tests, when compared to other samples. This is justified by the in-depth hardness and the ceramic compound layer of nitriding treatment together with the low friction coefficient and high hardness of DLC film. Nitriding treatment has shown intermediate wear behavior, explained by the compound layer produced with diffusion zone, formed during treatment. Although DLC film with a compound layer has shown the best wear resistance, it showed different behavior by itself. Figure 2 highlights this, showing similar wear properties to the other samples for the first five minutes. After that, the test reaches the matrix of the sample and the wear volume increases, but it remains lower than the base material. This indicates that once removed, the remnants of the film still act as a resistance factor for the material. Thus, it can be concluded that all three procedures improve wear resistance of AISI 4340 steel.

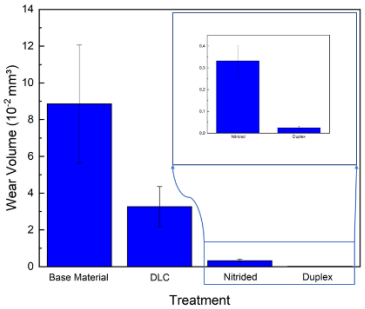

Fig. 1. *Wear volume of different treatments*

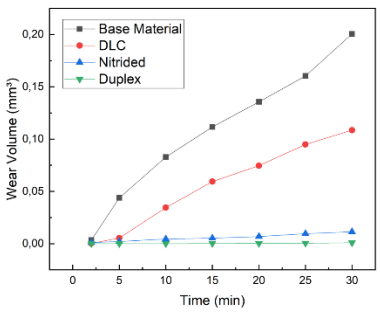

Fig. 2. *Wear volume progress over time*

4. References

[1] Dalibon *et al.* Surface and Coatings Technology, **255**, 22-27 (2014).

Acknowledgments
We acknowledge FAPESP (2019/13041-3) for the financial support and FATEC-Sorocaba for the laboratory.

*Corresponding author: edialbertosilva@gmail.com

BIOASSAY USING ONION AND LETTUCE SEEDS TO EVALUETE BIOPOLYMERS RESIDUES

Silva, G. M.[1]*, Irazusta, S. P.[2].
[1,2]*Faculdade de Tecnologia de Sorocaba – José Crespo Gonzales*

1. Introduction

Biopolymers or bioplastics have a similar structure to synthetic plastic meanwhile, they have a biological base or are biodegradable, or even have both characteristics [1], making biopolymers a solution for the synthetic plastic in instance for food packing. However, these biopolymers have benefits in replacing synthetic plastic is necessary to study the impacts of the soil degradation residues to guarantee its environmental safety. The objective was to determine the phytotoxicity and genotoxicity of these degradation residues.

2. Experimental

Two biopolymers films laminated with PBS (Polybutylene-succinate), NatureFlexTM 25NK Matt and NatureFlexTM 20 NKME metalized (film 1) and other with PBAT/PHBH (Polybutylene adipate-co-terephthalate/Poli 3-hydroxybutyrate-co-3-hydroxyhexanoate) (film 2) were submitted to degradation in compost soil following DIN EN 13432 norm. After, a concentrate solution of each soil sample, after 12 weeks of degradation, was prepared, so that PBS, PBATH/PHBH, 25NK MATT, 20 NK ME, film 1 and film 2. Then, onion and lettuce seeds were exposed to these elutriates following the Marin-Morales (2008) protocol. The sample controls were distilled water (negative) and ethyl methanesulfonate (EMS) 4.10^{-4} M (positive). We determined the germination and the genotoxicity indexes.

3. Results and Discussions

The results showed that none of the samples were phytotoxic to onion seeds as well as to lettuce seeds (Figure 1 A and Figure 2 A), although the film 2 inhibit the growth of lettuce plant (hypocolite) (Figure 1 B). The genotoxicity analysis results showed that none of the samples had significative alterations when compared to the control (Figure 2 B). In conclusion, the film 1, with the PBS polymer had better behavior in soil than film 2, with PBATH/PHBH blend as considering the inhibitory effect of the blend on the plant lettuce growth and development.

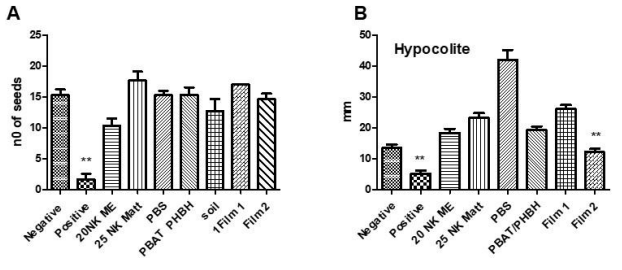

Fig. 1. *On A is showed the germination of the lettuce seeds and on B the seeds hypocolite growth showing the film 2 inhibition on the seeds. ** p<0,05*

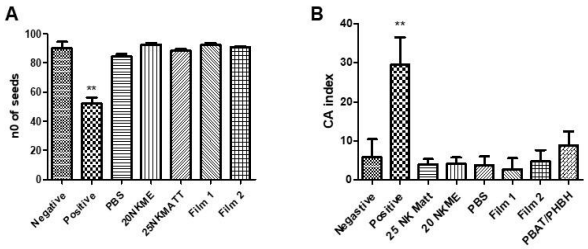

Fig. 2. *On A is showed the germination of the onion seeds and on B is showed the chromosomic aberration index addressing that none of them were affected. ** p<0,05*

4. References

[1] G.F.A. Brito, *et al*. REMAP, **6**, 127-139, (2011).
[2] M.A. Marin-Morales. *"A Utilização de Allium cepa como Organismo Teste na Detecção da Genotoxidade Ambiental"*, 1ª Ed. Unesp – SP. 2008.

Acknowledgments
We acknowledge the CNPq for the grants.

*Corresponding author: silvam.giovanna29@gmail.com

OPTICAL SENSORS: TERRESTRIAL DATA COLLECTION

Silva, M. A.[1]*, Damião, A. J.[2]
[1]*Instituto Tecnológico da Aeronáutica (ITA)*
[2]*Institunstituto de Estudos Avançados (IEAv)*

1. Introduction

The use of optical sensors embedded in satellites or in aircraft has leveraged the possibilities of terrestrial mapping to an unprecedented level, enshrining terrestrial monitoring satellites, as well as the sensors involved for terrestrial data collection as an indispensable data source in Remote Sensing (SR) applied to agriculture, natural resource management, urban planning, military planning and others. With the technological advances of the last decades, it is now possible to obtain orbital images of high temporal, spatial, spectral and radiometric resolution that cover large areas of the surface, enabling the identification of the most diverse targets. However, there are factors to be evaluated to ensure the accuracy of the cartographic products generated from these data.

2. Theory

Through technological advances and the need for human locomotion in environments of difficult access to collect data on land occupation, limits of areas, among other aspects, means were sought to obtain information so that, in addition to minimizing the risks, Relevant spatial geodata can be collected to be applied for various purposes. Due to the ease of performing photogrammetric flight by ARP, it suggests its use to extract updated information from the earth's surface [1]. Therefore, it is interesting to analyze the height and scale of flight, the scale of the project, to evaluate the operational costs and to allocate these primary choices according to the purpose of the cartographic product. As for orbital images, according to what one wants to identify in an image processing, one must pay attention to the resolutions.

3. Result and Discussions

Although the advances, there are still great challenges related to the construction, launch and maintenance of these satellites in orbit, since they are in low orbits, with great temperature variation, presence of radiation, vacuum, deposition and friction with atomic oxygen and other particles, causing optical surface degradation and reduced sensor life. The understanding of how these factors affect the data obtained by the equipment is essential to guarantee the quality of these data and the correct use in the various possible applications, especially regarding techniques whose analyzes are essential to represent the surface and identify targets throughout the geographic extension [2]. As an example, multispectral and hyperspectral satellites can be cited that eventually show faults in one of the bands, generating noisy images that cannot be corrected, as occurred with the thermal band of the Landsat 3 satellite [3]. In addition to that, for image processing purposes, atmospheric correction is necessary, which demands detailed coefficients and with sensor degradation there is a loss in pre-processing quality, which can lead to erroneous analyses. In short, it is essential that the analyzes carried out through geoprocessing take these sources of interference into account.

4. References

[1] MITISHITA, E. E., J.; GRAÇA, N. de.; CENTELHO, J.; MACHADO, A. O Uso de Veículos Aéreos Não Tripulados (VANTs) em Aplicação de Mapeamento Aerofotogramétrico. XXVI CONGRESSO BRASILEIRO DE CARTOGRAFIA, (2016).
[2] PONZONI, Flávio Jorge; REZENDE, Ana Carolina Pinto. Revista Árvore, **26**, 403-410, (2002).
[3] BARRETO JÚNIOR, M. S. et al. Utilização do geoprocessamento para acompanhar a transformação da paisagem oriunda do processo de instalação de parques eólicos na serra de Santa Luzia/PB, (2018).

Acknowledgment
Ao CNPq, ITA e IEAv pela oportunidade de pesquisa.

*Corresponding author: micaela.allmeida@gmail.com

CLASSIFICATION OF IMAGES REMOTE THERMAL SENSING

Silva, M. A.[1]*, Damião, A. J.[2]
[1]*Instituto Tecnológico da Aeronáutica (ITA)*
[2]*Institunstituto de Estudos Avançados (IEAv)*

1. Introduction

The use of Remote Sensing (SR) for extraction, detection and interpretation of objects on the earth's surface has been one of the essential means for carrying out the monitoring and mapping of natural resources, urban management, defense issues, strategic planning and so on. With technological advances and the development of new sensors, it became possible to obtain orbital images with better spatial, spectral and temporal resolution, expanding applications in several areas of knowledge. The SR has also helped in the segmentation and classification of objects, generating information that can be applied to decision making; contributing to the increase in precision and better manipulation of spatial data [1]. This summary proposes to evaluate the initial parameters of thermal data collection, for later segmentation, classification and production of cartographic products.

2. Experimental

Orbital, on-board and airborne sensors contribute to the detailed generation of terrain information, so image classification can strengthen the foundation and planning of territorial logistics. The set of techniques and sensors have the ability to obtain data without interaction with the physical world, using radiation characteristics along the electromagnetic spectrum. For better use of images, it is important to have primary analyzes that are determining factors for decision making in relation to sensors, platforms and processing methods [2]. In order to determine the best conditions for obtaining thermal aerial photos, a first data collection was performed, using the FlirDUO thermal camera coupled to a Remotely Piloted Aircraft (RPA) - Phantom 4 v.2. Thus, obtaining a set of sequence images, which were processed in a single orthophoto of 10 cm of spatial resolution. Using the QGIS software, a false color composition was performed, making it possible through photointerpretation to identify different targets and their respective behaviors, allowing for further analysis to define the best methodology for segmentation and classification.

3. Results and Discussions

Through the photointerpretation of thermal images, it was possible to identify targets classified into soil, vegetation, construction, paving and vehicles, and it was also possible to identify subclasses such as bridges, dense vegetation, undergrowth and different construction coverages. However, there are some difficulties due to different targets that have the same temperature, so that only the spectral classification is not enough for its correct distinction, making it necessary to use geometric classification algorithms. In order for the quality of the classification to be adequate, it is essential that there is significant variation between the targets, therefore, the time with the highest incidence of sunlight, little shade and low humidity must be considered as adequate conditions for data collection. It is also important to analyze through these factors whether an algorithm will be applied or developed for the classification of thermal images, due to the unconventional nature of the data.

4. References

[1] S. D. M. Guarda, E. S. Bias, E. E. Sano, E. F. Castejon, P. N. Happ, R. R. Antunes, A. A. Teixeira and R. B. Sousa, Anuário do Instituto de Geociências, **42**, 514-526 (2019).
[2] F. J. Ponzoni and A. C. P. Rezende, Revista Árvore, **26**, 403-410 (2002).

Acknowledgment
Ao CNPq, ITA e IEAv pela oportunidade de pesquisa.

*Corresponding author: micaela.allmeida@gmail.com

VEGETABLE IVORY MICROPARTICLES COATED BY PLASMA JET ACTIVATION OF SILICONE OIL AND MULATEIRO EXTRACT

Silva, Y. F. da[1]*, Almeida, G.[2], Veiga, A. T. V.[1], Zoghlami, A.[3], Oliveira, R. N.[4], Perré, P.[3], Simão, R. A.[1]
[1]*Federal University of Rio de Janeiro, Department of Metallurgical and Materials Engineering, Brazil*
[2]*Université Paris-Saclay, INRAE, AgroParisTech, France*
[3]*Université Paris-Saclay, CentraleSupélec, Laboratoire de Génie des Procédés et Matériaux, France*
[4]*Federal Rural University of Rio de Janeiro, Department of Chemical Engineering, Brazil*

1. Introduction

As the awareness of the environmental hazards caused by polymer microbeads increases, a large number of eco-friendly alternatives, e.g., minerals and plant products, has been investigated [1]. Among these resources, microparticles ground from the endosperm of Amazonian palm seeds of the genus *Phytelephas* have been highlighted owing to their ivory-like color and biodegradability. On the other hand, their chemical composition essentially based on pure mannan [2], a low-substituted polysaccharide constituted by mannose residues, makes them vulnerable to the degradation by micro-organisms, especially when exposed to moisture. With this in mind, this work aimed at developing coatings on vegetable ivory microparticles using cold plasma technology.

2. Experimental

Vegetable ivory microparticles (~ 125-250 µm) were immersed in a 1:1 mixture of silicone oil and mulateiro extract (*Calycophyllum spruceanum*). Further, the liquid was treated during 30 s by an atmospheric pressure plasma jet (PlasmaPen™, PVA TePla America) fed with ambient air compressed at 7 bar. A distance of 1.5 cm was kept between the plasma jet nozzle and the surface of the liquid. Later, particles were abundantly washed in distilled water during vacuum filtration followed by ultrasound cleaning for 15 min. Finally, sample characterization was performed by scanning electron microscopy (SEM), atomic force microscopy (AFM) and Raman imaging.

3. Results and Discussions

Air plasma jet activation of silicone oil and mulateiro extract resulted in the formation of water-stable coatings on the particle surface produced by liquid-phase crosslinking reactions. This result was substantiated by SEM and AFM images, in which an increased surface smoothness and an extensive coverage of particle pores could be observed. Furthermore, Raman imaging results (Fig. 1) for coated samples presented regions abundant in Si-O bonds (490 cm^{-1}) and aromatic groups (1616 cm^{-1}) in comparison to the mannan-rich (890 cm^{-1}) matrix, evidencing film composition by moieties from both precursors. The coatings, produced in a single step, could act as a protection barrier against moisture and micro-organisms, enhancing vegetable ivory durability.

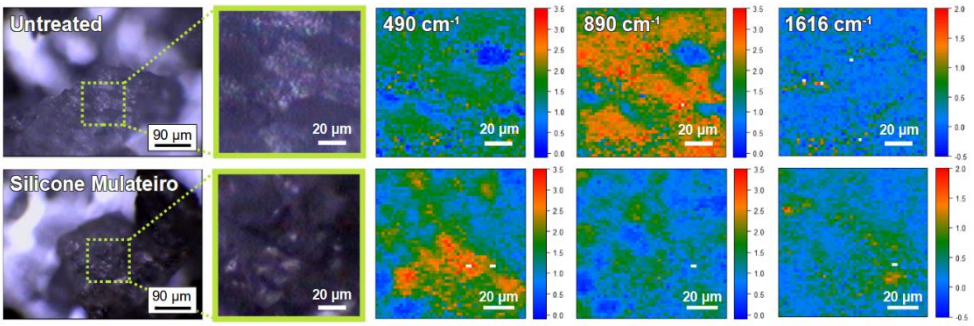

Fig. 1. *Optical microscopy images and Raman average intensity maps (490, 890 and 1616 cm^{-1}) for untreated and plasma coated vegetable ivory microparticles using silicone oil and mulateiro extract as precursors.*

4. References

[1] C.F. Hunt, W.H. Lin, N. Voulvoulis, Nat. Sustain., **4**, 1102-1106, (2021).
[2] S. Ghysels, A.E.E. Léon, M. Pala, K.A. Schoder, J.V. Acker, F. Ronsse, Chem. Eng. J., **373**, 446-457, (2019).

Acknowledgments
The authors would like to thank CAPES, CNPq and Chaire de Biotechnologie de CentraleSupélec for the support received during this study.

*Corresponding author: yuri@metalmat.ufrj.br

OXIDE FILMS DEPOSITED ON ALUMINUM ACETYLACETONATE PLASMA

Souza, A. L.[1]*, Almeida, L. S. de[2,3], Rossino, L. S.[2,3], Cruz, N. C.[1], Rangel, E. C.[1]
[1]*Laboratory of Technological Plasmas (LaPTec), São Paulo State University (UNESP), Av. Três de Março, 511, 18087-180, Sorocaba, SP, Brasil.*
[2]*Sorocaba Technological College – FATEC, Av. Engenheiro Carlos Reinaldo Mendes, 2015, 18013-280, Alto da Boa Vista, Sorocaba, SP, Brasil.*
[3] *Federal University of São Carlos (UFSCAR), Sorocaba Campus, Rod. João Leme dos Santos, km 110, 18052-780 Sorocaba, SP, Brasil.*

1. Introduction

Alumina thin films are materials that have a wide variety of practical applications. The diversity of alumina applications and its wide range of properties is related to the different possible crystalline phases [1]. The chemical vapor deposition methodology is the most commonly applied. However, in order to make it possible to obtain alumina films on substrates sensitive to high temperatures, many studies are being developed based on methods that involve plasma, such as PECVD.

2. Experimental

Argon plasma was established in the presence of (0.80 g) of aluminum acetylacetonate (AAA) powders for deposition of films on substrates of different materials. The effects of deposition time on deposition kinetics and film properties were investigated.

3. Results and Discussions

The process is divided into 3 steps as a function of time. The first occurs at $t < 4$ min, in which the etching of the AAA is the predominant process of transporting the compound to the plasma. The second stage ($4 < t < 8$ min) is favored by a high density of AAA fragments favored by AAA sublimation with increasing temperature. The third step, which occurs for $t > 8$ min, is characterized by high temperatures and low pressures.

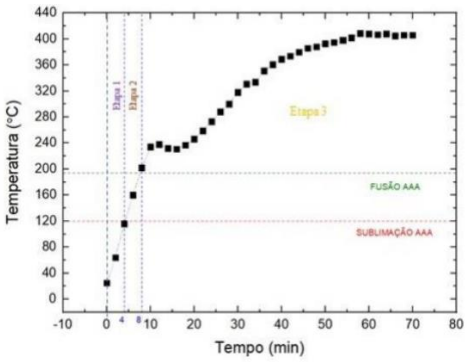

Fig. 1. *Sample holder temperature as a function of plasma exposure time. The horizontal dashed lines represent the sublimation and melting temperatures of AAA.*

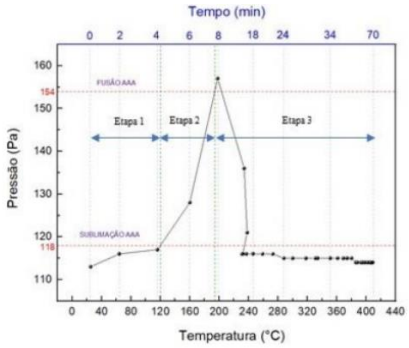

Fig. 2. *Process pressure as a function of temperature. The vertical dashed lines represent the sublimation and melting temperatures of AAA and the horizontal lines the system pressure in this situation.*

4. References

[1] DING, J. C. et al. Low-temperature deposition of nanocrystalline Al2O3 films by ion source-assisted magnetron sputtering. Vacuum, **149**, 284–290, (2018).

Acknowledgments
The authors would like to thank LabTes and LabTec for their support and use of the equipment.

*Corresponding author: adriano.luiz_souza@hotmail.com

DEPOSITION OF SiO_2 THIN FILMS USING TRIS(DIMETHYLAMINO) SILANE BY PLASMA ENHANCED ATOMIC LAYER DEPOSITION

Spigarollo, D. C. F. S.*[1], Camargo, D. H. S. de[2], Ivanof, G. P. S.[1], Cruz, N. C.[1], Rangel, E. C.[1]
[1]*Science and Technology Institute of Sorocaba (ICTS), São Paulo State University (UNESP), 511 Av. Três de Março, Sorocaba, 18087-180, Brazil*
[2]*Brazilian Nanotechnology National Laboratory (LNNano), Brazilian Center for Research in Energy and Materials (CNPEM), 10000 R. Giuseppe Máximo Scolfaro, Campinas, 13083-970, SP, Brazil*

1. Introduction

Thin SiO_2 films have a variety of applications, since corrosion protection films, until their application in microelectronics. Plasma Enhanced Atomic Layer Deposition was explored to deposit thin films of SiOx since it allows a decrease in temperature, when compared to ALD, and a faster and more uniform deposition, enabling the deposition of different materials [1].

2. Experimental

Plasma Enhanced Atomic Layer Deposition of Oxford Instruments – OpAL was utilized for films depositions. The precursor used was tris(dimethylamino) silane (TDMAS) and O_2 was used as an oxidizing agent. The temperature adopted was 150 and 200 ºC. The number of cycles was varied from 1271 to 2966 and layers with thicknesses of 150, 300 and 350 nm were obtained at looking glass to obtain different thickness of film.

3. Results and Discussions

In all cases the growth per cycle was 1,18 Å/cycle. Figure 1 shows the IRRAS spectrum of the samples. It is possible to observe the characteristic bands of the presence of the Si-O bond in 1059 cm^{-1} and the presence of CH_3 groups in 1238 cm^{-1}[2, 3, 4]. Some authors [3, 4] cite the presence of the third dimethylsilane group in precursor as energetically unfavorable to the reaction. The presence of groups CH_3 may indicate a residue of the precursor due to this high energy required for complete breakdown of TDMAS. This data can be corroborated by EDS data (fig 2), that indicates the presence of carbon in the deposited film. The film deposited via PEALD presented also characteristics of a SiO_2 structure and impurities due to incomplete breakdown of the TDMAS molecule. Further studies are needed to elucidate this process of deposition of SiOx films.

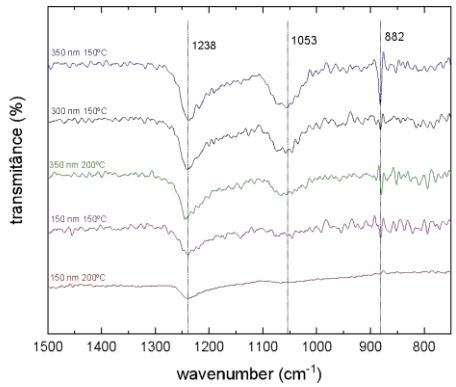

Fig. 1. *IRRAS spectrum for looking glass deposited with different film thickness.*

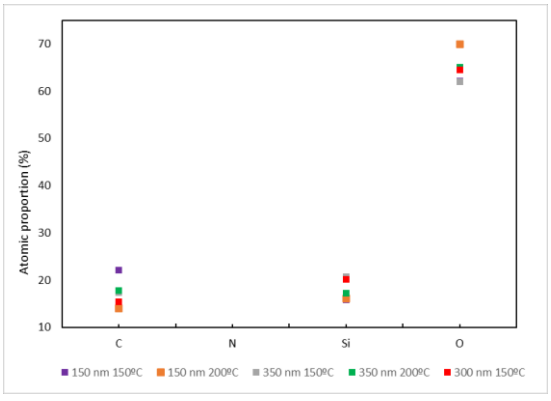

Fig. 2. *Atomic percentages of the elements's determinated by EDS in deposited films with different tickness.*

4. References

[1] M. Napari, et ali, Surface and Coatings Technology, **326**, 281-290, (2017).
[2] R.C. Rangel, et ali, Surface and Coatings Technology, **378**, 124996, (2019).
[3] B.B. Burton, et ali, The Journal of Physical Chemistry C, **113**, 8249-8257, (2009).
[4]F. Hirose, et ali., ECS Transactions, **19**, 417, (2009).

Acknowledgments
The authors would like to thank LNNano/CNPEM for the use of PEALD.

*Corresponding author: daniellespigarollo@gmail.com

ARTIFACTS IN XPS ANALYSIS DUE TO INCORRECT SAMPLE HANDLING

Steffen, T. T.*, Sagás, J. C.
Laboratory of Plasmas, Films and Surfaces, UDESC, Joinville, Santa Catarina, Brazil

1. Introduction

The use of X-ray photoelectron spectroscopy (XPS) is more often every day. At the same time, a large amount of misinformation has been inferred from the technique [1] due to analysis errors and inappropriate sample handling. As the XPS is very sensitive to the surface, proper handling of the samples must be done to not compromise the use of collected data [2]. That considered, this work aims to show how XPS spectra are affected by the way silicon samples are handled before analysis.

2. Experimental

Silicon wafers were analyzed by XPS after going through different handlings. Only one of the samples was not cleaned with isopropyl alcohol in ultrasound by 10 minutes (Si_P). Another one (Si_C) was cleaned and analyzed as so. Three samples were manually touched – by finger (Si_F), by nitrile glove (Si_NG), and by latex glove (Si_LG) – before putting them into XPS. Analyses were conducted at a base pressure of 10^{-8} mBar, with an Al Kα (1486.6 eV) radiation source in a Thermo Scientific K-Alpha equipment. Survey spectra were obtained after 10 scans, with 200.00 eV pass energy, 10 ms dwell time, and 1.000 eV step size. For high resolution scans those parameters were set, respectively, as 10 scans, 20.00 eV, 100 ms, and 0.025 eV. In the curve fitting a Gaussian (70%) Lorentzian (30%) sum function was used in combination with a Shirley background.

3. Results and Discussions

For Si_P and Si_C samples, survey spectra do not show significant change, with the chemical composition varying by no more than 1 at.%. The samples which were touched, however, present a significant increase in carbon concentration (20-35 at.%), coming from adsorbed carbon. Comparing the high-resolution spectra with the Si_C sample (Fig. 1) as a reference, it is observed the appearance of a peak in 102.00 eV, related to organic silicon [3], for Si_F (Fig. 2) and Si_LG samples. These results highlight the importance of correctly handling the samples, in a way to prevent contaminations that affect the XPS results.

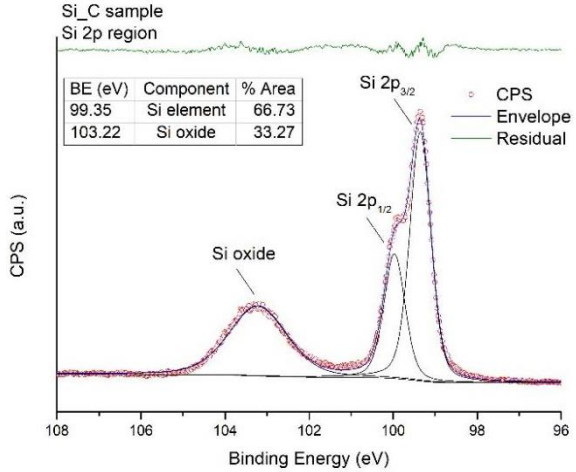

Fig. 1. *XPS Si 2p fitting for Si_C sample.*

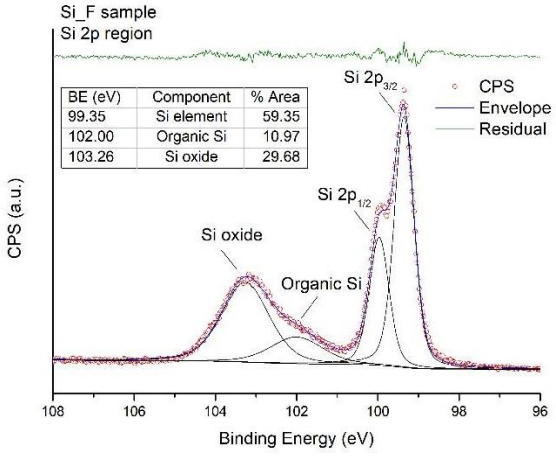

Fig. 2. *XPS Si 2p fitting for Si_F sample.*

4. References

[1] G. H. Major et al., J. Vac. Sci. Technol. A, **38**, 061204, (2020).
[2] F. A. Stevie et al., J. Vac. Sci. Technol. A, **38**, 063202, (2020).
[3] P. M. Dietrich et al., Appl. Surf. Sci., **363**, 406-411, (2016).

Acknowledgments
The authors are thankful for the Multi-User Facility infrastructure from Santa Catarina State University's Technological Sciences Center.

*Corresponding author: teretromm@hotmail.com

EFFECT OF SAMPLE SHAPE ON PLASMA TREATMENT BY A CONICAL SHAPED APPJ-LIKE

Tavares, T. F.*, Kodaira, F. V. P., Kostov, K. G.
São Paulo State University (UNESP), School of Engineering, Guaratinguetá, SP, Brazil.

1. Introduction

Atmospheric plasma treatments are commonly used to modify the surface properties of polymers [1]. The atmospheric pressure plasma jet (APPJ) used in this work has a conical shape, with a larger nozzle in comparison with traditional APPJs, it was built to overcome some limitations of other previous popular configurations, such as, small treatment spot. In this work polymers samples of high-density polyethylene (HDPE) were treated using a conical shaped (APPJ). There are many possible applications for the HDPE in the industry, due to their combinations of different properties, like: flexibility, chemical resistance, and a great balance among hardness, flow and processability [2]. Different shapes and sizes were treated to evaluate their influence.

2. Experimental

The plasma device is made of a glass funnel with Ø75mm nozzle and 70mm in height, the plasma was generated in a pin-to-plate configuration, with the pin electrode placed inside the funnel and fed by a pulsed voltage at 25KHz in burst mode with 2ms period and 12 cycles, the plate electrode was grounded and positioned right below the funnel nozzle and was covered with glass, which works as a sample holder and a dielectric barrier. Samples of HDPE were cut in square and circular shapes, varying its diameter and square sides (from 30 to 50 mm) making it possible to examine if the shape and the size of the samples have an influence on the polymers when the treated. They were treated for 300 seconds, and water contact angle (WCA) measurements were made.

3. Results and Discussions

All the samples were treated for 300 seconds. The changes on the homogeneity of the samples were evaluated by its wettability, analyzed through the WCA. The samples were treated directly with one side of the surface facing up, which will be called the top side, and the other facing the sample holder. What interests us the most here is the bottom side of the samples, square and circular ones, which makes it possible to see how the shape has an influence on polymers treatment. It can be observed that the WCA for square samples (Fig.1) is homogeneous all over the sample and does not depend on the size. However, for round samples (Fig.2) a less homogeneous treatment is observed and there is a dependence of the WCA on the sample size.

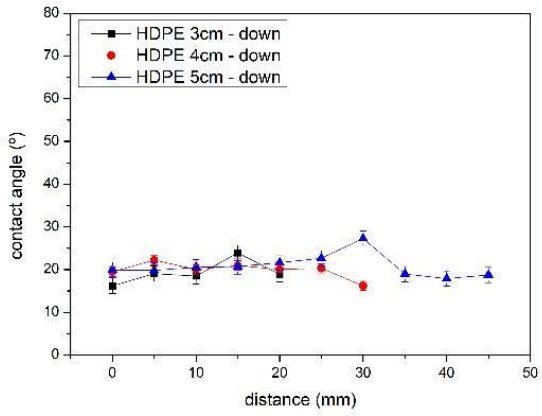

Fig. 1. *WCA of square HDPE samples, bottom side analysis, with their respective sides: 3cm, 4cm, 5cm.*

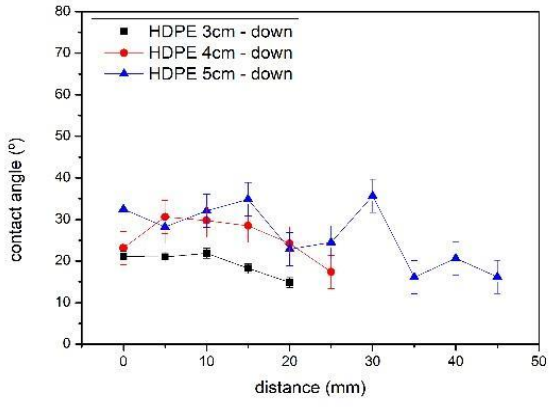

Fig. 2. *WCA of circular HDPE samples, bottom side analysis, with their respective diameters: 3cm, 4cm, 5cm.*

4. References

[1] R. Morent, et al., Surf Interface Anal, **40**, 597-600, (2008).
[2] C. Mezaroba, et al., Matéria (Rio de Janeiro), **23**, 1-10, (2018).

Acknowledgments
The authors would like to thank CNPq for financial support.

*Corresponding author: thayna.tavares@unesp.br

COMPARATIVE STUDY OF THE WEAR BEHAVIOR OF HARD COATING BY MICRO-ABRASIVE WEAR AND RUBBER WHEEL TEST

Teodoro, M. R.[1]*, Maluf, O.[2], Manfrinato, M. D.[1,3], Rossino, L. S.[1,3]
[1]*Universidade Federal de São Carlos, PPGCM, UFSCar Campus Sorocaba, Sorocaba-SP*
[2]*Faculdade de Tecnologia do Estado de São Paulo (Fatec Sertãozinho), CEETEPS, Sertãozinho-SP*
[3]*Faculdade de Tecnologia do Estado de São Paulo (Fatec Sorocaba), CEETEPS, Sorocaba-SP*

1. Introduction

Laboratory wear testing is a quick and relatively inexpensive means of obtaining information on wear rates and wear mechanisms [1]. In the literature, there are several methods for evaluating the wear resistance of hard coatings. In this work, the wear behavior of hard coatings deposited by welding was studied through the micro-abrasive wear test by fixed ball and rubber wheel wear test.

2. Experimental

The wear behavior of hard coatings containing carbides was studied, namely FeTiCW with titanium, tungsten, and chromium carbides, FeCrC with chromium carbides, and FeNbC with chromium and niobium carbides deposited by electric arc welding. The micro-abrasive wear test by fixed ball was carried out using an AISI 52100 steel sphere etched with 30% Nital. The test time was 15 minutes, with a load of 8N and abrasive with 30% SiC and 70% deionized H_2O, dripped between the sphere and the sample every 15 seconds. The rubber wheel wear test was performed considering the ASTM G65:2016 standard with a load of 130N, wheel rotation at 2,000 rpm, and a time of 30 minutes, with AFS 50/70 abrasive sand.

3. Results and Discussions

For the rubber wheel test (Figure 1), the FeNbC coating was the most wear resistant, followed by the FeCrC and FeTiCW coatings, respectively. Niobium carbide proved to be more resistant than titanium, tungsten, and chromium carbides, which are fragile and detach from the metallic matrix, becoming abrasive and increasing the severity of the test. This behavior is also observed in the micro-abrasive wear test (Figure 2). These two kinds of wear tests cannot be directly compared as the test parameters are different. Also, the sphere in the micro-abrasive wear test affects a smaller area compared at the rubber wheel wear test, being more indicated to evaluate thinner coating while the rubber wheel test is more severe and indicated to evaluate thicker and hard coatings. Even so, both tests showed the same behavior and wear resistance of the studied coatings.

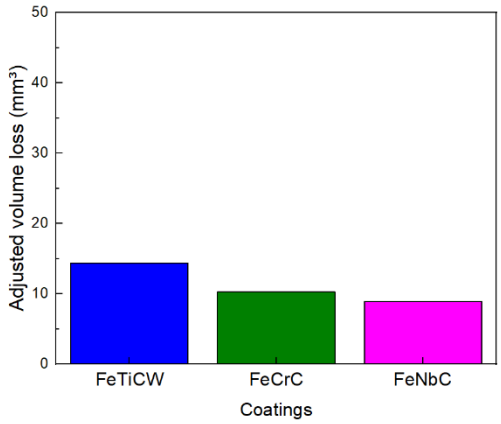

Fig. 1. *Wear resistance obtained by the rubber wheel test*

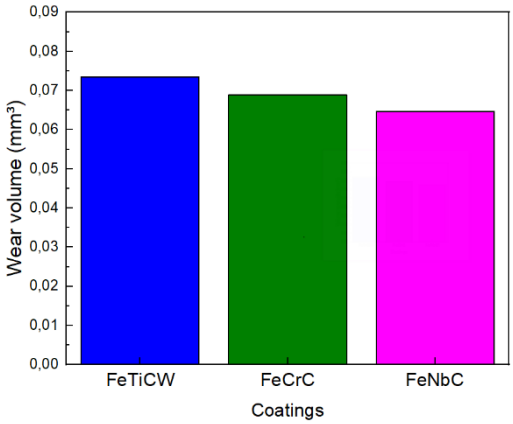

Fig. 2. *Wear resistance obtained by the micro-abrasive wear test*

4. Reference

[1] J. Konstanty et al. Materials Science Forum, **534–536**, 125–1128, (2007).

Acknowledgments
We would like to thank Capes (001).

*Corresponding author: teodoro.maicon001@gmail.com

MICROSTRUCTURE AND SELECTED MECHANICAL PROPERTIES OF AGED HIGH ENTROPY ALLOYS FOR POTENTIAL USE AS AN IMPLANTABLE MATERIAL

Torrento, J. E.[1]*, Sousa, T. S. P. de[1], Afonso, C. R. M.[2], Grandini, C. R.[1], Correa, D. R. N.[1,3]
[1]*Univ. Estadual Paulista - Laboratório de Anelasticidade e Biomateriais*
[2]*Univ. Federal de São Carlos - Department of Materials and Engineering*
[3]*Instituto Federal de Educação, Ciência e Tecnologia de São Paulo*

1. Introduction

HEAs are recognized for their superior strength, ductility, and corrosion resistance. In the biomedical area, the current research effort is looking for the development of HEAs with properties compatible with use as implantable materials [1]. This study aims to design, process, and characterize novel HEAs' structure, microstructure, and selected mechanical properties, composed of non-toxic elements for possible application as biomedical implants.

2. Experimental

The alloys were cast by arc melting and subjected to a heat treatment for microstructural homogenization. Then, aging treatments were performed at 300 ºC, 400 ºC, and 500 ºC for 6 hours (Fig. 1). The samples were characterized by density, EDS, chemical mapping, XRD, optical, scanning electron and transmission electron microscopy, elastic modulus, and Vickers microhardness measurements.

3. Results and Discussions

The chemical characterizations indicated an excellent quality of the produced samples. The structural characterization stated the majority of BCC crystalline structure, as predicted by the *ab initio* design parameters, has the secondary phase precipitation of an HCP structure in the TiZrNbTaMo sample. In the microstructural characterization, both alloys in the as-cast condition showed an irregular formation (Fig. 2). After the heat treatments, it is possible to observe grain boundaries, characteristic of the BCC crystalline structure. For the TiZrNbTaMo sample, some acicular structures in the boundary region indicated some microstructural modifications, confirmed by transmission electron microscopy. The TiZrNbTaMo sample showed substantial variation in elastic modulus related to the precipitation of secondary phases in the microstructure after heat treatments. Both HEAs showed higher Vickers microhardness (around 500 HV) and lower elastic modulus (around 80 GPa) than some commercial biomedical biomaterials (SS 316L, CP-Ti grade 2, and Ti-6Al-4V ELI). This study produced new HEAs, and the TiZrNbTaMn alloy showed the best potential for use in the orthopedical area, especially as joint replacement devices.

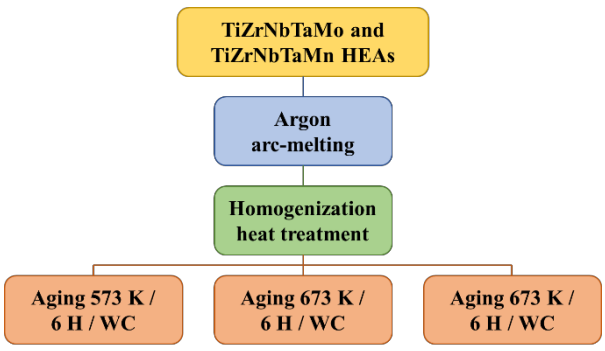

Fig. 1. *HEAs processing diagram.*

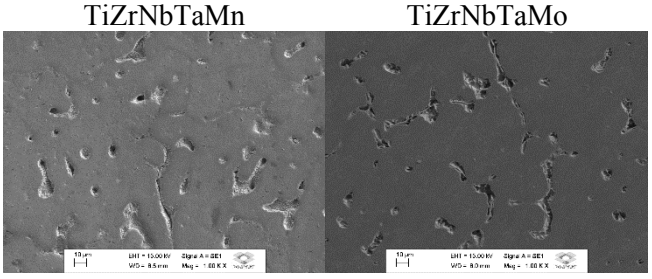

Fig. 2. *Micrography of the alloys in the as-cast condition.*

4. References

[1] T. NAGASE et al., Materials Science and Engineering: C, **107**, 110322, (2020).

Acknowledgments
Financial support: FAPESP, CNPq, and CAPES.

*Corresponding author: jhuliene.torrento@unesp.br

EFFECT OF TEMPERING TEMPERATURE ON THE DEGREE OF SENSITIZATION OF AISI 420 STEEL

Vacchi, G. dos S.[1]*, Varavallo, R.[2], Rossino, L. S.[3], Manfrinato, M. D.[3], Rovere, C. A. D.[1]
[1]*Universidade Federal de São Carlos, Departamento de engenharia de materiais, UFSCar*
[2]*Escola Técnica Estadual Sylvio de Mattos Carvalho, ETEC*
[2]*Faculdade de Tecnologia de Sorocaba, FATEC*

1. Introduction

The martensitic stainless steels (MSS) containing more than 11wt% chromium (Cr) are generally selected for special applications which require, in addition to moderate corrosion resistance, a combination of mechanical properties like high strength with adequate toughness, abrasion resistance, good fatigue resistance after certain heat treatments [1]. After tempering, these steels are brittle and need to undergo tempering to become applicable. The tempering temperature is extremely important to meet the design specifications, but it can increase the possibility of intergranular corrosion in these steels through the precipitation of chromium carbides during the treatment. To evaluate the susceptibility to intergranular corrosion, Electrochemical potentiokinetic reactivation (EPR) tests (single and double loop) were performed on samples submitted to tempering at temperatures ranging from 300°C to 600°C [2].

2. Experimental

A commercial AISI 420 stainless steel was used during the present work. These specimens were austenitized in a furnace at 1020°C for 30 minutes followed by oil quenching. Subsequently, the austenitized specimens were tempered at different temperatures, from 300 to 600°C in steps of 50°C for 30 min followed by air cooling. Microstructural examination was done using an optical microscopy. For electrochemical tests, a conventional three-electrode cell using a Pt foil as the auxiliary (counter) electrode and a saturated calomel electrode (SCE) as the reference electrode was used. The working electrode was constructed using the MSS specimen mounted in an epoxy resin to obtain a 0,278 cm^2 exposed area. The DL-EPR tests starts after obtaining the stable open circuit potential (OCP), the potential was scanned from -0.1V cathodic to the OCP to + 0.6V_{SCE} (activation scan) and then scanned back to the OCP (reactivation scan) at a scan rate of 100 mV/min at room temperature.

3. Results and Discussions

Table 1 shows the calculation of the degree of sensitization after at least 5 tests for each tempering temperature. Note that the degree of sensitization increased with increasing tempering temperature, which was expected, because the higher the temperature was, the greater the carbon diffusion velocity will be. This fact will increase the precipitation chromium carbides in the grain boundaries. This result shows that the region that presented the lowest degree of sensitization was the sample tempered at 300°C and the one that presented the highest degree was the one tempered at 600°C.

Temperatura de revenimento	**300°C**	**350°C**	**400°C**	**450°C**	**500°C**	**550°C**	**600°C**
Grau de sensitização (%)	17,2 ± 1,7	24,1 ± 1,3	27,5 ± 4,5	32,1 ± 3,0	68,6 ± 2,6	75,2 ± 2,5	150,5 ± 1,9

Tab. 1: *DL-EPR values with different tempering temperatures.*

4. References

[1] A.J. Sedriks *"Corrosion of stainless steel"*, 2nd edition, John Willy and Sons Inc, USA(1996).
[2] N. Alonso-Falleiros, M. Magri, and I.G.S. Falleiros, Corrosion, **55**, 769-778, (1999).

Acknowledgments
The authors gratefully acknowledge CNPq (National Council for Scientific and Technological Development–rant no. 312614/2020-9) and FAPESP (São Paulo Research Foundation –grant no. 2020/03205-6)

*Corresponding author: guilherme.vacchi@yahoo.com.br

POLYMER FILM DEPOSITION ON METALLIC SURFACES THROUGH ELECTROPOLYMERIZATION ACTIVATED BY PULSED VOLTAGE BIAS

Valcanaia, A. [1]*, Wiener, L.[1], Recco, A. A. C.[1], Steffen, T. T.[1], Becker, D.[1], Dalmolin, C.[1], Fontana, L. C.[1]
[1]*Laboratory of Plasmas, Films and Surfaces, Santa Catarina State University (UDESC), Joinville, Brazil*

1. Introduction

Corrosion is a major problem in engineering, as it is responsible for several damages, such as surface degradation, and therefore, solutions are needed to reduce or avoid it [1]. Present paper sets out to investigate an electropolymerization process, which consists of the growing of polymeric layers on metallic surfaces, activated by electrical pulses. The pulses can be controlled in intensity and period (in order of µs). The methodology proposed in this work aims to improve the corrosion resistance of steel parts previously coated with Zn layers.

2. Experimental

Polymeric layers were growth on zinc plated surfaces, by submerging the sample in aqueous solution containing alcohol monomers and nanoparticles SiO2 (50nm). The electrochemical cell was composed by a low carbon steel zinc plated substrate, which consist in the working electrode, and a counter electrode of stainless-steel grid. The specimens were polarized through high voltage pulses (periods of 1µs) using an Asymmetric Bipolar Pulsed Power Supply (ABiPPS). As the electrode is positively biased, the zinc layers corrode, and thus zinc atoms diffuse to the solid/liquid interface and act as catalysts, helping to form the polymeric layer on the solid surface [2]. The samples were characterized by scanning electron microscopy and X-ray excited photoelectron spectrometry (XPS).

3. Results and Discussions

The survey spectrum obtained in the XPS (Figure 1) indicates that the polymeric layer analyzed contains 11% of Silicon, 7% of Zinc, 40% of Carbon and 42% of Oxygen. The Silicon present in the polymeric film comes from the nanoparticles in the liquid solution, while the Zn atoms come from the surface of zinc coated parts. The electron microscopy analysis shows that the monomer is completely adhered to the metallic surface, as shown in Figure 2. Corrosion tests are currently being performed and it indicate substantial improvement in the corrosion resistant.

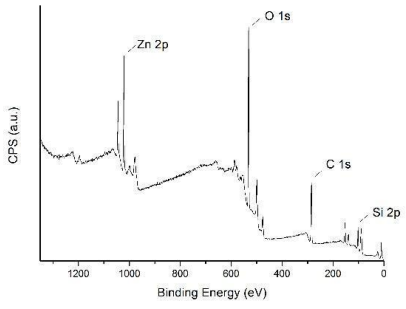

Fig. 1. *XPS results of generated polymer layer*

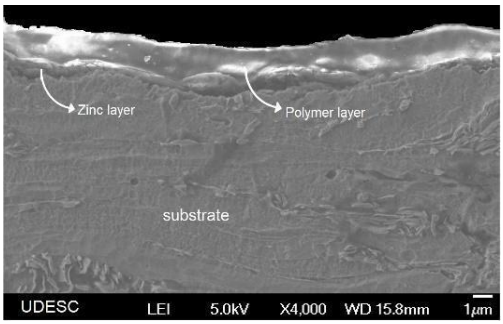

Fig. 2. *Cross section image of the layers*

4. References

[1] Roberge, P. R. *Corrosive Engineering: Principles and Practice.* New York: McGraw-Hill, (2008).
[2] Coelho, D.; Luiz, G. M.; Machado, S. A. S. Journal of the Brazilian Chemical Society, **32**, 1912-1917, (2021).

Acknowledgments
This research was partially supported by FAPESC 2021TR874. We thank PIBIC/UDESC/CNPq for the grants and CISER S.A. for providing samples and supplies.

*Corresponding author: amandavalcanaia@outlook.com

TRIBOLOGICAL STUDY OF STAINLESS STEEL 420 PLASMA NITROCEMENTATE

Varavallo, R.[1], Almeida, L. S. de[2], Vacchi, G. dos S.[3], Manfrinato, M. D.[2,4], Rossino, L. S.[2,4]
[1]*Escola Técnica Estadual Sylvio de Mattos Carvalho - ETEC, Matão. SP, Brasil*
[2]*Universidade Federal de São Carlos – UFSCAR Campus Sorocaba, Sorocaba/SP, Brazil*
[3]*Universidade Federal de São Carlos – UFSCAR Campus São Carlos – DEMA, São Carlos/SP, Brazil*
[4]*Faculdade de Tecnologia José Crespo Gonzales – Fatec Sorocaba, Sorocaba/SP, Brazil*

1. Introduction

Martensitic stainless steels type AISI 420 are many used in polymer and cutlery injection process molds, where it requires corrosion and mechanical resistance [1]. However, the method of repair carried out in the molds can be a factor for the useful life of the same, as it requires knowledge in metallurgical processes and welding. As alternatives to prolong the useful life of the material, surface treatments are adopted, such as hardening by diffusion of carbon and nitrogen [2]. The aim of this study is to compare the wear resistance of nitrocementation treatments performed in thermal treatments/revenues in stainless steel AISI 420.

2. Experimental

The samples were tempered to 1000 ° C in olive oil, reset to 400 ° C, 450 ° C and 500 ° C and nitrocement for 4 hours at 400 ° C, 450 ° C and 500 ° C. The metal surfaces were analyzed using metallographic analysis, hardness, microabrasive wear test and dispersive energy spectroscopy (EDS) by scanning electron microscopy (MEV).

3. Results and Discussions

Nitrocement layers at 400 ° C, 450 ° C and 500 ° C showed respectively microdurity and thicknesses of 839 HV, 920HV and 650 HV, 20µm, 23µm and 25µm. Figure 1 shows the microstructural formation of the nitrocement sample at 400 ° C, as well as the formed coarse thickness and secondary precipitation. Figure 2 shows the wear profile performed by nitrocement. The best condition for wear was 450 ° C, such condition comes from the rate of wear and secondary precipitation that form the nitrocementation.

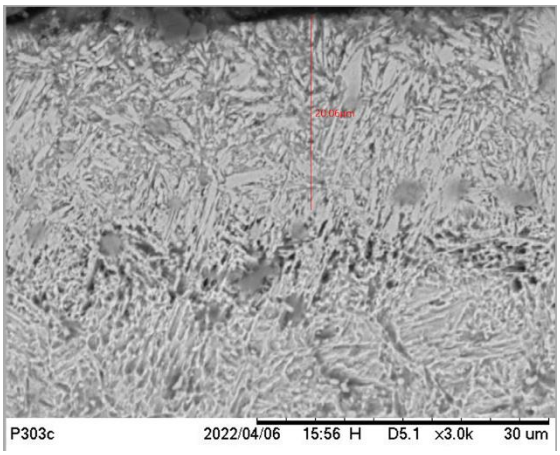

Fig. 1. *MEV of the Nitrocement sample at 400 ° C.*

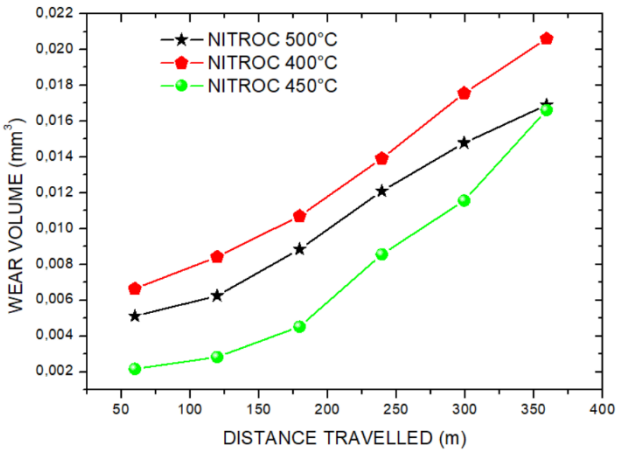

Fig. 2. *Wear out nitrocemented samples.*

4. References

[1] C. E. Pinedo, W. A. Monteiro, Techn. in Metall. Mat. and Min., **8**, 86-90, (2011).
[2] C. P. Rocha, H. B. Pereira, L. S. Rossino, M. D. Manfrinato. Braz. Jour. of Devel., **7**, 5837-58393,(2021).

*Corresponding author: rogerio.varavallo@gmail.com

ZINC-NITRIDING TRHOUGH PLASMA: A SIMULTANEOS ZN FILM DEPOSITION AND NITRIDING PROCESS

Wiener, L.[1]*, Valcanaia, A.[1], Recco, A. A. C.[1], Dalmolin, C.[1], Becker, D.[1], Steffen, T. T.[1], Fontana, L. C.[1]
[1]*Laboratory of Plasmas, Films and Surfaces, Santa Catarina State University (UDESC), Joinville, Brazil*

1. Introduction

Low temperature plasma has been used in the field of surface treatment for several purposes, namely: plasma nitriding, film deposition by sputtering, surface functionalization, plasma etching, etc [1]. Sometimes, it is possible to combine two processes as, for example, the combined effects on the surface mechanical and tribological properties by nanosecond pulse laser irradiation in nitrogen atmosphere, to produce simultaneous nitriding and texturing of the Ti6Al4V surface [2]. Present paper sets out to investigate the simultaneous plasma nitriding and zinc film deposition on AISI 1015 steel. This combined treatment is carried out in a very simple set up, through Zn sputtering from a solid target in a low-pressure Ar/N_2 plasma. The treatment proposed in this work produces simultaneously effects of nitriding and Zn film deposition, which can combine surface hardness (nitriding) with corrosion resistance (Zn film).

2. Experimental

AISI 1015 samples are placed between Zn targets in a vacuum chamber, where the plasma was generated. Both, the Zn target, and the samples work as cathode discharge and the chamber walls (anode) are connected to the ground. The main treatment parameters were P=8.0 Torr, T=330°C, time t=30 min, working gas 60%N_2/20%H_2/20%Ar. The plasma was generated by an asymmetric bipolar pulsed power supply (ABiPPS). The samples were characterized by optical microscopy, x-ray diffraction, Vickers microhardness, scanning electron microscope (SEM) and electrochemical corrosion tests.

3. Results and Discussions

Results show that the simultaneous effects of plasma nitriding and zinc film deposition was successfully performed, as showed in figure 1, where it is indicated the Zn film layer on surface of the sample. It was not observed the generation of compound nitride layers (Fe_4N or Fe_2N) in the subsurface of the samples. However, the microhardness results (fig. 2) indicate that may occur nitrogen diffusion toward the sample core because the hardness increased until typical values of diffusion zone of nitrogen in steel. The Microhardness depth profiles (fig 2) was splatted by two trends, namely: 1- Zn film + diffusion zone; 2-steel core. Electrochemical corrosion tests are currently being performed and it indicate substantial improvement in the corrosion resistant.

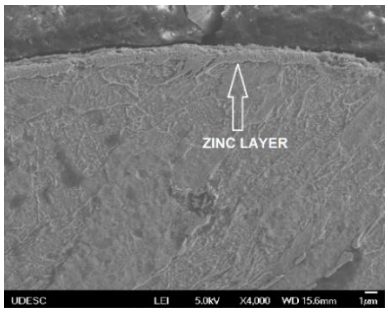

Fig. 1. *Zinc layer on AISI 1015 steel substrate*

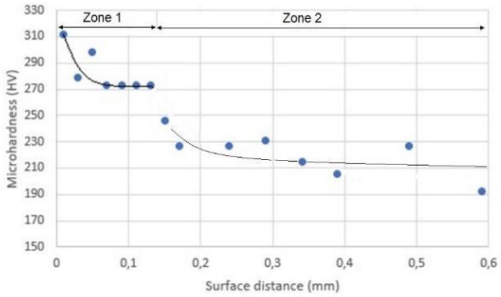

Fig. 2 *Microhardness–depth profile*

4. References

[1] Adamovich et al., J. Phys. D: Appl. Phys., **50**, 323001, (2017).
[2] WANG, Chao; HONG, Jing; CUI, Mingming; HUANG, Hu; ZHANG, Lin; YAN, Jiwang, Surface And Coatings Technology, **437**,128358, (2022).

Acknowledgments

This research was partially supported by PRONEM FAPESC-CNPq - 2020TR730. We thank PIBIC/UDESC/CNPq for the grants and CISER S.A. for providing samples and supplies.

*Corresponding author: lucaswiener1999@gmail.com

INFLUENCE OF THE ABRASIVE WEAR MODES ON THE FRICTION COEFFICIENT OF THIN FILMS

Wilcken, J. T. de S. L.[1], Júnior, S. M.[1], Silva, F. C. da[2], Luna-Domínguez, J. H.[3], Verma, V.[4], Schön, C. G.[5], Cozza, R. C.[1,2]*

[1] *University Center of FEI – Educational Foundation of Ignatius "Priest Sabóia de Medeiros" – Brazil*
[2] *CEETEPS – State Center of Technological Education "Paula Souza" – Brazil*
[3] *Universidad Autónoma de Tamaulipas – Mexico*
[4] *Research & Development Cell, R.V. Institute of Technology, Bijnor – India*
[5] *USP – University of São Paulo – Brazil*

1. Introduction

The micro-abrasive wear test by rotative ball is an important method adopted to study the abrasive wear behavior of materials (Figure 1) [1,2]. "*Wear craters*" are generated on the specimen and two abrasive wear modes are usually observed on the surface of the worn crater: "*grooving abrasion*" is observed when the abrasive particles slide on the surface, while "*rolling abrasion*" results from abrasive particles rolling on the specimen.
The purpose of this work is to measure the coefficient of friction in coated systems submitted to micro-abrasive wear, using the "*ball-cratering*" wear test method.

2. Experimental

Experiments were conducted with thin films of TiN, CrN, TiAlN, ZrN, TiZrN, TiN/TiAlN, TiHfC and TiHfCN. For counter-body, it was adopted one ball made of AISI 52100 steel, with diameter of $D = 25.4$ mm.
The normal force value defined for the wear experiments was $N = 0.4$ N, with two abrasive slurries concentrations (C), C_1 = 5% SiC + 95% glycerin and C_2 = 50% SiC + 50% glycerin (volumetric values). The average particle size of the SiC is 3 μm. The coefficient of friction was calculated using the equation $\mu = T/N$; T: tangential force.

3. Results and Discussions

Table 1 shows the values of the coefficient of friction as a function of the abrasive wear mode. An increase of the volume of abrasive particles (from 5% SiC to 50% SiC) caused a decrease lower on the friction coefficient. The abrasive slurry concentration and, consequently, the actions of the abrasive wear modes, show an important influence on coefficient of friction. The values of coefficient of friction reported under the occurrence of grooving abrasion were higher than the values of the coefficient of friction reported under the occurrence of rolling abrasion. In rolling abrasion, the abrasive particles are free to roll between the ball and the specimen, facilitating the relative movement between these elements and decreasing, consequently, the coefficient of friction on the tribological system. In other hand, in grooving abrasion, the abrasive particles are fixed on the counter-body (in the case, on the ball), limiting then, their movements and requiring higher tangential forces. With the low concentration of abrasive slurry, it was observed the action of grooving abrasion and, consequently, high values of friction coefficient were reported. In other hand, when was adopted the high concentration of abrasive slurry, there were the occurrence of rolling abrasion and low friction coefficients values.

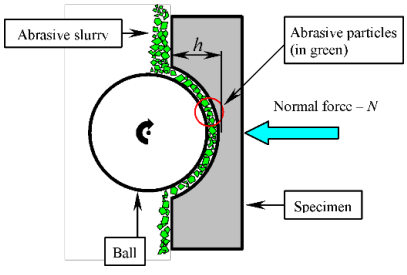

Fig. 1. *Schematic illustration of the principle of the micro-abrasive wear test by rotating ball* [1]

Thin film ⇓	$\mu_{Grooving}$ Grooving abrasion (5% SiC)	$\mu_{Rolling}$ Rolling abrasion (50% SiC)
TiN	1.37	0.57
CrN	0.35	0.24
TiAlN	0.72	0.32
ZrN	0.46	0.17
TiZrN	0.14	0.11
TiN/TiAlN	1.10	0.97
TiHfC	1.67	1.20
TiHfCN	0.68	0.51

Tab. 1. *Values of the coefficient of friction. Maximum error observed: $\mu = 0.11$.*

4. References

[1] R.C. Cozza, Surface & Coatings Technology, **215**, 224-233, (2013).
[2] M.M. Macedo, J.H. Luna-Domínguez, V. Verma, C.G. Schön and R.C. Cozza, Wear, **476**, 203664, (2021).
*Corresponding Author: rcamara@fei.edu.br, ronaldo.cozza@fatec.sp.gov.br

Sumário dos Autores

ISBN: 978-65-00-78788-7
CBL
9 786500 787887